

EOG-VR

ElectroOculoGraphy (EOG) Eye-Tracking for Virtual Reality

MASTER THESIS FINAL REPORT

1/7/2019



FEDERICO ALTOBELLI



*Delft University of Technology
Faculty of Industrial Design Engineering
Master in Integrated Product Design*

Graduate Student

Federico Altobelli

Student number: 4624858

Address: Oude Delft 174, 2611 HH Delft, The Netherlands

University email: f.altobelli@student.tudelft.nl

Personal email: federicoaltobelli@hotmail.com

Phone: +39 345 591 1109



University

Delft University of Technology

Industrial Design Engineering

MSc Integrated Product Design



Supervisory team

Chair

Dr. Huysmans, T.

Toon Huysmans - Expert in Ergonomics

Department of Industrial Design - Applied Ergonomics & Design

t.huysmans@tudelft.nl

Mentor

Ing. Kooijman, A.

Adrie Kooijman - Expert in Mechatronics

Department of Design Engineering - Technical Support

a.kooijman@tudelft.nl

A short story...

Dear reader, this is my graduation thesis with the title ElectroOculoGraphy (EOG) Eye-Tracking for Virtual Reality. It is written within the context of Industrial Design Engineering at Delft University of Technology, Master programme Integrated Product Design.

This project was initiated by the chair Toon Huysmans by advertising it on the graduation opportunities board of the faculty. I came to know about it during August 2018 and became immediately interested. Indeed, the proposal fitted perfectly my interest in working on the Virtual Reality field and as well with advanced ergonomics and electronics.

The proposal initially expected the collaboration with a company, but for various reasons this collaboration was not possible to initiate in a short time. However, since the topic was extremely appealing to me, I then decided to start this graduation project at the beginning of December 2018.

Executing a graduation project without a company can be highly challenging in terms of building know-how that could rather be transferred quite quickly and easily by the company instead. On the other hand, as an advantage the project was executed with less restrictions that would be present in a company that has to design, produce and launch a product on the market and, ultimately of course, make profit.

The project was conducted in the academic context with the collaboration of the supervisory team composed by Toon Huysmans and Adrie Kooijman, in the space of the Applied Labs.

Acknowledgments

During the master, culminated with this graduation project, I experienced highs and lows and I have improved a lot both as a designer and as a person. I challenged myself in multiple ways and fields, and I always tried to give the best of myself and of my abilities.

I take this opportunity to thank my family and all the people that surrounded me in the last years in Delft, the people at the Applied Labs and in particular both of my coaches, Toon and Adrie.

Both of them have strong competences in their fields and at the same time were highly available and friendly. They coached me by sharing their knowledge and tools while giving a good ratio between support and freedom.

Thank you all!

Abstract

The key factor for the success of virtual reality is immersion, which is the condition where the user loses awareness of being in an environment which is not real. Immersion is achieved by replicating human senses. In this context, introducing eye-tracking into VR can increase the immersion and open up a wide variety of applications.

Among eye-tracking methods, ElectroOculoGraphy (EOG) has the big advantage of having low requirements in terms of processing power and energy. This allows an efficient integration also in less powerful VR headsets.

EOG eye-tracking exploits a property of the eye which behaves as an electric dipole. When the eyes rotate, the dipole vector rotates accordingly. Signals that are a measure of the rotations can be obtained with the EOG technique by placing electrodes on the skin around the eyes.

It is recognised that these electrodes can be efficiently integrated on a VR headset on the foam mask surface which is contacting the user's face. With a minimum total of five electrodes it is possible to record signals that are a measure of horizontal and vertical conjugate (parallel) eye rotations, which can be converted into coordinates of the user's gaze point in the virtual reality

environment.

In order to receive EOG signals, a stable contact between electrodes and the user's skin must be assured. Standard VR headset masks do not provide uniform contact for all users, due to high variability of the human face shape. For this reason, the foam mask piece was re-designed by creating multiple sizes that could better accommodate different face shapes.

An anthropometric analysis was conducted on a database of 3D scans of European subjects, with the aim of identifying three clusters of face shapes. Such results were then used to create digital mannequins to be exploited in the design of three mask sizes, with the ultimate purpose of improving the contact with the face and the overall comfort.

Electronics and materials were researched and a final prototype with the desired characteristics was built with the purpose of demonstrating the integration of EOG into a VR headset and conducting user-tests. Finally, testing was successful to prove that with such a sizing system there is at least one size out of three that ensures stable contact with EOG electrodes for each subject tested.

Abbreviations

VR = Virtual Reality

PCA = Principal Component Analysis

CPU = Central Processing Unit

GPU = Graphic Processing Unit

HMD¹ = Head Mounted Device

HMD² = Head Mounted Display

EMG = ElectroMyoGraphy: recording of the electric potentials of the muscles

ECG = ElectroCardioGraphy: EMG specific of the heart

EEG = ElectroEncephaloGraphy: recording of the electrical potentials resulting from brain activity

EOG = ElectroOculoGraphy

PLR = Pupillary Light Reflex

FoV = Field of View / Field of Vision

LoS = Line of Sight

FP = Fixation Point

PC = Pupil Center

PA = Pupillary Axis

Table of Contents

1 CONTEXT

1.1 Virtual Reality context

1.1.1 VR headsets categories

1.2 Eye-tracking Context

1.2.1 Eye-tracking methods overview

1.2.2 Eye-tracking in Virtual Reality

1.2.3 EOG eye-tracking entering VR

1.2.4 Face electrodes VR products

1.3 Eye-tracking applications

1.3.1 Summary of eye-tracking general applications

1.3.2 Eye-tracking VR applications

1.4 Sizing system approaches

1.4.1 One-size-fits-all

1.4.2 Multiple sizes

1.4.3 Custom design

2 THE VISUAL SYSTEM

2.1 Introduction

2.1.1 The eyes

2.1.2 Rotations of the eye

2.2 Positional eye movements

2.2.1 Saccades

2.2.2 Smooth movements

2.2.3 Vergence movements

2.2.4 Miniature movements

2.2.5 Nystagmus

2.3 Non-positional eye movements

2.3.1 Adaptation

2.3.2 Accommodation

2.3.3 Blinking

3 ELECTROOCULOGRAPHY (EOG)

1.1 Virtual Reality context

3.1.1 Introduction

3.1.2 Corneo-retinal potential

3.1.3 ElectroOculoGraphy working principle

3.2 Electrodes configurations

3.2.1 Horizontal component

3.2.2 Vertical component

3.2.3 Torsional component

3.2.4 Ground placement

3.3 EOG signals

3.3.1 Amplitude of the signals

3.3.2 Artefacts

3.4 Calibration

3.5 Electrodes

3.6 EOG electronics

4 VR HEADSET PRODUCT ANALYSIS

4.1 HTC Vive product analysis

4.1.1 Choice of headset

4.1.2 HTC Vive taxonomy of parts

4.1.3 The harness system

4.1.4 The mask

4.1.5 Connections

4.2 3D-scanning and reverse-engineering of the mask

4.2.1 Insights gained

5 IDEATION

5.1 Electrodes

5.1.1 Configuration

5.1.2 Materials of the electrodes

5.1.3 Shape and dimensions

5.2 Mask design

5.2.1 Sizing system

5.2.2 Materials of the mask

6 ANTHROPOMETRIC STUDY

6.1 CAESAR database

6.1.1 Demographic data

6.2 Landmarks, planes, axes and measurements

6.2.1 Landmarks

6.2.2 Axes and planes, new coordinate system

6.2.3 Traditional style measurements

6.2.4 Digital measurements

6.3 Statistical analysis

6.3.1 Visualizations

6.3.2 Principal Component Analysis (PCA)

6.4 Clustering and generating mannequins

6.4.1 Clustering

6.4.2 Averaging and extremes

7 PROTOTYPING AND TESTING

7.1 Prototyping iterations

7.1.1 Experiment with EOG signals

7.1.2 Testing of Sparkfun board

7.1.3 Testing of custom-made dry electrodes

7.2 Final prototype

7.2.1 Foam part

7.2.2 Translation of mannequins into physical sizes

7.2.3 Main body

7.2.4 Physical prototype

8 USER TESTS

8.1 User test

8.1.1 Research questions

8.1.2 Equipment and test setup

8.1.3 Procedure

8.1.3 Questionnaire description

8.1.4 Video stimuli description

8.1.5 Subjects

8.1.6 Limits of the user test

8.2 Evaluation of the signals

8.2.1 Filtering

8.2.2 Plots

8.3 Summary of results

8.3.1 Signals

8.3.2 Comfort/discomfort

RECCOMENDATIONS, REFLECTIONS AND REFERENCES

1

Chapter 1
CONTEXT

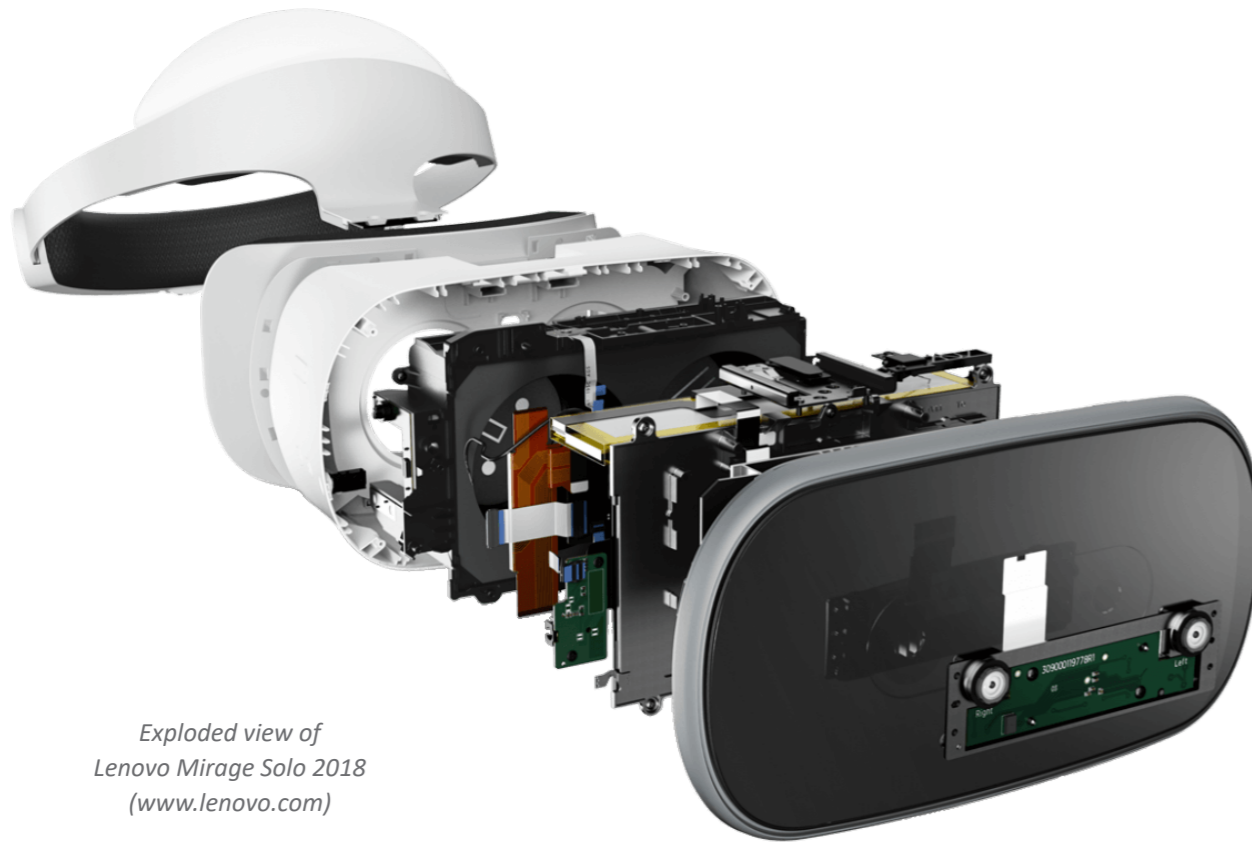
1.1 Virtual Reality context

Virtual reality (VR) is an immersive computer simulation of a three-dimensional environment where the user experiences sensory feedbacks and can interact with the surrounding through various kinds of controllers and devices.

Virtual Reality is experienced through VR headsets that project images with a pair of displays and lenses (optics) placed few centimetres from the user's eyes in order to create the illusion of a three-dimensional world.

The key factor for the success of VR is immersion, which is the condition where the user loses awareness of being in an environment which is not real. Immersion is achieved by virtually replicating human senses stimuli.

Big investments are made by companies on technologies and devices that can improve the level of immersion. Most popular VR devices (other than headsets) are hand-held controllers. Many other devices are oriented towards offering motion tracking and haptic feedback for the whole body or for a specific body feature, such as the hands.



Exploded view of
Lenovo Mirage Solo 2018
(www.lenovo.com)

1.1.1 VR headsets categories

Nowadays, the VR market is filled with a large variety of headsets differing in technology, price, and application fields.

They can be categorized in three main groups:

- Mobile
- Tethered
- Standalone

Mobile / Smartphone-based

Mobile or smartphone-based headsets mainly consist of a case and the optics and its regulation system (focus and distance between lenses). The VR experience is run by the smartphone's processor and graphic unit and displayed on its screen through the lenses. These kinds of headsets may also exploit the smartphone's cameras, audio system and sensors (accelerometer and gyroscope) for head tracking.

Smartphone-based headsets do not enable to run complex content and provide overall low levels immersion and quality. They are in fact targeted mainly to users who want to experience VR (often for the first time), but are not able or not willing to spend a lot on a product that they are not familiar with.

Main advantages	Main disadvantages
These kinds of headsets are typically low cost	The limit of the smartphone hardware translates to low immersion due to low graphics and framerate, pixelated images, inaccurate head tracking, and short battery life
The movements of the user are not constrained by wires	The motion tracking is limited to the head (no positional body tracking)
These kinds of headsets are typically low cost	Often no other devices as controllers can be connected
Setting up these headsets and running VR experiences are relatively easy jobs	In most VR experiences the user is just a spectator (360 photos and videos)



Google Cardboard
(www.vr.google.com)

Most diffused headsets in this category:

- Google Cardboard (2014)
10€
- Google Daydream View (2016)
110€ - 135€
- Samsung Gear VR (2015)
40€

Tethered

Tethered headsets are physically connected to a computer or console to exploit their processing and graphic power to run complex and detailed VR experiences. The headset consists of high-end hardware that is specifically designed for VR, as high-resolution screens, optics, precise head and body motion tracking. Moreover, such a system often includes hand-held controllers and external

motion tracking cameras that allow the user to interact and move accurately in VR environments.

Tethered headsets are targeted to users who are motivated to experience the highest quality of VR experience and can also afford or already own a high-end computer or console. These users are hardcore gamers, developers, and corporates which business can benefit from VR applications.

Main advantages	Main disadvantages
This kind of headsets can provide the highest level of immersion in VR	High costs both of the headset and of a gaming computer or console
	The system is not portable and generally requires to dedicate a whole room to it
	Cables may restrict users' movements
	Setting up such a system is relatively difficult

Most diffused headsets in this category:

- Oculus Rift (2016)
350€ (only headset) - 400€ (with controllers)
- Oculus Rift S (2019)
450€ (with controllers)
- HTC Vive (2016)
600€ (with controllers and motion tracking accessories)
- HTC Vive Pro (2018)
880€ (headset only) - 1200€ (with controllers and motion tracking accessories)
- HTC Vive Pro Eye (2019)
1700€ (with controllers and motion tracking accessories)
- Sony PlayStation VR (2016)
300€ (with motion tracking accessories)



HTC Vive
(www.vive.com)

Standalone / Untethered / All-in-one

Standalone headsets offer VR experiences without the need of any other additional device. They provide a level of performance and immersion that lies in between the mobile and the tethered headsets. However, the development of hardware that is specific for VR, in particular processors and cameras for positional tracking, may rise standalone headsets to a higher level in the future, bringing them closer to tethered headsets.

The main advantage of standalone headsets is allowing users to experience VR without cables, practically anywhere.

Their price range widely, based on the complexity of technology contained in it, opening to a wider variety of customers with different needs and budget.

For these reasons, latest trends saw the increase of interest from the market and investments of companies on the standalone category of headsets. Analysts predict that the Oculus Quest (May 2019), will be the biggest VR hit of the year 2019 (Venturebeat.com, 2019).

Main advantages	Main disadvantages
No need for other devices, the headset can be used anywhere and anytime	The device is dependent on a compact battery
The movements of the user are not constrained by wires	
Setting up these headsets and running VR experiences are relatively easy jobs	
Setting up such a system is relatively difficult	



Oculus Go
(www.oculus.com)

Most diffused headsets in this category:

- Oculus Go (2018)
220€ (32GB) - 270€ (64GB)
- Oculus Quest (2019)
450€ (64GB) - 550€ (128GB)
- Lenovo Mirage Solo (2018)
400€
- HTC Vive Focus (2019)
580€

1.2 Eye-tracking Context

Eye-tracking is a sensor technology that enables one or multiple of the following measurements performed on the eyes:

1. Identification of the different kinds of eye movements (Chapter 2 paragraphs 2.2, 2.3)
2. Identification of the direction of gaze (left, right, top, bottom and combinations of those)
3. Measurement of the angles of eye rotations along three axes around the center of the eyeball (Chapter 2 paragraph 2.1.2)
4. Measurements of the position of the user's gaze point on a surface (two-dimensional coordinates), usually a screen
5. Measurements of the position of the user's gaze point in the surroundings (three-dimensional coordinates)

1.2.1 Eye-tracking methods overview

There are three kinds of eye-trackers based on different working principles and technologies:

Tracking contact lenses (scleral contact lens search coils)

The user wears a pair contact lenses that embed small search coils connected to electronic instrumentation with wires. This method is extremely intrusive and rather out-dated; it was mainly in use for experiments on animals. For further details see Appendix 3.1.

Image/camera-based methods

They use a setup of optical devices (commonly infra-red cameras) to detect and track some distinguishable features of the eyes (typically the pupil) and derive the gaze point through image processing software. For further details see Appendix 3.2.

ElectroOculoGraphy (EOG)

EOG consists on capturing and analysing the electrical properties of the skin around the eyes in order to track eye movements. It is achieved by placing electrodes in strategic points of the user's face. EOG is discussed in detail in Chapter 3.

In order to convert the angles of eye rotations (3) into gaze positions on a surface (4) or in space (5), the user's head must be fixed, or must be tracked in order to disambiguate eye rotations from head movements.

Finally, it is possible to distinguish:

- Real time eye-trackers: measure with an unnoticeable delay.
- Offline eye-trackers: record and store the data in order to be further analysed after the recording session



(www.chronos-vision.de)



Dikablis Glasses 3 (www.ergoneers.com)



(www.youtube.com/user/BiopacSystems)

1.2.2 Eye-tracking in Virtual Reality

One of the biggest factors for achieving a higher level of immersion in VR is the ability to simulate human vision. For this purpose, new technologies are being developed as improved optics and higher resolution screens.

In this context, eye-tracking is taking place in virtual reality. Indeed, introducing eye-tracking into VR can bring many advantages and open up a wide variety of applications (Section 1.3).

Market overview

The integration of eye-trackers in VR headsets is relatively recent. In fact, only few products already reached the market while most others are still in development (Appendix 1.1). Nevertheless, analysts forecast a rapid growth. Road to VR (2018) expects eye-trackers to become a standard of consumer VR headsets.

In this rapid growing market, there are some relevant facts and trends that can be observed.

Tracking methods

First of all, VR eye-trackers on the market and in development are all camera-based. The reason is that camera-based eye-tracking is a well-established technology which has been also already implemented in commercial products. An example is the Tobii 4C selling at 170€ (www.tobii.com) for research and gaming purposes.

On the other hand, EOG did not see the same development efforts outside of the medical diagnostic field. The main reason is the fact that EOG requires a trained doctor to place single-use adhesive electrodes on the patient's face.

Headset categories

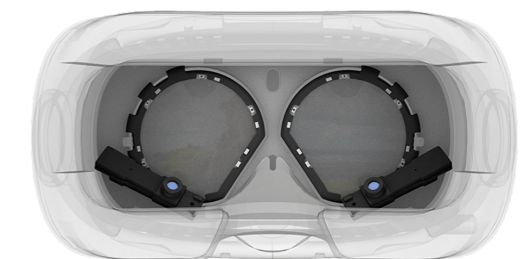
Another relevant fact is that camera-based eye-tracking is being integrated mainly in tethered headsets. Indeed, high costs of camera hardware, and high consumption of computational and battery power, oriented the initial adoption towards the more powerful tethered headsets, mainly targeting business customers. The example is the launch of HTC Vive Pro Eye with camera-based eye-tracking at 1700 €, 500€ more than the standard HTC Vive Pro.

Kinds of integration

Finally, there are two kinds of integration of camera-based eye-tracking in VR: headsets with built-in eye-tracking hardware and eye-tracking add-on modules for existing headsets (Appendix 1.1). The second option allows a great business opportunity for eye-tracking companies to focus on the development of a modular product which can be targeted to the wide base of consumers who already own a VR headset.



Qualcomm 845 VRDK Headset with integrated camera-based eye-tracking (www.qualcomm.com)



Camera-based eye-tracking add-on (www.pupil-labs.com)

1.2.3 EOG eye-tracking entering VR

Main advantages of camera systems are that they are highly accurate and do not require contact with the user. On the other hand, EOG is cheaper (infrared cameras are more expensive than electrodes), and less hungry of processing and battery power. In fact, the analysis of EOG signals (facial skin voltages) does not require extremely powerful CPUs and energy even at high frequency; while real-time video analysis algorithms of camera-based eye-trackers are extremely more complex.

These properties make EOG suitable not only for tethered headsets, but also for standalone ones, which are relatively less powerful and are running on compact batteries.

Moreover, recent developments in electrodes technology overcame the biggest limit of EOG (Chapter 3 section 3.5). Namely, dry electrodes are not adhesive but only require contact with the skin to capture signals. This enables an efficient integration of EOG in wearable products.

This was proven by two companies: imec and J!NS developed eyeglasses that integrate dry electrodes for EOG. While J!NS focuses its product on general activity tracking, its limited number of electrodes (three) provides EOG signals that are only able to recognize gaze directions and blinking. On the other hand, imec claims that with a total of five electrodes and a high sample rate (256 samples per second) it is possible to precisely capture eye movements and translate them into gaze positions in the surroundings (the accuracy is not specified).

In a similar way it is recognised that it is possible to integrate electrodes on the VR headset soft mask, which covers the strategic positions of the electrodes that are required for EOG (Chapter 3 section 3.2)

The aforementioned advantageous properties of the EOG, and the fact that its integration in VR is yet unexplored, motivates to explore this topic as graduation project.



imec - Non-commercial product (www.imec-int.com)
J!NS MEME - 370€ (www.jins-meme.com)



1.2.4 Face electrodes VR products

It is relevant to observe that there are two products under development that are integrating dry electrodes on a VR headset mask, but with a different purpose than EOG. Their purpose is instead to capture signals from facial muscles to sense facial expressions.

Their main fields of application are:

- Enhancing virtual avatars with human-like movements in VR social applications
- Detection and treatment of medical conditions of the facial muscles (e.g. facial palsy)
- Measure alertness and attention (from facial expressions) for performance monitoring
- Research on users' reactions to stimuli (behaviour research and marketing)

Emteq

- Add on for unspecified headset
- 8 electrodes
- Not yet on the market



www.emteq.net

Mind Maze

- Add on for unspecified headset
- 8 electrodes
- Not yet on the market
- Mind Maze claims that it can identify facial expressions as including smiling, speaking, winking, blinking and smirking



www.mindmaze.com

1.3 Eye-tracking applications

1.3.1 Summary of eye-tracking general applications

First eye-tracking technologies were developed at the beginning of '900. They were initially exploited by researchers of the visual system to study eye movements during visual scanning and reading, and by doctors as diagnostic tools for the diagnose of oculomotor system pathologies. Also, eye-trackers were also specifically developed for military purposes as input devices for aiming at targets during combat.

Developments in eye-tracking technologies increased the accuracy, lowered costs and enabled its integration in more compact and lighter devices enabling a wider variety of applications.

- Eye-controlled computer interfaces for entertainment, gaming and assistance of disabled people (e.g. pointing with gaze to select and navigate buttons and letters, blinking to click)
- Measure attention, interest and arousal as a tool for human behaviour research in neuroscience and psychology
- Assessment the effectiveness of marketing media to understand what information attracts consumers and influence their decisions
- Human factor studies to understand how humans work and interact with environments, products and digital interfaces.
- Assessment of the performances of highly skilled jobs (e.g. performing surgeries, operating complex machinery, piloting an aircraft) and sports.

1.3.2 Eye-tracking VR applications

Integrating eye-tracking in VR enables to leverage the benefits of both technologies. VR allows to port users into any kind of environment; eye-tracking can give useful insights on the visual stimuli that are presented in VR and enable interactions through gaze. In the following paragraphs the applications of eye-tracking in VR are presented, with a specific section for applications that are not achievable with EOG but only with camera-based eye-tracking.

Foveated rendering / Eye-driven video compression

One specific application of eye-tracking for VR applications is foveated rendering. The name comes from the "fovea" a small region of the eye that enables detailed vision at the center of the field of view. By knowing where users' gaze is pointing at, it is then possible to render only a small central area of the VR 3D scene at a high resolution, while drastically cutting down the complexity of the scene at the periphery of vision. This illusion can be done in a way that is completely invisible to the user.

As the display resolution of VR headsets and the field of view increases, as more headsets are becoming untethered from powerful gaming computers but instead integrate smartphone-like hardware, foveated rendering can greatly contribute to reduce the load of the GPU, improving graphics on lower-powered devices, and dedicating processing resources elsewhere.

Requirement: (4) Measurement of the position of the user's gaze on a surface (VR screens)



Demonstration of foveated rendering (www.getfove.com)

Gaze as an input in VR interfaces and games

Eye-tracking input is likely to be helpful for making VR interfaces faster and more productive, allowing users to select items, press buttons and navigate much more quickly than if they had to move their body or hands to achieve the same (Road to VR, 2018).

Moreover, eye-tracking can facilitate more natural and intuitive interactions in games. For example, it could be helpful to improve the aim of players by correcting the trajectory towards the gaze point.

Requirement: (4) Measurement of the position of the user's gaze on a surface (VR screens)



Demonstration of foveated rendering (www.getfove.com)

Researches on consumer focus and behaviour

In VR, the user can be ported in a controlled virtual environment, where stimuli are presented while keeping track of the participant's gaze, with the purpose of analysing their attention and focus points for scientific research or marketing.

An example is the simulation of a virtual store, where researchers can analyse eye-tracking data to gain insights on product packaging designs, product placements, and the overall layout of the store.

Requirement: (4) Measurement of the position of the user's gaze on a surface (VR screens)



Demonstration of foveated rendering (www.tobii.com)

Complex jobs training

In VR complex and safety-critical work environments can be simulated in order to train workers. Eye-tracking provides insight into how employees react under pressure and make decisions in simulated challenging scenarios or emergency situations with no risks and at lower costs.

Requirement: (4) Measurement of the position of the user's gaze on a surface (VR screens)



Simulation of an aircraft in VR integrated with eye-tracking data (www.tobii.com)

Medical diagnosis and treatments

Eye-tracking in VR enables to collect prolonged eye movements data which can be analysed to diagnose pathologies of the oculomotor and vestibular systems. Moreover, these pathologies can be treated by immersing the patients in a virtual environment where they can perform rehabilitation exercises.

In a similar way, phobias can be treated by exposing patients to a controlled VR environment specific to a treatment protocol, where eye-tracking can provide insights on how specific visual stimuli trigger emotional responses.

Requirements: (1) Identification of the different kinds of eye movements; (2) Identification of the direction of gaze (left, right, top, bottom and combinations of those); (3) Measurement of the angles of eye rotations along three axes around the center of the eyeball

Design and architecture

In VR, products, interfaces and environments, can be tested without the need to physically build the actual prototype or structure. Designers and architects can test a new concept with people all over the world, and receive relevant user experience insights from eye-tracking data.

Requirement: (4) Measurement of the position of the user's gaze on a surface (VR screens)



Eye-tracking heat map on the VR simulation of the interior of car (www.smivision.com)

Enhancing virtual avatars

In social VR content and applications, eye-tracking can enhance avatars with human-like eye movement including gaze direction, blinking, squinting, pupil dilatation.

Requirements: (2) Identification of the direction of gaze (left, right, top, bottom and combinations of those); (3) Measurement of the angles of eye rotations along three axes around the center of the eyeball



Eye-tracking enhanced VR avatar (www.tobii.com)

Pedagogy

Eye-tracking can be used to measure students or employee's engagement with educational/training contents and offer valuable insights into the effective adjustment of their learning process.

Requirement: (4) Measurement of the position of the user's gaze on a surface (VR screens)



Students using VR in class (www.looxidlabs.com)

Camera-based eye-tracking specific applications

User identification / Privacy

Collecting eye-tracking data can arise privacy issues whereas not handled responsibly or hacked. On the other hand, camera-based eye-trackers could increase security as biometric identifier of the iris. This could be also useful for setting up multiple user profiles across a single headset, and removing the need for user authentication.



Fictional demonstration of user identification from eye-tracking data (www.tobii.com)

Headset adjustments

With camera-based eye trackers it would be possible to measure users' Inter Pupillary Distance (IPD) in order to assist them in its regulation, or warn them that their IPD is outside of the supported range.

1.4 Sizing system approaches

1.4.1 One-size-fits-all

One-size-fits-all means that there is only one size of the product. Normally the product is designed around the average of the target population (50th percentile).

This strategy brings advantages in the reductions of costs of development and production of multiple sizes. On the other hand, the product might provide good fit only on a small percentage of users (close to the average).

There are a number of occasions whereas this approach might be preferred.

- The variability of the anthropometric feature is low.
- Good fit is not necessary because the product is tight to the body.
- Good fit is not necessary because the product is used for short time.
- The product is not personally owned but is available in shared or public spaces.

In order to improve the fit of one-sized products, materials that are adaptable (e.g. highly stretchable textiles in clothing) can be used, or the product may include a regulation feature.

One size with regulation system

The second is to include a regulation feature that allows the product to increase or decrease its dimensions. This allows the product to adapt to the variability of the anthropometric feature it needs to fit. Example is the watch: customers can buy a watch only in one size and then can regulate its strap for optimal fit to the wrist.

1.4.2 Multiple sizes

Creating a product in multiple sizes is helpful to better accommodate the anthropometric variability of the target population and, as a result, increase the overall comfort.

A common approach in the design of a sizing system is to use a set of anthropometric measurements (that relate to critical dimensions of the product) to create plots of subjects along each dimension. If the subjects are normally distributed, the distribution is then plotted along an axis scaled to standard deviations. Each standard deviation represents a fixed percentile.

Subsequently, the range of population percentiles between the 5th and the 95th is considered and divided into a specific amount of groups/clusters that will correspond to sizes. Each size will then accommodate the range of anthropometric measurements variability within the relative group.

This approach is commonly used in products that fit relatively close to the body as the whole category of wearables such as clothes, helmets, (affordable) prosthesis.

1.4.3 Custom design

Another strategy in the design of a product is to create a custom design for a specific user. This strategy is preferred for high performance products which require a perfect fit with the user's body and/or that need to achieve high levels of comfort. Costs of development and production increase because skilled personnel have to directly measure or 3D-scan the user and the production is limited to a one-off.

Custom designed products often fall in the categories of luxurious products (e.g. tailored dress), medical devices (e.g. custom prosthesis), and professional sports (e.g. custom shoes for a runner).

1 Context - Summary and conclusions

- The integration of eye-tracking in VR should not lower the level of immersion. Key factors for this project are the comfort of the mask and the non-intrusive integration of the EOG technology.
- Smartphone-based headsets provide too basic VR experiences to benefit from eye-tracking.
- Tethered headsets are suitable to integrate EOG eye-tracking.
- Low requirements of processing power and energy of EOG allow an efficient integration also in standalone headsets.
- Measuring the kind of eye movements and/or their direction allow only few applications
- Most of the applications require the measurement of the position of the user's gaze point on the VR headset screens.
- In VR, even during head and body motions, the position of the screens in front of the users' eyes remains constant. It is then relatively easy to convert angles of eye rotations into point coordinates on the VR headset screens.
- For this project it is more feasible to design an add-on EOG module for an existing headset.
- A sizing system may improve the fit of a VR headset.

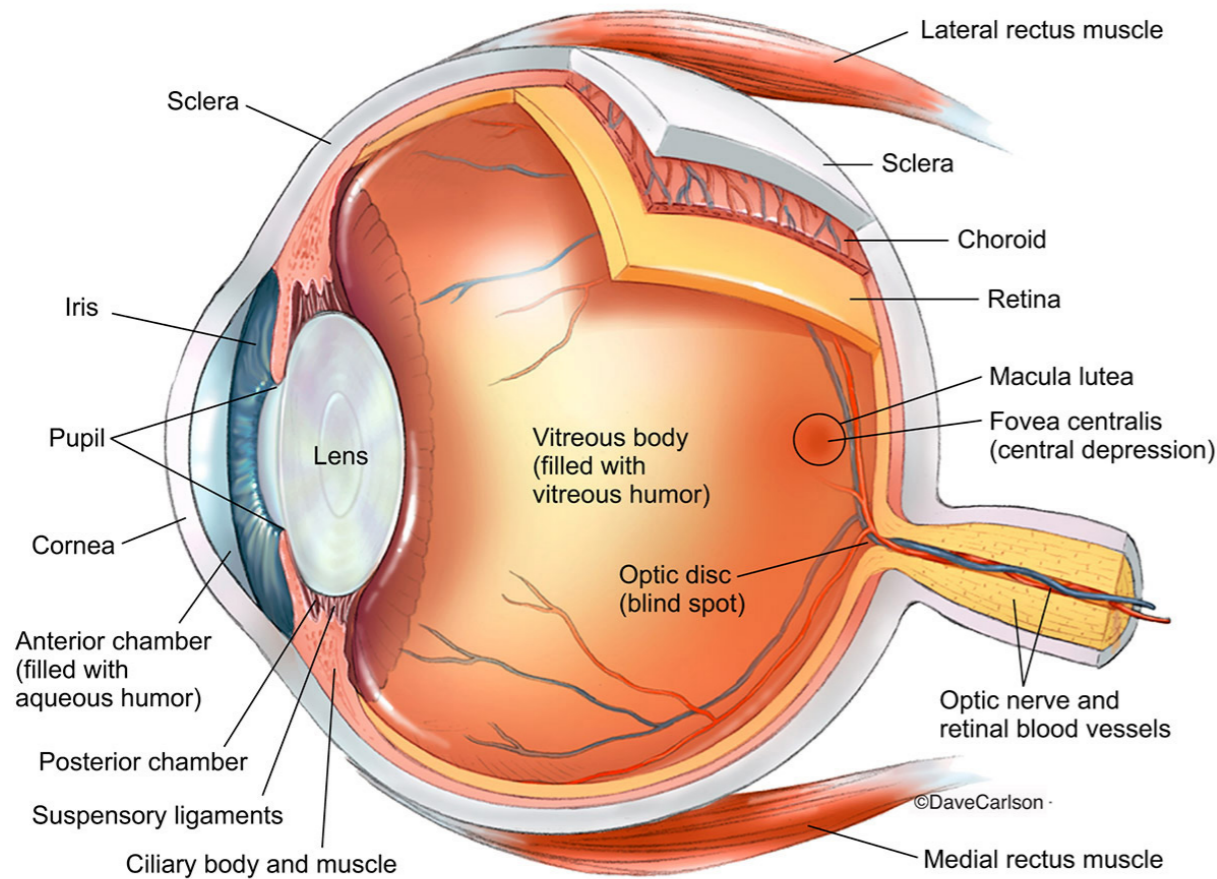
Chapter 2
THE VISUAL SYSTEM

2

2.1 Introduction

The visual system is the part of the central nervous system which gives humans the ability to detect and interpret information from visible light to build a representation of the surroundings,

as well as enabling the formation of several non-visual light responsive functions. The visual system includes the eyes, parts of the brain (primarily the visual cortex), and the connecting pathways.



Right Eye (viewed from above)

(www.carlsonstockart.com)

2.1.1 The eyes

The human eyes react to light and pressure to provide a three-dimensional coloured image.

In short, firstly light enters the eye at the cornea. The iris expands or contracts to let more or less light enter the pupil. The lens refracts and focusses the light rays on the back of the retina. The retina consists of photosensitive cells called photoreceptors (cones and rods) which convert light into electrical neural impulses to be transmitted to the brain across the optic nerve. A small area of the retina called fovea has the highest concentration of photoreceptors and is responsible for high resolution vision at the centre of the field of view, while the rest of the field of view, called peripheral vision, perceives less details and colours but is more sensitive to movements.

A complete description of all the parts of the eyes and their function can be found in the Appendix 2.1 and 2.3.

Eye movements

In order to build an impression of the surroundings, humans perform eye movements to fixate at different parts of the visual scene, in a process called visual scanning. Positional eye movements are rotations of the eye actuated by a combination of muscles attached to the eyeball (extraocular muscles). The function of these rotations is to bring targets of the scene to detailed vision (at the fovea).

Other non-positional eye movements are the blinking of the eyelids and the deformations of the optical elements to regulate the amount of light entering the eye and to focus targets at different distances.

Average dimensions of the eyeball

The eyeball has an approximately spherical shape with the cornea slightly protruding. The eye attains its full size around the age of 13 to an average diameter of 24mm. This dimension varies by only one or two millimetres among adults and is remarkably consistent across different sexes, ages and ethnicities. For this reason, the eye is often approximated to a sphere of 24 mm in diameter.

Complete information on the dimensions of the eye can be found in the Appendix 2.2.

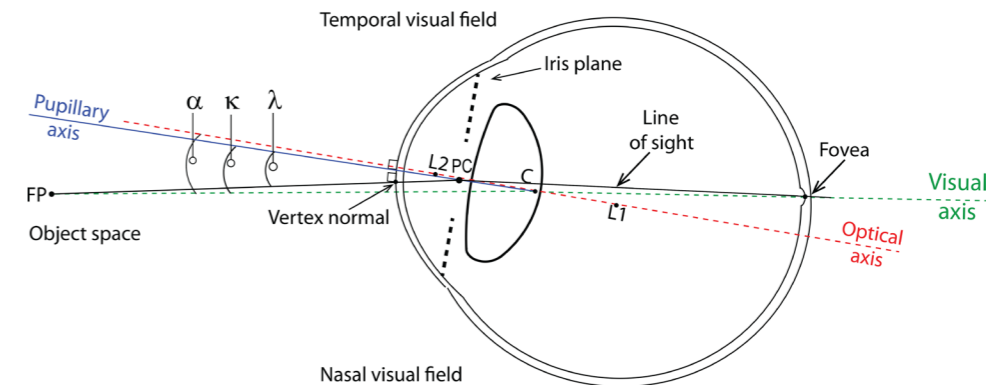
Centres and axes of the eye

Since the parts of the eye are not exactly spherical, each optical element has its own geometrical center, center of curvature and optical axis.

The trackable axes of the eye are not ultimately aligned with the gaze point. In order to derive the gaze point in space it is then necessary to perform corrections that depend on the determination of the angles between the trackable axis and the visual axis, which is the actual path that the light follows to reach the fovea.

Another relevant axis is the Line of Sight (LoS), which is the line connecting the pupil center with the fovea. This is useful to approximate the center of rotation of the eyeball to a point lying on the LoS at 13.5 mm from the cornea (Park & Park, 1933).

A detailed description of the centres and axes of the eye can be found in the Appendix 2.4.



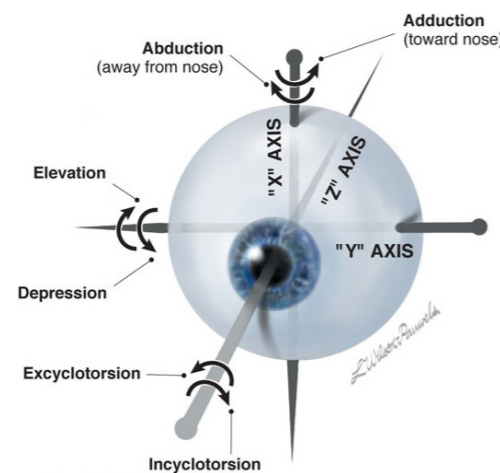
Centres and axes of the eye (Nowakowski et al., 2012)

2.1.2 Rotations of the eye

In order to describe rotations of the eye for eye-tracking purposes, it is possible to model the eye as a sphere (of 24 mm) that rotates with three degrees of freedom, from a standard position, around its center, about the following axes:

- X - Vertical axis: to generate horizontal eye movements (abduction and adduction)
- Y - Horizontal axis: to generate vertical eye movements (elevation and depression)
- Z - Anteroposterior axis (corresponding to the Line of Sight, the axis connecting the pupil center to the fovea): to generate torsional eye movements (excyclotorsion and incyclotorsion)

More detailed information about the standard position, the axes and planes of the eye (Listing's law), and the terminology of the rotations can be found in the Appendix 2.4, 2.5 and 2.6.



(Wilson-Pauwels et al., 2010)

2.2 Positional eye movements

Positional eye movements include voluntary or involuntary rotations of the eyes performed to move fixation point or track visual stimuli. There are four basic types of positional eye movements: saccades, smooth pursuit movements, vergence movements, and vestibulo-ocular movements. The repetitive combination of saccades and smooth movements is defined as nystagmus.

A special type of Rapid Eye Movement (REM) occurs during sleep but will not be discussed because it is not relevant for eye-tracking.

Eye rotations can be:

- Conjugate: the eyes move parallelly (the angular relationship between the right and left eyes are preserved)
- Disconjugate: the eyes move in opposite directions

Positional eye movements are described with the following characteristics:

- Amplitude (deg): the amplitude is the rotation the eye can travel during the movement
- Angular Speed (deg/sec): the rate at which the radius sweeps out a certain angle in one second
- Angular Acceleration/Deceleration (deg/sec²): the rate of change of angular speed
- Delay (msec): the time it takes to initiate the movement after a stimulus is presented
- Duration (msec): the time it takes to perform the movement, it is a function of its amplitude and angular speed

2.2.1 Saccades

Saccadic eye movements are the rapid conjugate movements by which the eyes change fixation from one point to another. They are useful to move the fovea rapidly from one point of interest to another. Saccades commonly occur during the scanning of a visual scene or during reading (from word to word).

Saccades are described as ballistic. Once the movement has started its trajectory and the speed cannot be updated with new information (the end point of a saccade cannot be changed when the eye is already moving). According to Malmivuo & Plonsey (1995), saccades usually undershoot the target and requires another small saccade to reach it. Overshooting is common only for small saccades under 2 deg.

During a saccade, due to the fast movement, the image on the retina is of extremely poor quality and information intake thus happens mostly during the fixation period.

Amplitude

The amplitude of saccadic eye movements is in the range of 1 to 40 deg vertically and up to 90 deg horizontally. Typical saccades are 20 deg in amplitude. Usually, when a target exceeds 30 deg, head motion is involved.

Angular speed

The peak velocity varies proportionally to the amplitude of the saccade and is not controllable: the eyes move as fast as they are able. A 10 deg amplitude is associated with a velocity of 300 deg/sec, 20 deg with 400 deg/sec, 30 deg with 500 deg/sec, until a maximum of 900 deg/sec at 60 deg.

Angular acceleration/deceleration

Very high acceleration and deceleration, up to 40,000 deg/sec².

When following a target moving in stepwise jumps, the eyes normally accelerate rapidly, reaching the maximum velocity about midway to the target. When making large saccades (>25 deg), the eyes reach the maximum velocity earlier, and then have a prolonged deceleration (Malmivuo & Plonsey, 1995).

Delay

Saccades take between 100 to 300 msec to initiate, typically 200 msec. Small saccades under 2 deg have longer latencies up to 400 msec (Wyman and Steinman, 1973).

Duration

The duration of a saccade varies from 20 to 200 msec, approximately linearly correlated to its amplitude (Malmivuo & Plonsey, 1995). Typical saccades during visual scanning are of are of 80 msec, while during reading are between 20 to 40 msec.

Other facts

Rashbass (1961) reported the absence of saccadic responses to targets appearing closer to the fovea than about 0.25 deg, this area is called "foveal dead zone".

Saccades can be also made in the dark, or with the eye closed.

Saccades do not always have simple linear trajectories.

2.2.2 Smooth movements

Smooth movements are slow rotations of the eye that enable to maintain fixation on a moving target (pursuit) or during body and/or head movements (compensatory / Vestibulo-Ocular Reflex).

Pursuit movements

Pursuit, or slow-tracking movements are conjugate eye movements used to follow moving visual targets.

Smooth pursuit movements are voluntary but can be generated only in presence of a moving object (Robinson, 1965; Westheimer, 1954). Therefore, it is impossible to generate smooth pursuit eye movements in a stationary visual scene, in the dark and with the eyes closed.

Angular speed

Speed is most often in the range of 1 to 30 deg/sec (Malmivuo & Plonsey, 1995). When a target moves at higher speeds, the eyes start to perform saccades in order to follow the it.

Compensatory movements - Vestibulo-Ocular Reflex (VOR)

Compensatory eye movements or Vestibular-Ocular Reflexes (VOR) are smooth movements that compensate for motion of the body and/or the head.

For example, when fixating a target, if the body and/or the head is turned, the VOR causes the eye to move in the opposite direction with same speed in order to keep the fixation point stable on the same target.

They are attributable to stimulation of the semicircular-canal of the ears and to neck proprioception.

Angular speed

The speed of the eye equals the speed of head or body motion.

2.2.3 Vergence movements

Vergences are equal but horizontally opposite (disconjugate) movements of the eyes. They are performed to obtain or maintain vision on extremely near objects (nearer than 10 cm from eyes). For this reason, vergences are quite uncommon; most of the time eyes are performing conjugate eye movements. Indeed, usually eyes are parallel, but in presence of extremely close objects, the eyes cross horizontally: the eyes rotate towards each other (convergence). When moving back to a far target, the eyes rotate away from each other (divergence).

Vertical disconjugate eye movements are not naturally possible without the presence of a disorder of the oculomotor system

Vergence movements are closely connected to depth perception and accommodation of the eye (change of focal distance) in an automatic process known as the accommodation-convergence reflex.

Amplitude

Vergences have amplitudes in a range of 15 deg.

Angular speed

Vergence movements are slow and smooth, and reach maximum speed of 10 deg/sec.

2.2.4 Miniature movements

When there is absolutely no motion of the eyes, images fade and disappear (perceptual fading). For this reason, even during fixation, the eyes are not perfectly still. Involuntary miniature or fixation movements include three small (less than 1 deg) motions: tremor, drift and microsaccades or flicks.

Tremor

During fixation there is a high-frequency tremor in the range of 30 to 150 Hz. Its speed is related to its frequency. Typical tremor of 70 Hz has a speed of around 0.01 deg/sec.

Drift

Drift movements are slow random motions of the eye away from a fixation point. They are small, occurring within the foveal dead zone (0.25 deg around the center of the fovea) with a speed of around 0.1 deg/sec

Microsaccades / Flicks

Microsaccades or flicks, are small rapid eye movements which correct the other involuntary miniature movements. They occur at intervals as little as 30 msec.

2.2.5 Nystagmus

Nystagmus is a combination of involuntary movements of the eyes characterized by the repetition of a slow phase (smooth pursuit), and a fast phase (saccadic jump).

The minimum time between fast phases is approximately 0.2 sec, resulting in a maximum frequency of approximately 5 Hz. The amplitude of nystagmus generally varies from 1 to 10 deg.

Optokinetic nystagmus

Optokinetic nystagmus, also known as "train nystagmus," is induced by looking at a moving visual field containing moving patterns (e.g. looking outside of the window of a running train).

Vestibular nystagmus

Vestibular nystagmus is attributable to stimulation of the vestibular system during rotation of the head.

Nystagmus can also occur when the vestibular system is being stimulated by other means of head motion, for example with changes in temperature (caloric nystagmus) or by diseases of the vestibular system.

2.3 Non-positional eye movements

Other movements refer to non-positional aspects of the eye.

2.3.1 Adaptation

Adaptation is the ability of the eyes to adjust to various levels of light. An automatic Pupillary Light Reflex (PLR) contracts or expands the iris in order to let more or less light enter the pupil and reach the retina.

The adaptation process takes approximately 20 to 30 minutes to adapt from bright sunlight to complete darkness. However, it takes only five minutes to adapt from darkness to bright sunlight.

2.3.2 Accommodation

Accommodation is the process by which the lens changes its focal power to focus objects at various distances. Accommodation is usually an automatic process part of the accommodation-vergence reflex, but it can also be consciously controlled.

The focal power of the lens relates to its shape and curvature, which is controlled by the ciliary muscles. When the ciliary muscles contract, the lens thickens (becomes more spherical), resulting in higher refractive power, allowing to focus objects at short distances. When the ciliary muscles relax, the lens flattens and is able to focus objects at greater distances.

The eyes can change focus from distance (infinity) to as near as 6.5 cm from the face. This process can occur in as little as 350 milliseconds.

2.3.3 Blinking

Blinking is the automatic or voluntary rapid closing of the eyelid. The main functions are to maintain the eye lubricated by spreading tears across and remove irritants from the surface of the eye.

Blink speed and rate can be affected by elements such as level of attention, level of fatigue, eye injury, medication, drugs, and diseases. For this reason, eye-trackers may monitor the blinking rate.

2 The visual system - Summary and conclusions

- Only a small central area which corresponds to the fovea is perceived at high resolution. The center of this area is the gaze point. The periphery of the field of view is perceived at lower resolution but is more sensitive to movements.
- For eye-tracking purposes it is possible to model the eye as a sphere rotating around its center. However, misalignments between trackable axes of the eyes and the actual visual axis must be accounted and corrected via calibration.
- Torsional eye rotations are not voluntary and are not interesting to track.
- The most common eye movements are saccades. They are extremely rapid (up to 900 deg/sec) thus eye-trackers must operate at high frequencies to be able to track these movements.
- Disconjugate vertical eye rotations are naturally not possible. Disconjugate horizontal eye rotations are not common (because happen when objects are placed as near as 10 cm from the eyes) and not possible in VR because the headset screens are virtually placed far (between 1 and 3 metres) by the optics.
- Blinking is interesting to track because it can enable applications as measuring the level of attention, tiredness and diagnosis of diseases.

3

Chapter 3
ELECTROOCULOGRAPHY (EOG)

3.1 ElectroOculoGraphy (EOG)

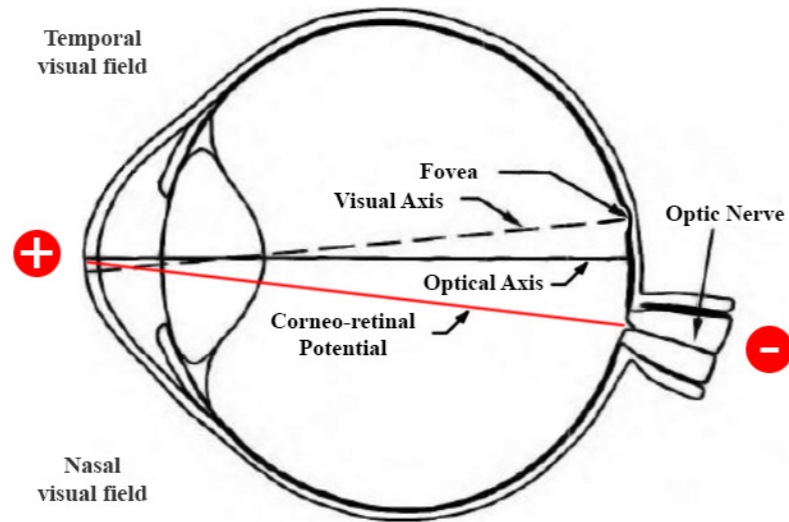
3.1.1 Introduction

Emil du Bois-Reymond (1848) observed that the cornea of the eye is electrically positive relative to the back of the eye.

In 1922, Schott discovered that by placing electrodes on the skin in the region of the eyes, it was possible to record electrical activity which changed in synchrony with movements of the eyes.

It was initially believed that these signals reflected the action of the extraocular muscles. However, it is now agreed that the signals are generated by the potential field which exists between the cornea and the retina.

When the eyes move the potential field rotates accordingly. Signals that are a measure of the rotations can be obtained with the ElectroOculoGraphy (EOG) technique by placing electrodes on the skin around the eyes. The recorded signal is called electro-oculogram (EOG).



Corneo-retinal potential and axes of the eye in the horizontal section (Shkoukani & Abusaimh, 2012)

3.1.2 Corneo-retinal potential

The collective activity of the retina generates a potential field in the surrounding volume of the eye. This potential field, called corneo-retinal potential behaves as a dipole oriented:

- From the retina (negative) approximately at the optic disk, 15 deg displaced from the macula (Young & Sheena, 1975)
- To the center of the cornea (positive)

This means that the electric dipole is not aligned with any axes of the eye and especially it is not aligned with the visual axis (the path that

the light follows from the fixation point to the fovea). A correction angle and/or a calibration procedure is helpful in deriving the gaze point in space. The magnitude of this potential can be measured at the cornea with a technique called ElectroRetinoGraphy (ERG) with the use of electrodes embedded in a corneal contact lens. The obtained values slowly vary between 0.4 and 1 mV (Malmivuo & Plonsey, 1995), mainly accordingly to the level of adaptation of the eyes to the lighting conditions of the surroundings.

3.1.3 ElectroOculoGraphy working principle

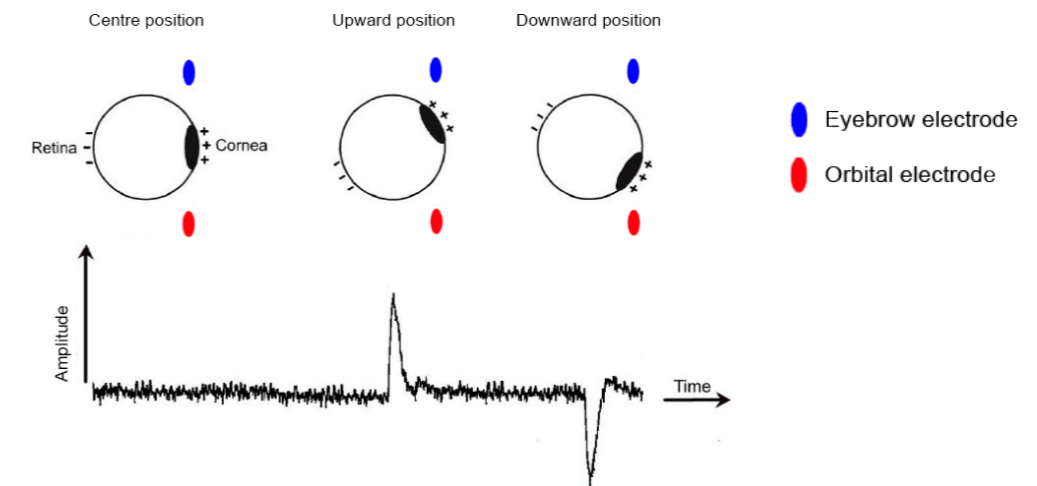
When the eye rotates, the dipole vector rotates accordingly, causing a change in potential in the surrounding tissues.

This signal can be captured by comparing a reference input (ground) with the input of an electrode placed in the vicinity of the eye. The signal becomes more positive when the eye rotates towards the electrode and less positive (negative) when it rotates in the opposite direction (Heide et al., 1999).

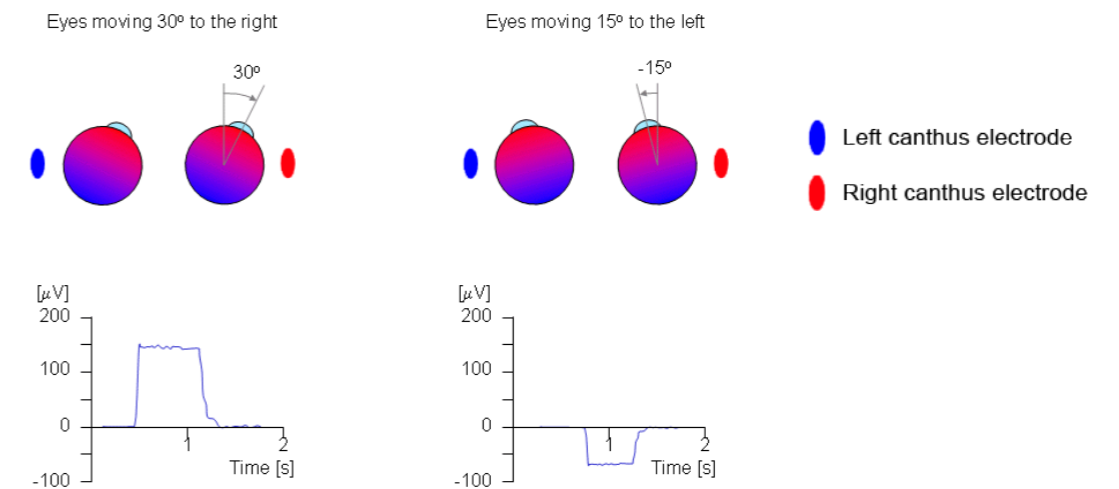
Another method is to use a ground and two electrodes as differential inputs. The differential signal is the difference between the signals of the two electrodes, with the ground useful to

stabilize the signal. According to Krupiński & Mazurek (2012) differential signalling is preferred for EOG because of better signal-to-noise ratio. A movement of the eye in a certain direction results in a potential difference: the electrode in the direction of the movement becomes more positive relative to the other electrode.

Signals that are a measure of the horizontal, vertical and torsional components of the eye rotations are sensed with electrodes placed in strategic positions of the face. While the ground is placed in positions where there is low or none muscles activity (Malmivuo & Plonsey, 1995): on the middle of the forehead, or on the earlobe.



An illustration of the EOG signal generated by vertical eye rotations (Abo-Zahhad et al., 2015)



An illustration of the EOG signal generated by horizontal eye rotations (Malmivuo & Plonsey, 1995)

3.2 Electrodes configurations

The properties of the EOG change depending on the quantity and placement of electrodes. Different configurations are used for different applications. A configuration with a higher number of electrodes is the most accurate and is the most diffused for medical applications. However, a configuration with a reduced number of electrodes may be preferred for applications where the touching of the human face must be reduced. A configuration is defined by choosing:

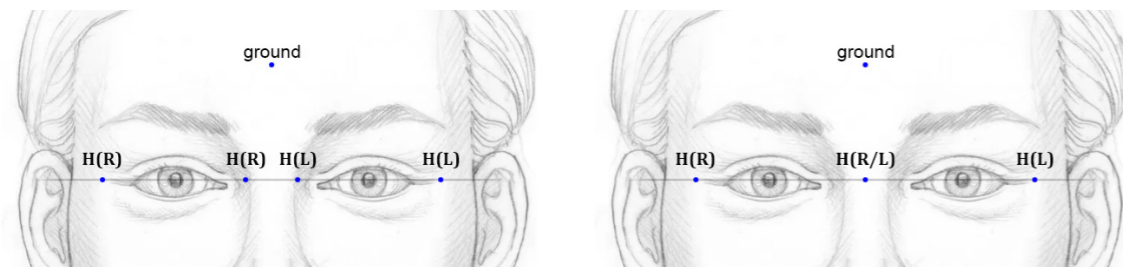
- One of the three horizontal component configurations
- If to measure the vertical component on one or both eyes
- Placement of the ground

3.2.1 Horizontal component

The horizontal component of eye rotations can be measured with electrodes in the following positions:

- Medial electrode: between the eye and the bridge of the nose (medial).
- Lateral electrode: at the outer canthi (the bone on the side of the eye)

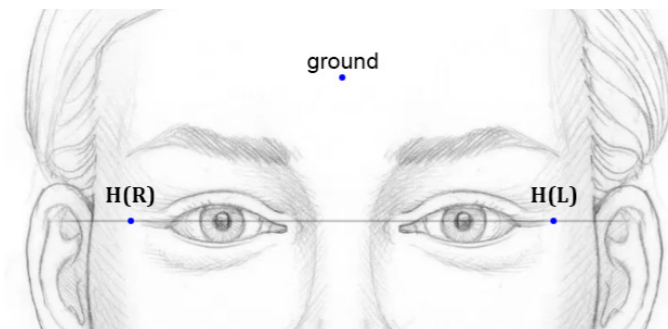
For conjugate and disconjugate (vergences) horizontal eye rotations, each eye must be measured individually. Two pairs of electrodes are used for each eye (picture below-left). According to Young & Sheena (1975), the two medial electrodes can also be reduced to a common one for both eyes, placed over the bridge of the nose (picture below-right)



Two medial and two lateral electrodes allow to measure conjugate and disconjugate horizontal eye rotations

The two medial electrodes may be reduced to a common one

Since disconjugate horizontal movements are not common (Chapter 2 paragraph 2.2.3), for many applications it is not necessary to measure disconjugate eye rotations. In this case, the two lateral electrodes are sufficient.

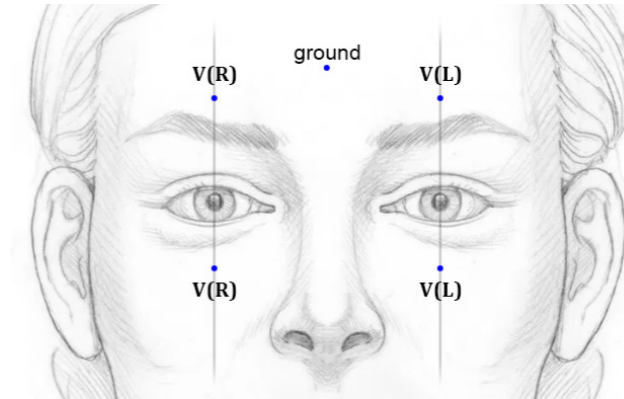


Two lateral electrodes allow the measurement of conjugate horizontal eye rotations

3.2.2 Vertical component

The vertical component of eye rotations can be measured by placing the electrodes on an imaginary para-sagittal plane passing by the pupil center in the following positions:

- Top electrodes: over the eyebrows
- Bottom electrodes: on the lower orbit



The signals of the vertical component are easily contaminated by face muscle artefacts: facial expressions (e.g. smiling), talking and especially blinking of the eyelids (paragraph 3.3.2)

Since disconjugate vertical eye movements (e.g. one eye looking up and one eye looking down) are naturally not possible, it is sufficient to perform the measurement at either one of the eyes. However, measuring both eyes and averaging the signal is helpful in improving the accuracy and reduce the negative effects of artefacts.

3.2.3 Torsional component

The torsional component cannot be directly measured by dedicated electrodes but it may be estimated by signal analysis: since the corneo-retinal dipole is slightly not aligned with the axes of the eye, any torsional eye rotation introduces a slight potential change in the horizontal and vertical components signals. However, this method is not reliable, and torsional rotations are often mistaken for other movements. For this reason, this measurement is often treated as artefact and filtered out by software or through calibration.

3.2.4 Ground placement

The torsional component cannot be directly measured by dedicated electrodes but it may be estimated by signal analysis: since the corneo-retinal dipole is slightly not aligned with the axes of the eye, any torsional eye rotation introduces a slight potential change in the horizontal and vertical components signals. However, this method is not reliable, and torsional rotations are often mistaken for other movements. For this reason, this measurement is often treated as artefact and filtered out by software or through calibration.

3.3 EOG signals

3.3.1 Amplitude of the signals

With the eye at primary/rest position (see Appendix 2a.6) the pair of electrodes are at the same potential and the signal is stable at a certain level. A movement of the eye in a certain direction results in a potential difference where the electrode in the direction of the movement becomes positive relative to the other.

The amplitude of the potential difference varies proportionally to the angle of rotation of the eye. The measured signals are small, in the range of 15 to 200 microVolts (μV), with nominal sensitivities of the order of 5-20 $\mu\text{V}/\text{deg}$ (Shackel, 1967) which allows a spatial resolution between 1 and 2 deg (Malmivuo & Plonsey, 1995).

Non-linearity

According to Young & Sheena (1975), theoretically the potential difference varies as the sine of the angle of rotation. In reality, linearity becomes progressively worse at angles greater than 30 deg, especially in the vertical (Young & Sheena, 1975).

Conducting tissues

The non-homogeneous nature of the conducting medium (the skin around the eyes) causes wide departure from the theoretical values (Young & Sheena, 1975). Values differ according to the metabolic state of the tissues (pO₂, pCO₂, and temperature).

The amplitude of the corneo-retinal potential

The corneo-retinal potential (measured with the ElectroRetinoGraphy technique) varies between 0.4 and 1 mV. Its value varies mainly according to the level of the adaptation of the eyes to the environmental lighting conditions, decreasing up to 50% following steady periods in the dark (Henn, 1993).

According to Heide et al. (1999) a stable corneo-retinal potential can be achieved after 15 minutes of adaptation of the eyes to the lighting conditions.

The corneo-retinal potential also changes slightly according to the state of alertness.

3.3.2 Artefacts

Artefacts are elements that appear in an experimental result, but are not actually characteristic of the actual entity being studied. In physiological signal acquisition, they are introduced from extraneous sources such as electrical or mechanical interference, or incorrect experimental protocol caused by the experimenter or the subject.

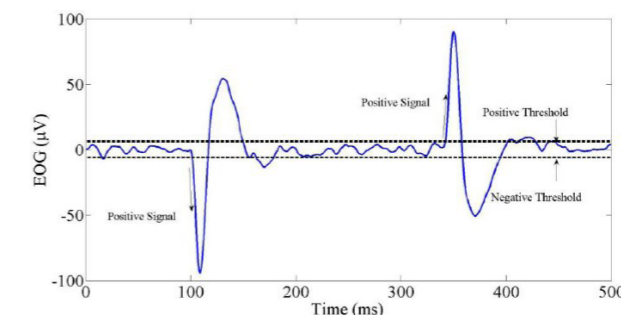
Software pattern recognition techniques can classify artefacts: some are considered noise, while others can be recognized as discreet events. The main sources of EOG artefacts are explained in the following paragraphs.

Eyes at primary/rest position

When the eyes are in the primary/rest position the potential difference between the two electrodes should be zero, but the signal might be shifted from zero upwards (positively) or downwards (negatively). A calibration procedure is required in order to shift the potential difference to zero.

Miniature and fixation movements

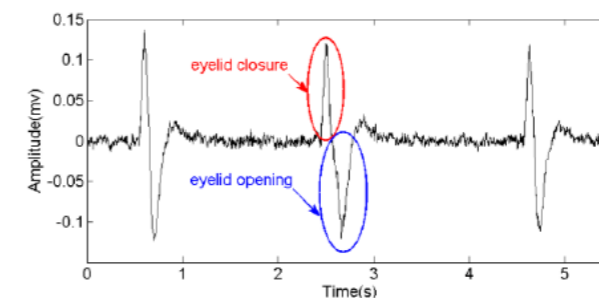
Even at a fixed eye position, the EOG is far not exactly constant. Miniature/fixation movements exist and cause small fluctuation in the signal. The software can filter out this information by setting a positive and negative threshold between which the signal is not recognized as an eye movement.



Example of miniature and fixation movements with amplitudes close to the zero (Rusydi et al., 2014)

Muscle artefacts and blinking

Main source of EOG artefacts are caused by the presence of potentials of facial muscles. In particular, movements of the eyelids, commonly blinks, generate artefacts in the shape of tall signal spikes, especially in the vertical component signal.



Example of blinking artefacts (Abo-Zahhad et al., 2015)

Torsional rotations

Any torsional rotation of the eye introduces a slight potential change which can be mistaken for others eyes movements.

Bad contact between electrodes and skin

A bad contact between electrodes and skin is a source of signal instability (Augustyniak, 2001)

Skin resistance

The signal may drift as a result of changes in skin resistance, commonly from sweating (Heide et al., 1999). The resistance can be reduced by using adhesive electrodes and/or an electrogel.

Electrical interferences

The main sources of electrical interferences are power line interferences caused by external electrical and electronic devices, especially incandescent light sources. Filtering techniques and appropriate shielded wiring are used for the reduction of power lines interferences.

Other biopotentials

Surface electrodes pick up other undesired biopotentials, such as the ECG, the EEG from frontal brain regions, and the EMG from the temporal and the orbicularis oculi muscles (eyelids muscles).

3.4 Calibration

Eye rotations are measured in degrees, however the potential differences that are a measure of eye rotations are recorded in volts. In order to determine the relationship between the amplitude of the measured voltage and the angle of rotation of the eyes, it is necessary to perform a calibration.

The calibration is performed by having the subject look at different points placed on the horizontal and vertical meridians of the visual field at known angles and distances and by recording the relative voltages. It is also important that the subject does not move their head during this process.

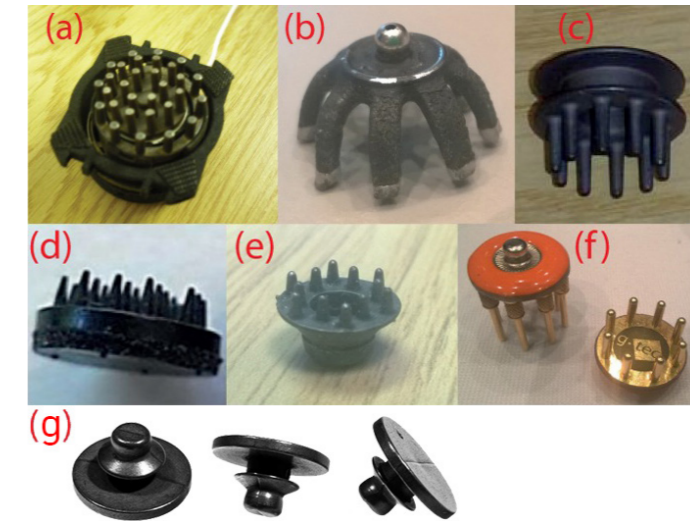
A few extreme orientations of eyes are recorded and the intermediate orientations are interpolated (Krupiński & Mazurek, 2012) to obtain a calibration curve, which can be used to convert voltages to degrees.

The calibration procedure might also include the subject to look straight ahead to set the zero level, and to track a point which moves slowly in known paths with smooth pursuit movements.

3.5 Electrodes

Traditionally, EOG makes use of adhesive electrodes. They are made out of a metal plate covered by electrogel. For medical purposes, disposable adhesive electrodes are attached by doctors to the subject's face and then thrown after the visit.

For applications of EOG where a repetitive use is required (as for the VR mask envisioned in this graduation project) the alternative are dry electrodes. They do not require to be stuck onto the skin to provide signal. On the other hand, they tend to catch more noise.



Example of dry electrodes on the market (Krachunov & Casson, 2016)

Dry electrodes technology is currently mostly developing around EEG devices, but seem also suitable for EOG. For this reason, EEG dry electrodes have indentations that are useful to better reach the user's scalp through hair (above picture, electrodes from a to f). On the contrary, a dry electrode with a flat shape is more suitable for EOG (above picture electrode g).

Materials of dry electrodes

Without the conductive gel present in an adhesive electrode, the material on surface dominates the performance in terms of noise and contact impedance (Krachunov & Casson, 2016). For this reason, dry electrodes are currently made out of a relatively cheap metal (usually brass, tin, nickel) or even plastic, plated by silver or gold.

The silver coating is usually converted to silver-chloride (Ag-Cl) with a chemical process. Silver-chloride is less sensitive to polarization and to changes in skin resistance (Krupiński & Mazurek, 2012).

Gold plated electrodes are also in use but may pick up more disturbance from electromagnetic fields (Krupiński & Mazurek, 2012).

3D-printed dry electrodes

Research from Krachunov & Casson (2016) demonstrates that dry electrodes can be also built by using low cost desktop 3D printers. This allows quick and inexpensive electrode manufacturing and opens the possibility of creating electrodes that are customized for each individual user. The research compares dry electrodes made out of conductive plastics (carbon based) with others made out of standard plastic coated with different metals.

Results of their study show that a dry electrode made out of standard plastic plated with silver-chloride holds the best performance.

3.6 EOG electronics

EOG electronic instrumentation mainly consists of:

- Instrumentation Amplifier (IA): generates a voltage that is proportional to the voltage of the inputs
- Operational Amplifier (OP Amp): adds additional gain
- Low-Pass Filter: reduces noise (mainly power line 50 Hz noise)
- High-Pass Filter: reduces the effect of motion artefacts

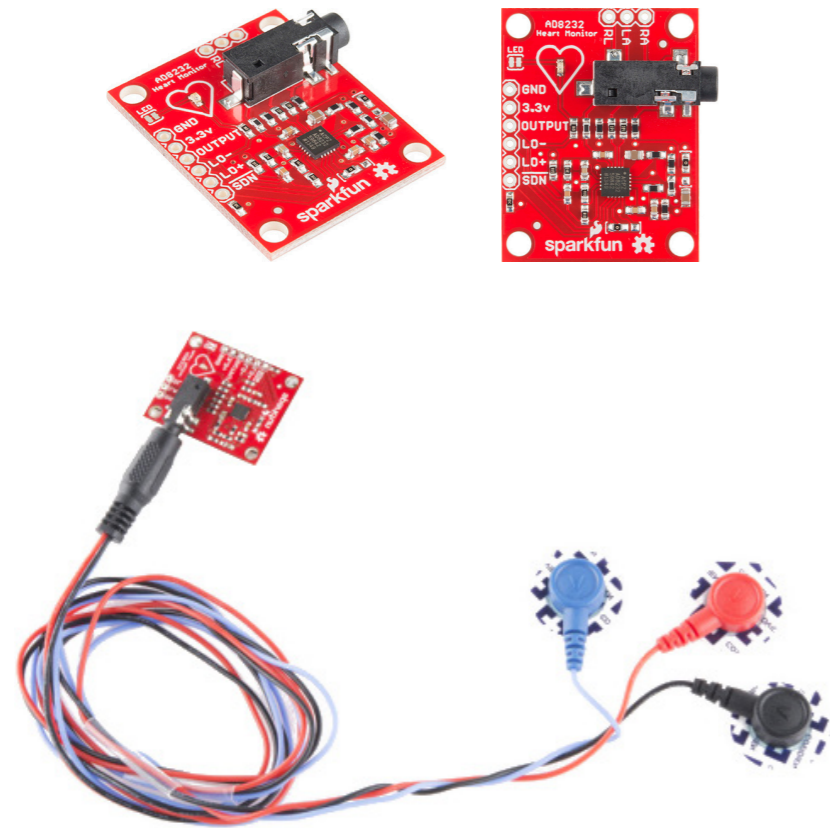
Online research shows that there is no electronic prototyping board specific for EOG. On the other hand, there are available several prototyping boards for EMG, ECG and EEG which also have the purpose of capturing, amplifying and recording biopotentials (body voltages) with electrodes.

Among all, ECG boards are the most suitable to be adapted for EOG because of similar amplification and because they make use of differential signalling.

Sparkfun AD8232

The Sparkfun AD8232 Arduino-compatible board for EMG resulted to be the best option for this project. It is designed to extract, amplify, and filter heart biopotential signals. It connects to two leads and one ground electrodes. It includes all the components in the previous list and also:

- Leads-off detector: puts the board in standby if the leads are not connected in order to save energy
- Fast restore circuit: brings back the signal shortly after leads are reconnected



Sparkfun AD8232 Heart Rate Monitor (www.sparkfun.com)

3 ElectroOculoGraphy (EOG) - Summary and conclusions

- The vector of the corneo-retinal potential dipole is not aligned with the visual axis. This must be accounted and corrected via calibration.
- The value of the corneo-retinal potential varies according to the level of adaptation to lighting conditions of the surroundings. Adaptation takes 20 to 30 minutes from light to dark and only 5 minutes from dark to light. However, in VR the user is constantly exposed to a lid-up screen.
- The properties of the EOG depend on the quantity and placement of the electrodes.
- The electrodes are placed on imaginary planes that cross horizontally and vertically the centres of rotations of the eyes.
- Two electrodes placed on the canthi are sufficient for measuring conjugate horizontal eye rotations.
- Two electrodes placed over the eyebrow and on the lower orbital bone can measure vertical eye rotations. Since disconjugate vertical eye movements are naturally not possible, performing the measurement on both eyes may be useful to lower the noise and increase accuracy.
- The biggest source of artefacts is the activity of other facial muscles.
- The torsional component of eye rotation is barely possible to measure with EOG and is rather filtered out.
- A calibration procedure is useful to map EOG signals to angles of eye rotations, and to correct misalignments between trackable factors and the actual visual axis.
- Single-use-adhesive electrodes cannot be used for the integration of EOG in VR. Dry electrodes are most suitable. The best material for dry electrodes performances is silver coated by silver-chloride.
- The Sparkfun AD8232 can be used for EOG measurements but needs modifications on its settings.

4

Chapter 4
**VR HEADSET
PRODUCT ANALYSIS**

4.1 HTC Vive product analysis

4.1.1 Choice of headset

Most diffused headsets on the market are HTC Vive and the Oculus Rift, both tethered. The choice fell on the HTC Vive because it was immediately available at the faculty.

In any case, this choice has small consequences on the design process and end result. In fact, the

anthropometric analysis and its results presented in Chapter 6 are independent from it. Moreover, regarding the mask and electronics design, most of the reasoning behind it can be extended to any other VR headset, with the only exceptions of differences in the mask-case attachment and power/data connection.

4.1.2 HTC Vive taxonomy of parts

The HTC Vive, and VR headsets in general, mainly consist of the following three main parts:

- Plastic case/housing: contains the electronic components and the optics (the lenses)
- Harness system: fits the headset on the user's head
- Mask: the soft part in contact with the user's face

The case and its contained parts are of no relevant influence for the graduation project.

On the other hand, HTC Vive, and VR headsets in general, are targeted to a vast variety of people of both sexes, different ages and nationalities, in static situations and during rapid movements of the head and the body. For these reasons the harness system and the mask piece are fundamental to:

- Accommodate the different head and face shapes
- Ensure comfort in the short and long term of usage
- Prevent slippage of the headset from the ideal position



HTC Vive 2016 (www.vive.com)

4.1.3 The harness system

The purpose of the harness system is to secure the headset on the user's head. The harness system can be regulated to make the headset tighter or looser to accommodate different head dimensions.

The regulation of harness system has a direct impact on the fit of the mask on the user's face. Tightening up the harness system has an effect on the mask, which deforms and adapts its shape to the user's face. An increased pressure prevents slippage of the headset from the ideal position but may cause discomfort in the long term.

Standard harness system

The HTC Vive standard harness system consists of multiple plastic parts secured to the headset by textile straps closed with velcro. The harness system is manually regulated by the user by closing the straps at a certain length.

Deluxe harness system

HTC also sells a harness system replacement (120€) which is fully made out of solid parts (plastic and metal) and allows the user to perform regulations in an easier and faster way, just by rotating a wheel placed at its back. Headphones are also mounted on it.



Standard and Deluxe HTC Vive harness systems (www.vive.com)

Other kinds of harness systems

Some headsets may have a simpler harness system consisting in one or two velcro straps. This solution is cheaper but does not achieve the same level of fit and comfort.



Samsung Gear VR 2015 (www.samsung.com)



Destek VR (www.destekgear.com)

4.1.4 The mask

The HTC Vive comes in the box with one standard mask. However, on HTC website it is possible to buy two extra sizes of the mask, narrow and wide.

Due to the unavailability of the narrow and wide masks sizes, only the standard size was analysed in detail. Nevertheless, it is likely that the sizing system designed by HTC Vive accounts only the width of the face as critical and representative of the variability of the human shape.

Finally, on the sides of the mask, it is possible to see an indented section. Its function is to fit the side bars of prescription glasses. It is normally possible to correct myopia by regulations of the distance between the user's eyes and the screens. However, this regulation is possible until a certain extent, after which prescription glasses are still required.



HTC Vive 2016 and mask replacements (www.vive.com)

Materials

The HTC Vive masks are made out of polymeric (plastic) foam. Some third-party masks are sometimes upholstered with leather or other

soft textiles. However, no detailed information is given by any producer about the foam or the cover materials.



Foam mask



Foam mask upholstered with leather

Velcro attachment system

The mask is attached to the support by velcro making it easily removable and replaceable. This is done for the following reasons:

- Replacing with a different size
- Replacing with a new mask: the mask is likely to get worn from use in the long term
- Using a personal mask: users may prefer to own a personal mask when sharing the headset with others for hygienic reasons (the mask usually gets humid with facial sweat)



Velcro attachment system (www.vive.com)

4.1.5 Connections

The HTC Vive has multiple connections: a power supply connector, an HDMI and two USB 3 (input/output and power). All the ports are already in use except one USB, which can be used to power and communicate with an eye-tracking module.



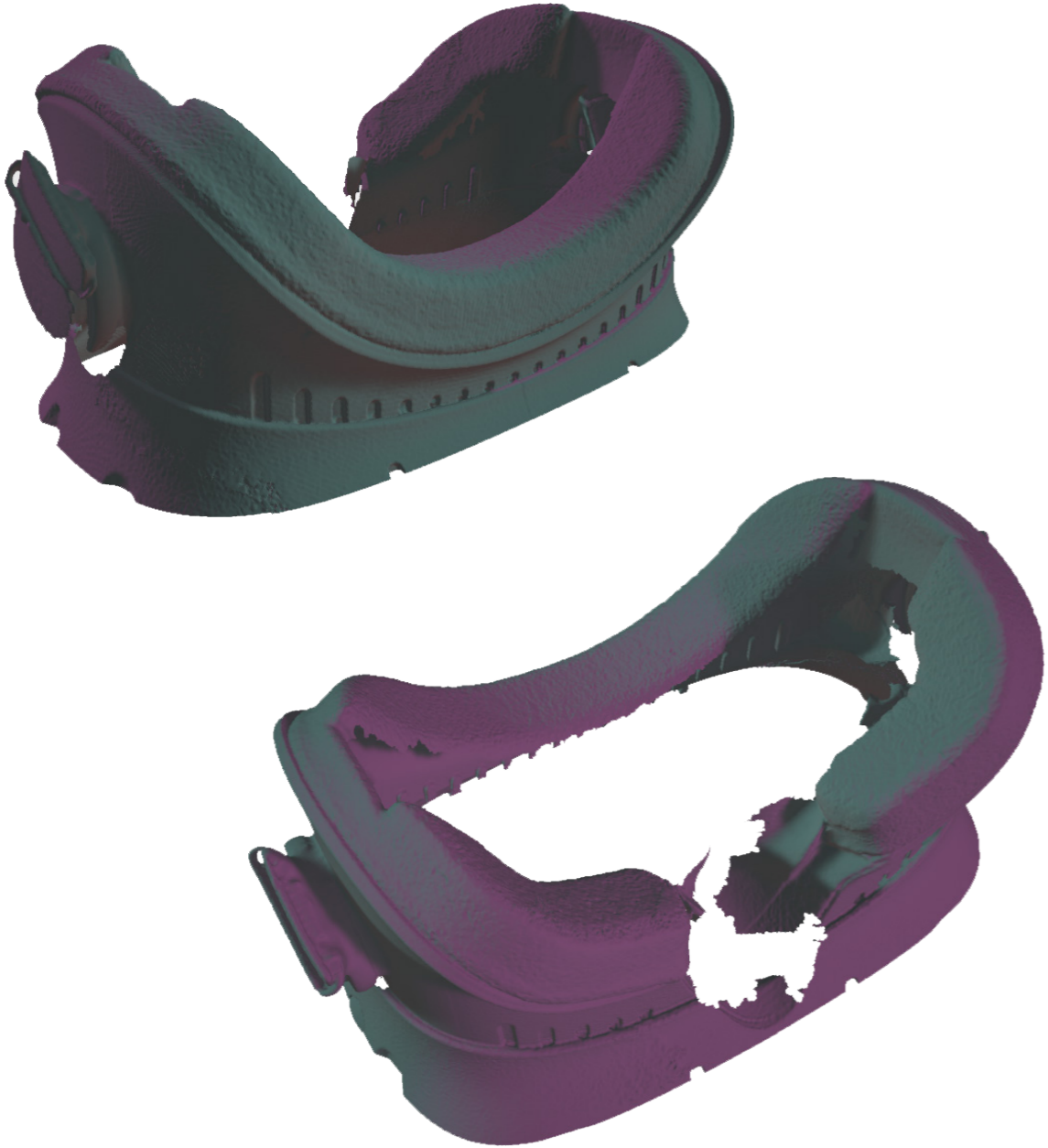
Top view of uncovered HTC Vive showing the connection ports (www.vive.com)

4.2 3D-scanning and reverse-engineering of the mask

Having a three-dimensional representation of the shape of the mask and its supporting part is fundamental for the design of an eye-tracking mask replacement. For this purpose, the HTC Vive was 3D scanned with and without the standard mask. The 3D scanners used were the Artec Spider and Artec Eva (different resolutions). The multiple scans were combined and cleaned thanks to several software: Artec Studio (www.artec3d.com), MeshLab (www.meshlab.net), Autodesk Meshmixer (www.meshmixer.com).



Artec Spider and Eva 3D scanners
(www.artec3d.com)

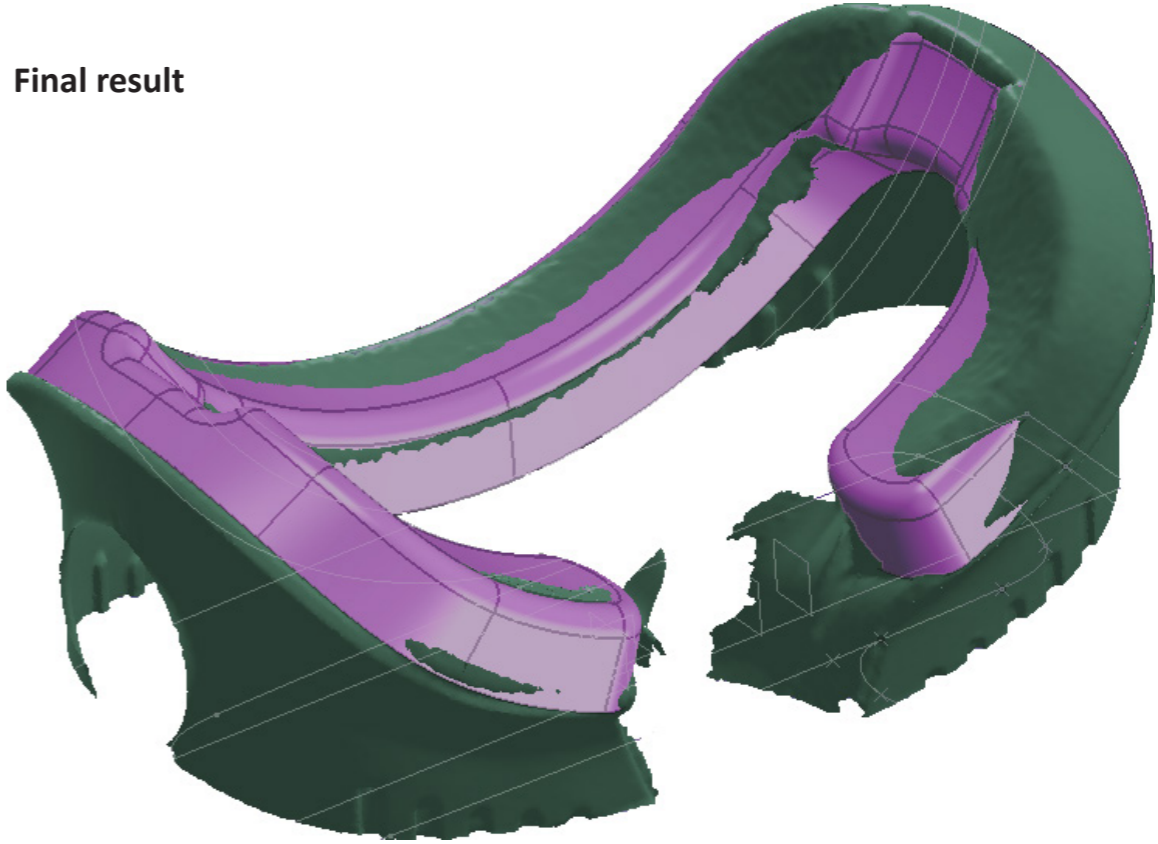


The 3D scan files of the mask and its support were then reverse-engineered. The process consists of reconstructing the surfaces of the 3D scan in a CAD software, Catia V5. To ensure the highest accuracy, the process also included using manual measurements taken with a caliper as a reference. These measurements were performed on the headset and also on the mask while it was detached from its support.

When removed, the shape of the mask can be approximately described as a rectangle with curved edges with the bottom segment disconnected to leave space for the user's nose. From being a "flat", the mask gets the shape of its supporting part when attached with the velcro.



Final result



4.2.1 Insights gained

The reverse-engineering process was useful to gain the following insights.

Production

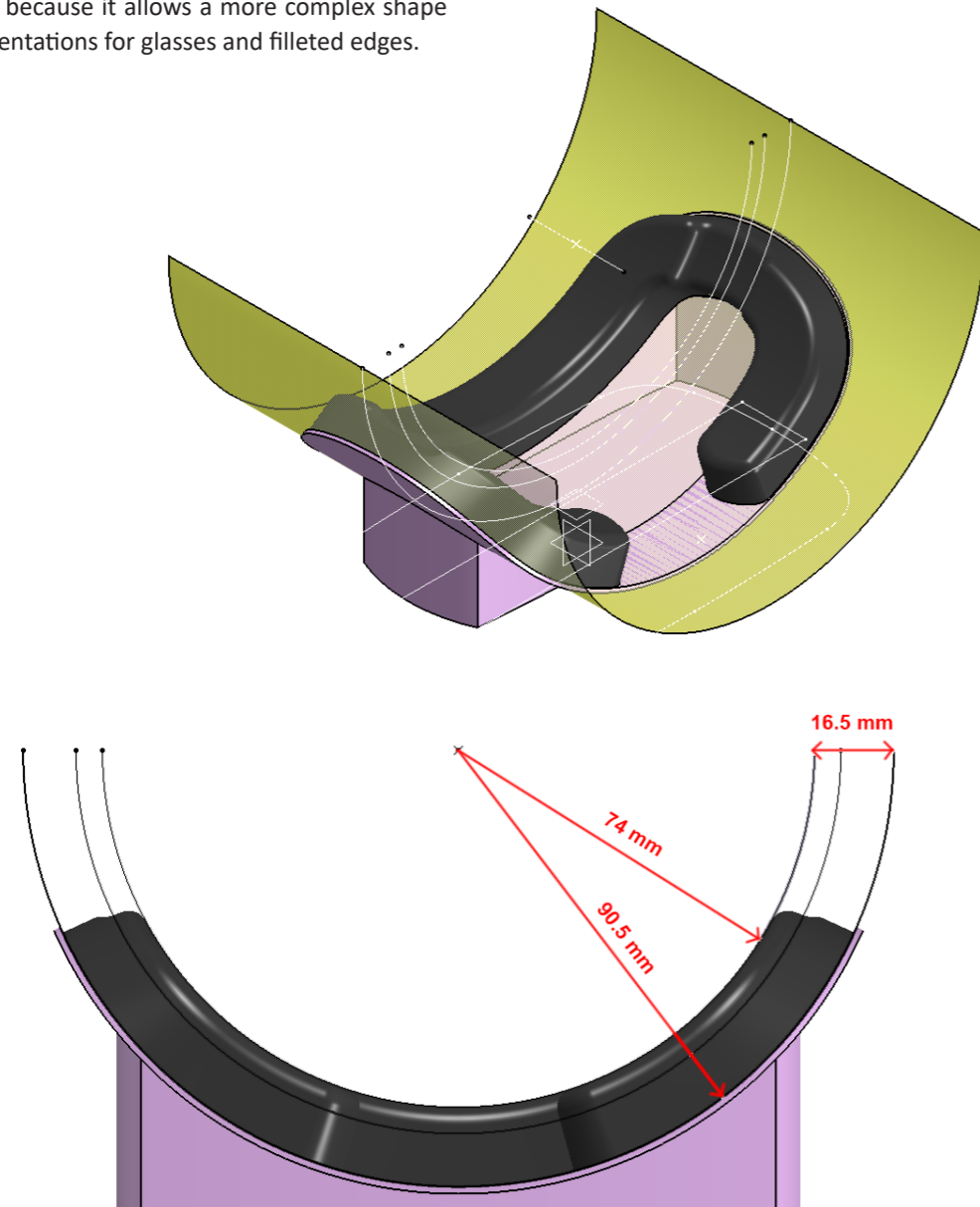
No official information can be found about the production of the HTC Vive mask. However, it may be produced the following three ways:

- Pressing a blade on a flat foam panel of 16.5 mm in thickness in the shape of the mask
- Laser-cutting a flat foam panel of 16.5 mm in thickness in the shape of the mask
- Injecting and letting expand foam in a three-dimensional mould in the desired mask shape

HTC Vive mask is expected to be produced in the last way because it allows a more complex shape with indentations for glasses and filleted edges.

Shape of the support and the mask

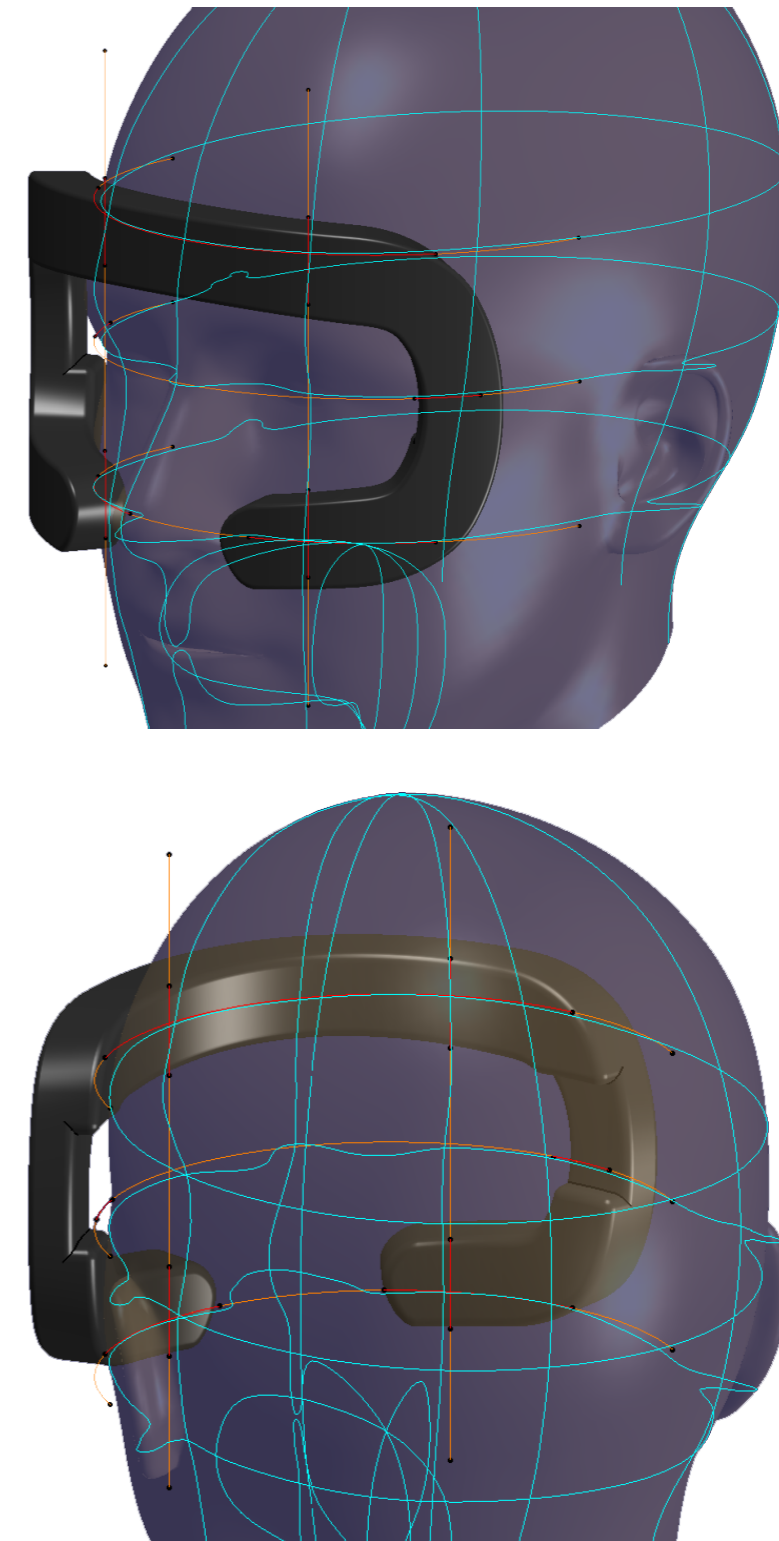
In the HTC Vive, the mask support surface is a section of a cylindrical surface (yellow) with a radius of 90.5mm. The mask is attached to this surface and has a thickness of 16.5mm. This means that the inner surface of the mask (in contact with the user's face) results in a cylinder with a radius of 74mm.



Corresponding size

By placing an average mannequin (Chapter 6) on the CAD model of the mask it is possible to see that the standard size of the HTC Vive is modelled around it. This is confirmed by the fact that the curvature of the face at the areas that

are contacting the mask are extremely tight, with a maximum distance of 3mm. This distance is supposedly accommodated by deformation of the foam.



4 VR headset product analysis - Summary and conclusions

- The choice of the HTC Vive has small consequences on the design process. The results of this project can be translated to other headsets relatively easily.
- The harness system has an influence on the mask contact and pressure on the face, and overall stability of the headset.
- There are three sizes of the mask, narrow, standard and face, that seem to accommodate different face shapes in terms of width.
- The properties of the foam and its thickness have an influence on its deformation (to fit the user's face).
- The mask is attached to the headset body with velcro and is easily replaceable. This gives the opportunity to substitute it with an EOG add-on module.
- The support of the mask piece is a cylindrical surface. When the mask is mounted on top of it, its inner surface has a radius of 74 mm. This dimension seems to be resulting from the fact that the standard size was modelled on the average human. The complex shape of the human face is then accommodated by deformation of the foam. Important factors are the physical properties of the material and its thickness.

5

Chapter 5 **IDEATION**

This section consists of the ideation and decision making on relevant aspects of the project. During this process it was important to distinguish choices to be taken for the purpose of building a prototype for testing purposes, and choices that are envisioned to be implemented in an actual product.

5.1 Electrodes

5.1.1 Configuration

Horizontal component

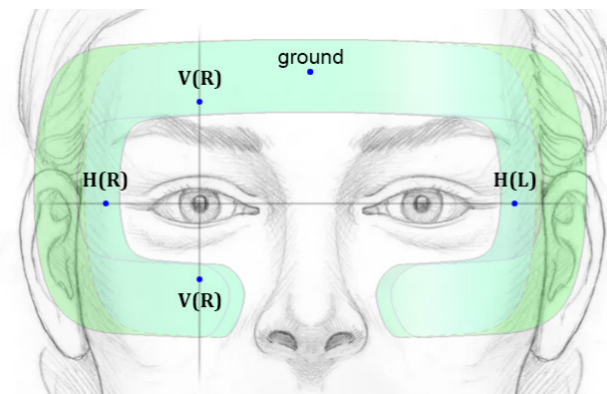
The mask shape offers placement for horizontal component electrodes only at the lateral canthi. This configuration is sufficient for capturing conjugate horizontal rotations of the eye. In any case it is not necessary to measure disconjugate eye rotations because they are not possible in VR. The users are fixating at a screen which is virtually placed by the lenses at distance that vary between 1 and 3 meters (depending on the headset), while vergences happen at distances smaller than 10 cm.

Ground placement

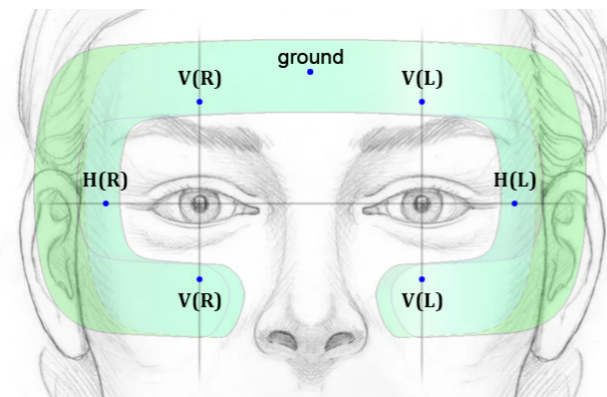
The best position for ground placement on the VR mask is the middle of the forehead.

Vertical component

Since disconjugate vertical eye rotations are naturally not possible, it is sufficient to measure the vertical component at one eye. However, research shows that by measuring both eyes the signals can be averaged to improve the accuracy and reduce the negative effect of artefacts (Chapter 3 paragraph 3.2.2). For this purpose, the envisioned final product will have vertical component measurements at both eyes. On the other hand, the prototype will have vertical component measurements at one eye only in order to simplify the signal acquisition process.



Prototype electrodes configuration (2x horizontal, 2x vertical, ground)



Envisioned product electrodes configuration (2x horizontal, 4x vertical, ground)

5.1.2 Materials

Due to lack of budget the dry electrodes that will be built for the prototype will be made out of a relatively cheap metal with good conductive properties.

On the other hand, research shows that the best performance is achieved with a silver chloride (Ag-Cl) coating.

Therefore, the dry electrode envisioned for the final product may be a relatively cheap metal plate coated with silver-chloride, or silver coated with silver-chloride.

5.1.3 Shape and dimensions

Literature shows that the shape and the dimensions of electrodes have an influence in the acquisition of biosignals.

As seen in electrodes VR products (Chapter 1 paragraph 1.2.4), the best shape for dry electrodes to be integrated optimally on the VR mask is flat. Then, the relevant dimension is the contact area between electrode and skin.

However, since there is no literature on this topic specifically for EOG, the impact of the contact area on the signal will have to be investigated during testing phase.

5.2 Mask design

5.2.1 Sizing system

By trying the HTC Vive standard mask on multiple subjects, big gaps were present between the subject's face and the foam, often around the canthi area. Even without complete contact it is still possible for most users ensure the headsets on their head and experience VR. For this reason, the other sizes of the mask are not included in the box, but are sold separately if users (likely far from average face shapes) experience discomfort and slippage.

However, for the purpose of recording EOG signals with dry electrodes, the uniform contact between the mask and the user's face (at the chosen electrodes positions) is necessary for ensuring constant signal acquisition.

Chosen approach for the prototype

A multiple size approach seems indeed the best solution to assure uniform contact and, at the same time, increase comfort and stability. The multiple size approach with three sizes is chosen by emulating the HTC Vive strategy (narrow, standard, wide). However, this strategy is intended to increase comfort and stability.

The hypothesis that it can also successfully ensure sufficient contact to all electrodes is an assumption that will need to be verified.

Whereas three sizes are not sufficient to accommodate the face shapes variability and provide uniform contact, it is then necessary to increase the number of sizes. On the other hand, if a three sizes approach is successful, it may be interesting to lower the number of sizes. Nevertheless, conducting the anthropometric analysis and designing a sizing system are long processes that may not be possible to repeat in the time given for this project.

For testing purposes, the most feasible option is prototyping a mask piece for each size, three in total (S, M, L). It would be beneficial to be able to swap the different sizes in an easy way.

Chosen approach for the envisioned product

Other than three swappable mask pieces, the envisioned product may include movable parts and a regulation system to give the possibility of adapting the shape of the mask to the user's face.

Such a system has advantages, disadvantages and differences in production and costs that would need to be investigated. This choice was not pursued for the prototype due to increased complexity and limited time. Anyway, insights from the generation of the three sizes (Chapter 6) can also be applied to the design of such movable parts.

5.2.2 Materials of the mask

The materials of the mask influence critical aspects as performance, comfort and hygiene. The main material of which a VR mask is composed is polymeric (plastic-based) foam. But, no VR-related company openly shares the composition and the properties of the foam used.

A known issue with foam is that it does absorb facial sweat. This is a problem especially VR headsets are likely to be shared between multiple users. For this reason, some companies sell more expensive replacement masks that have an outer

synthetic leather layer that does not absorb sweat and allows to be cleaned with antibacterial wipes.

Since EOG eye-tracking method makes use of electrodes that need to make good contact with the user's face, the challenges lay on ensuring the quality of the captured signals, while maintaining high wear comfort and stability also during motions. A special attention is also required on the choice of the materials in order to address thermal comfort and durability issues caused by prolonged use and sweat.

5 Ideation - Summary and conclusions

- The chosen configuration differs between the prototype and the envisioned product. The configuration chosen for the prototype has 2 electrodes (on the canthi) for the horizontal component measurements, and 2 electrodes (over the eyebrow and on the lower orbital bone) for the vertical component measurements, the ground is in the middle of the forehead. The envisioned product configuration differs only by the fact that the vertical component is measured at both eyes to reduce noise and increase accuracy.
- The dry electrodes for the prototype will be metal plates with good conductive properties, while the dry electrodes for the envisioned product will have silver-chloride coating.
- For flat dry electrodes the relevant dimension is the contact surface with the skin.
- The contact between the user face and the mask must be provided at all electrodes positions.
- For the purpose of providing uniform contact, a sizing system with multiple sizes is the best approach to accommodate the variability of the human face. The prototype will have separate parts for each size, while the envisioned product may have a regulation system with movable parts.
- The strategy chosen for the sizing system is emulating the HTC Vive masks
- The number of sizes will be three (S, M, L) by emulating HTC Vive strategy (narrow, standard, wide)

6

Chapter 6 **ANTHROPOMETRIC STUDY**

Traditional anthropometric data characterizes the human body with tables of measurements, averages, standard deviations and percentiles. For engineering and design applications this data format is not intuitive to use (Ball, 2011), and generally not suitable nor sufficient (Robinette et al., 2002). Especially for complex body parts as the face, measurements are challenging to gather and do not accurately describe the nuances of volumetric 3D space (Ball, 2011).

3D scanning technology makes it possible to digitize the surfaces of a large number of human bodies, providing much richer information about the body shape than the traditional anthropometric measurements (Azouz et al., 2005).

In this chapter, 3D scan data be analysed with the aim of identifying distinguishable clusters of face shapes and then creating digital mannequins. Such results will be used in the design of a sizing system for the VR headset mask, with the ultimate purpose of improving the contact with the face and overall comfort.

6.1 CAESAR database

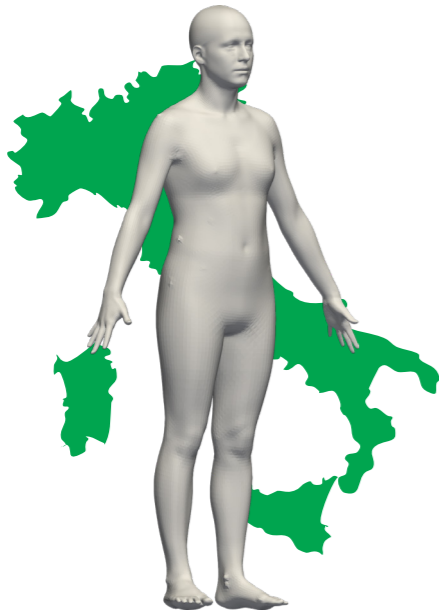
The use of 3D scanning equipment and software allowed to build populated databases of human 3D models for anthropometric research purposes.



The CAESAR (Civilian American and European Surface Anthropometry Resource) project is the first 3D whole-body surface anthropometry survey of civilian populations. The survey was conducted by NATO and representatives of the automotive, aerospace and apparel industry between 1998 and 2000.

About 6000 civilians between the age of 18 and 65 in three countries were sampled (scanned) in an effort to characterize the population of NATO countries as a whole. The Cyberware WB4 and Vitronic full-body scanners were used. A set of 74 white markers were also placed at anatomical landmarks prior to scanning.

Countries



Italy

Chosen because it has the shortest population (among NATO countries)



The Netherlands

Chosen because it has the tallest population (among NATO countries)



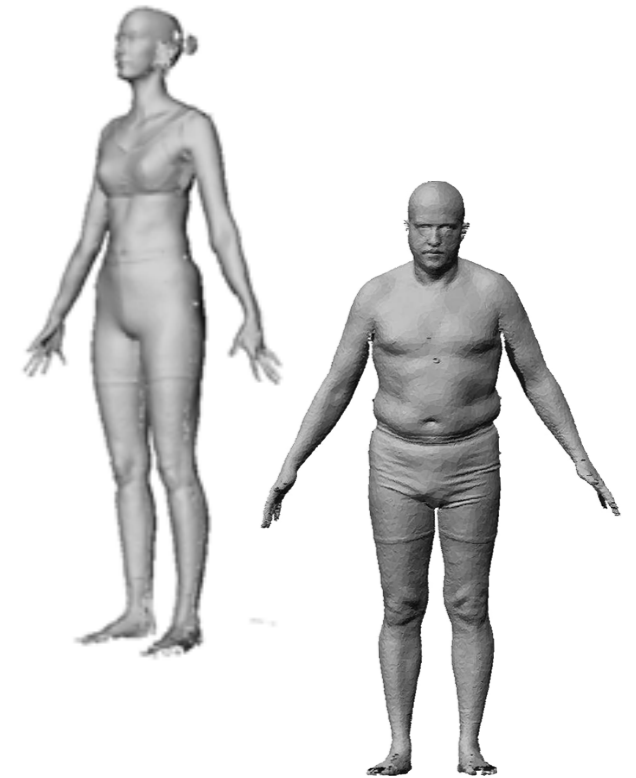
North America

(mostly USA + some subjects from Canada)
Chosen because it has the most diverse population (among NATO countries)

In order to streamline the analysis of the CAESAR data, mainly because of time limitations, the dataset will be reduced to the European population (Netherlands and Italy). Information on the North American database will be excluded in the rest of the Chapter. This choice will influence relevantly the resulting mannequins and consequently the shape and dimensions of the sizing system. However, this does not exclude the fact that extra-European users may be able to benefit from the design of such sizing system.

Outcomes of the survey

1. Demographic data
2. 3D scan for each subject
3. Landmarks
4. 1D traditional style measurements
5. 1D digital measurements extracted from 3D scans



6.1.1 Demographic data

CAESAR database contains a large amount of demographic data, the following is a selection of it which is considered to be relevant for the purpose of this project.

Subject Number	The Netherlands: from (1)1001 to (1)7079 (not sequential) Italy: from 4000 to 4800
Gender	Male or Female
Age in years	From ~17 to ~66
Birth State	The Netherlands: birth province Italy: birth region
Father Born	Country where the father of the subject is born
Mother Born	Country where the mother of the subject is born
Race	Dutch/Italian (both parents of the subject are born in the Netherlands/Italy), or Other (one or both parents of the subject are born in another country)

Demographic statistics

	Netherlands	Italy	Total
Total of subjects	1140	801	1941
Males	518 (45.5%)	388 (48.5%)	906 (46.7%)
Females	622 (54.5%)	413 (51.5%)	1035 (53.3%)
Age range	18 - 66	17.5 - 65	17.5 - 66
Average age	38.7	30.3	35.2

6.2 Landmarks, planes, axes and measurements

The first step taken in the anthropometric study was to identify a set of relevant anthropometric measurements that relates to the dimensioning of the product. The number of potential measurements is almost limitless. However, not all of these are equally reliable, anatomically meaningful, or relevant (Kolar & Salter, 1997). It is then important to choose the set of measurements which describes at best the craniofacial morphology that needs to be studied and that relates to the dimensioning of the product.

In order to perform anthropometric measurements, landmarks, axes and planes need to be identified. The landmarks are points of the body that relate to a specific feature of the body. The axes and the planes are used to define a coordinate system, to align the scans and to project measurements. An explanation of these features and procedures is presented in the following sections.

Name	ID	FARKAS Description	CAESAR description
Frontotemporale	ft	The most medial point on the temporal crest of the frontal bone.	
Frontozygomaticus	fz	The most lateral point on the frontozygomatic suture.	The most anterior point of the forehead between the brow ridges in the midsagittal plane.
Glabella	g	The most prominent point in the median sagittal plane between the supraorbital ridges.	Most anterior point of the forehead between the brow ridges in the midsagittal plane.
Ophryon	on	The point, at the mid-plane, of a line tangent to the upper limits of the eyebrows (sci-sci).	
Porion	po	The most superior point on the upper margin of the external auditory meatus when the head is in the Frankfort horizontal plane.	
Tragion	t	Located at the notch above the tragus of the ear, the cartilaginous projection in front of the external auditory canal, where the upper ridge of the cartilage disappears into the skin of the face.	Notch just above the tragus (the small cartilaginous flap in front of the ear hole).
Nasion	n	The midpoint of the nasofrontal suture.	
Zygion	zy	The most lateral point on the zygomatic arch.	
Orbitale	or	The lowest point on the margin of the orbit.	Lowest point on the inferior margin of the orbit (the bony eye socket), marked directly inferior to pupil.
Superciliare	sci	The highest point on the upper margin of the middle portion of the eyebrow.	
Sellion	s	The deepest point of the nasofrontal angle.	Point of greatest indentation of the nasal root depression.
Pupil	N/A		Center point of the pupil.

6.2.1 Landmarks

Anthropometric landmarks are points of the body that relate to a specific skin or bone feature of the body. Skin landmarks are identified by finding the most extreme point of a body feature (for example the tip of the nose). Bone landmarks are more easily identified on skeletal remains, while in living subjects are identified by palpation of the skin.

Since the product relates to the face, a selection was done between craniofacial landmarks. The selection initially included all the landmarks that are inside the area covered by the VR mask and that are useful in the definition of axes and planes.

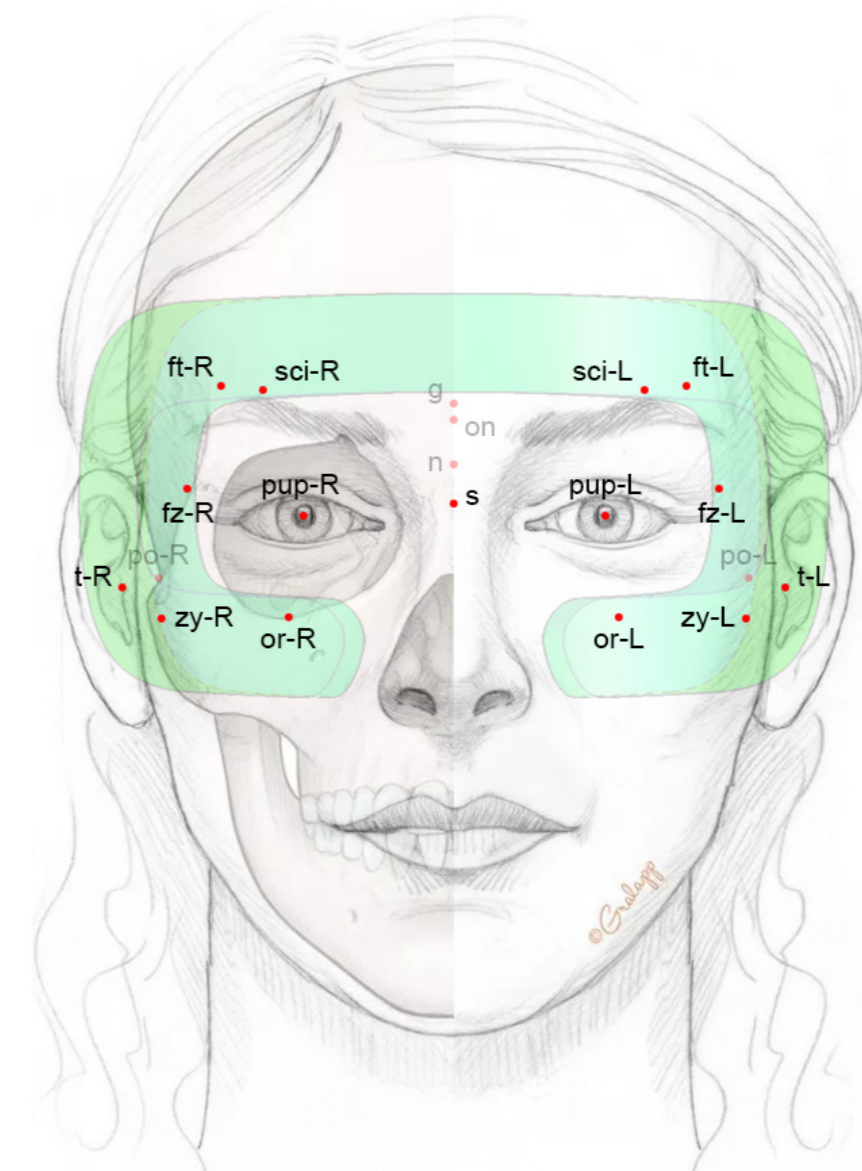
The landmarks are identified by the landmark name and (if applicable) its direction (Left or Right) with respect to the subject.

Further selection - Excluded landmarks

The selection of multiple landmarks in the proximity of the same facial feature is redundant. After a second selection some landmarks were excluded.

Glabella, ophryon and nasion were excluded in favour of keeping only the sellion, which is more easily identifiable on a 3D scan as the point of vertical tangency of the nasal root depression.

Porion was excluded by keeping the tragion. Indeed, the tragion is the corresponded skin projection of the bony landmark porion.



6.2.2 Axes and planes, new coordinate system

Axes and planes were defined in order to create a new coordinate system. This is useful for aligning the scans and project landmarks and measurements.

Three vectors were drawn, then they were normalized (reduced their magnitude to one) then the normal planes to the three vectors were created. An explanation of the vector and plane follows:

- Midsagittal plane - normal to the vector that is the average of all vectors drawn between each landmark and its respective symmetric

$$\text{midsagittal_normal} = (\text{t_t_vector} + \text{zy_zy_vector} + \text{fz_fz_vector} + \text{ft_ft_vector} + \text{sci_sci_vector} + \text{or_or_vector}) / 6$$

- Frankfort plane - normal to the vector that is the cross product (perpendicular) to the two vectors (left and right) drawn between the tragon and orbitale

$$\text{frankfort_normal} = \text{t_or_L_vector} \times \text{t_or_R_vector}$$

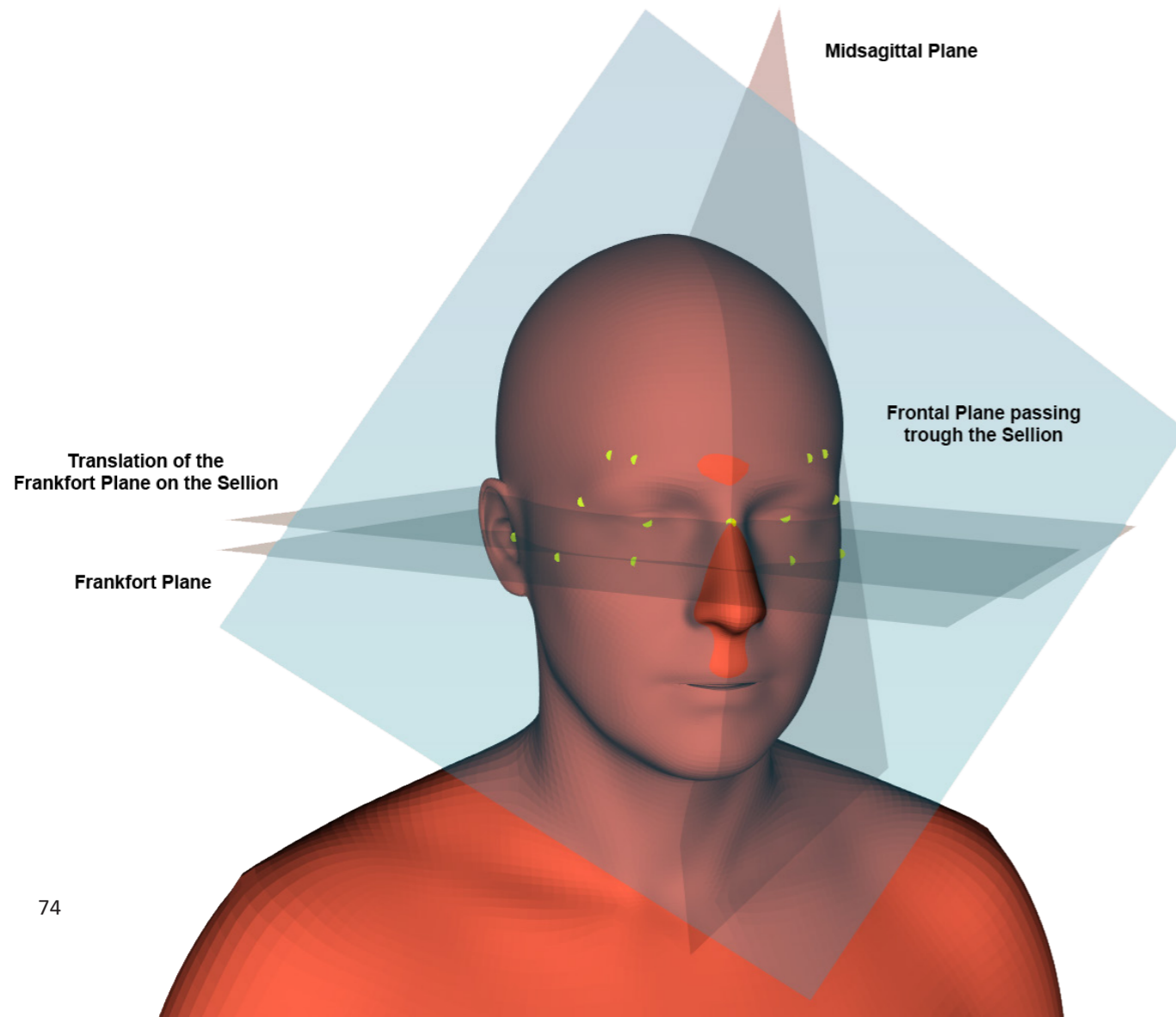
- Frontal plane - normal to the vectors of the previous two planes

$$\text{frontal_normal} = \text{midsagittal_normal} \times \text{frankfort_normal}$$

Then all the vectors (so the planes) were translated on the sellion, which then is the origin of the new coordinate system.

Ideally the sellion lies on the midsagittal plane, so the effect of the translation is minimal on the midsagittal plane. The other two planes will be then called

- Translation of the Frankfort plane on the Sellion
- Frontal plane passing through on the Sellion



Alignment

During the scanning procedure the subjects are asked to stand in a standard straight position, but it is likely that their heads are tilted. Before performing the averages, the head 3D scans needed to be aligned.

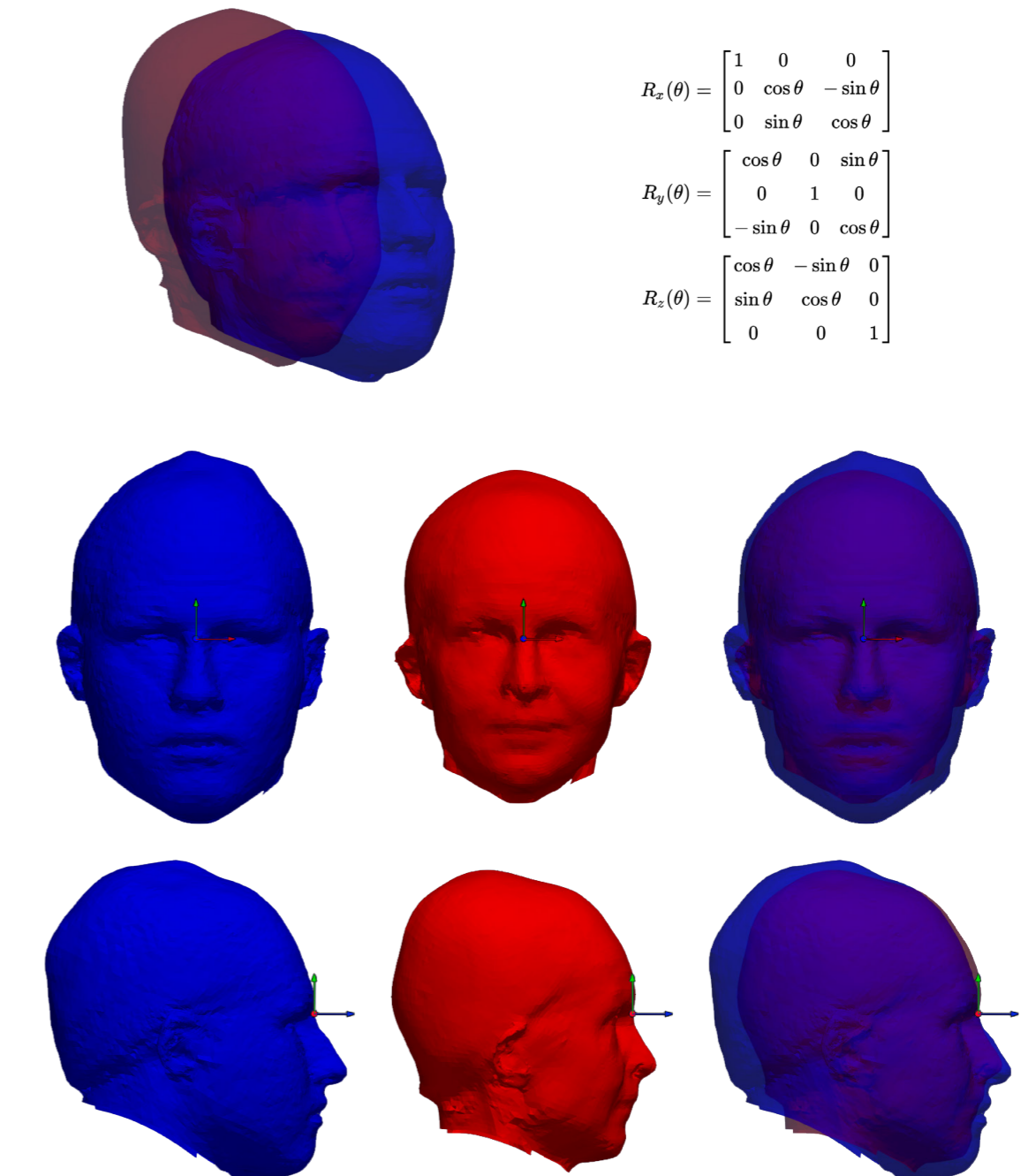
In the picture below, an example of two 3D scans (red and blue) before alignment. The scans are not aligned between each other and are not aligned with the world coordinate system. For each scan the following transformations were performed for alignment.

Translation

Firstly, the scan was translated with the purpose of moving the sellion to the origin of the world coordinate system. This is achieved by subtracting the coordinate of the sellion to the coordinates of all the others points of the scan.

Rotations

Then the scan was rotated in such a way that the normal vectors of the midsagittal, Frankfort and frontal planes are aligned with the XYZ vectors of the world coordinate system. This is achieved by calculating the angles between each vector of the two coordinate systems and from those build a 3D rotation matrix for each rotation.



$$R_x(\theta) = \begin{bmatrix} 1 & 0 & 0 \\ 0 & \cos \theta & -\sin \theta \\ 0 & \sin \theta & \cos \theta \end{bmatrix}$$

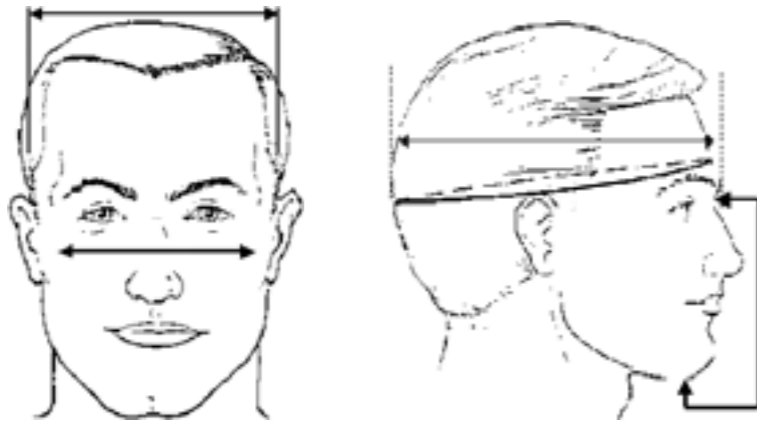
$$R_y(\theta) = \begin{bmatrix} \cos \theta & 0 & \sin \theta \\ 0 & 1 & 0 \\ -\sin \theta & 0 & \cos \theta \end{bmatrix}$$

$$R_z(\theta) = \begin{bmatrix} \cos \theta & -\sin \theta & 0 \\ \sin \theta & \cos \theta & 0 \\ 0 & 0 & 1 \end{bmatrix}$$

6.2.3 Traditional style measurements

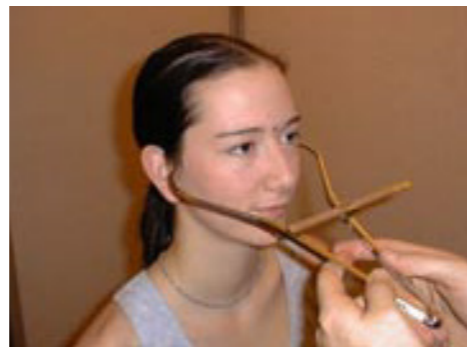
Traditional style measurements, also referred as manual measurements, are those measurements recorded from trained researchers with instruments (e.g. caliper, measuring tape) directly on the subject's body. This kind of data is considered to be highly accurate/reliable, but is

subject to human error and may present a small variability due to the fact that the researchers press and indent the skin with measurements tool, resulting in a slightly lower measurement.



Examples of traditional measurements (CAESAR Final Report, 2002)

CAESAR database includes an extensive dataset of traditional style measurements but only one was relevant for the dimensioning of the mask.



Name	Landmarks	Description	Instrument
Bizygomatic Breadth	zy-zy (zygion- zygion)	Maximum horizontal distance is measured across the face between the zygomatic arches (cheekbones)	Spreading caliper

6.2.4 Digital measurements

The scarcity of relevant traditional craniofacial measurements which relate to the dimensioning of the mask, motivates to take more measurements digitally.

Digital or virtual measurements are taken programmatically on the library of 3D scans. The process starts with the identification of 3D points in positions that correspond to relevant landmarks. Then the new coordinate system and the planes are defined. Finally, digital measurements are taken programmatically and stored in a table .

The biggest advantage is that this process allows to create new measurements not present in traditional anthropometric studies. At the same time, main drawbacks are that the identification of landmarks might be more difficult on a 3D scan compared to a real subject. Moreover, the measurement may be slightly deviated between boney landmarks, where the traditional measuring tools are pushed on the skin to reach the bone closer.

Digital measurements can be of the following 4 types:

3D distance between points

- A 3D vector is drawn between the two points
- The magnitude of the vector is calculated

Normal distance between a point and a plane

- A normal (perpendicular to the plane) vector is drawn between the point and the plane
- The magnitude of the vector is calculated

Normal projection of a vector on a plane

- A 3D vector is drawn between the two points
- The vector is projected normally on a plane
- The magnitude of this projected vector is calculated

Projection of a vector on an axis

- A 3D vector is drawn between the two points
- The vector is projected on an axis (another vector normally with unitary magnitude)
- The magnitude of this projected vector is calculated

CAESAR digital measurements

A collection of digital measurements was present in the CAESAR library.

Previous to the 3D scan, CAESAR's researchers placed stickers on each subject's body corresponding to landmarks. This was done in order to later identify the landmarks on the 3D scan from its texture in an easier and more precise way. All digital measurements present in the CAESAR library fall in the category of 3D distances between points.

Several craniofacial measurements were present in the CAESAR digital measurements library, but many regarded the overall dimensions of the head or the lower part of the face and were not relevant for the dimensioning of the mask. The only useful measurement is the following.

Name	Landmarks
Inter-Pupillary Distance (IPD)	pupil-pupil orbitale-orbitale (CAESAR)



It is important to note that CAESAR considers the distance between the pupils as equal to the distance between the infraorbitale landmarks. Indeed, CAESAR defines the infraorbitale as the projection of the pupil on the orbit bone.

Digital measurements (Python)

The two CAESAR measurements identified as relevant are still not sufficient to describe accurately the anthropometry of the face section underlying the mask. For this reason, more digital measurements were needed.

The process started with selecting points on the mesh in positions that correspond to the selected landmarks. Since the texture information (showing manually placed stickers on landmarks) was lost during the template registration process, the positioning of the points was performed by referring to landmarks definitions found in the literature (Farkas, 1994; Kolar & Salter, 1997). The positioning was performed on an average of all 3D scans and then projected on all scans (by correspondence) in this way the identification of landmarks was not relative only to a specific subject.

These points were then used to define the fundamentals planes and axes of the body and face. Finally, the measurements were taken programmatically with a Python script and stored in a spreadsheet.

This process included the use of Python code empowered by VTK library (Kitware Inc.), which enables operations on 3D files.

9 new digital measurements were taken with this method, plus two that correspond to the previous ones from CAESAR and are used as a matter of comparison (to check if the results from Python are accurate).

The variables are divided into three main groups: widths, depths and heights, corresponding to the approximate direction of the measurement.

Horizontal widths

The horizontal widths were all measured by drawing a vector between two landmarks and then projecting it onto the vector perpendicular to the midsagittal plane. In this way misalignments and asymmetries between the left and right landmarks are minimized.

Inter-Pupillary Distance and Bizygomatic Breadth were measured as a matter of comparison with measurements already present in the CAESAR database.

Symmetric Depths

The depths were calculated by projecting landmarks onto the frontal plane passing through the sellion along its normal vector. Then the distance (minimum distance between a point and a plane) between the landmark and its projection was measured.




Symmetric means that for each landmark two measurements were taken (left and right side of the face) and then averaged.

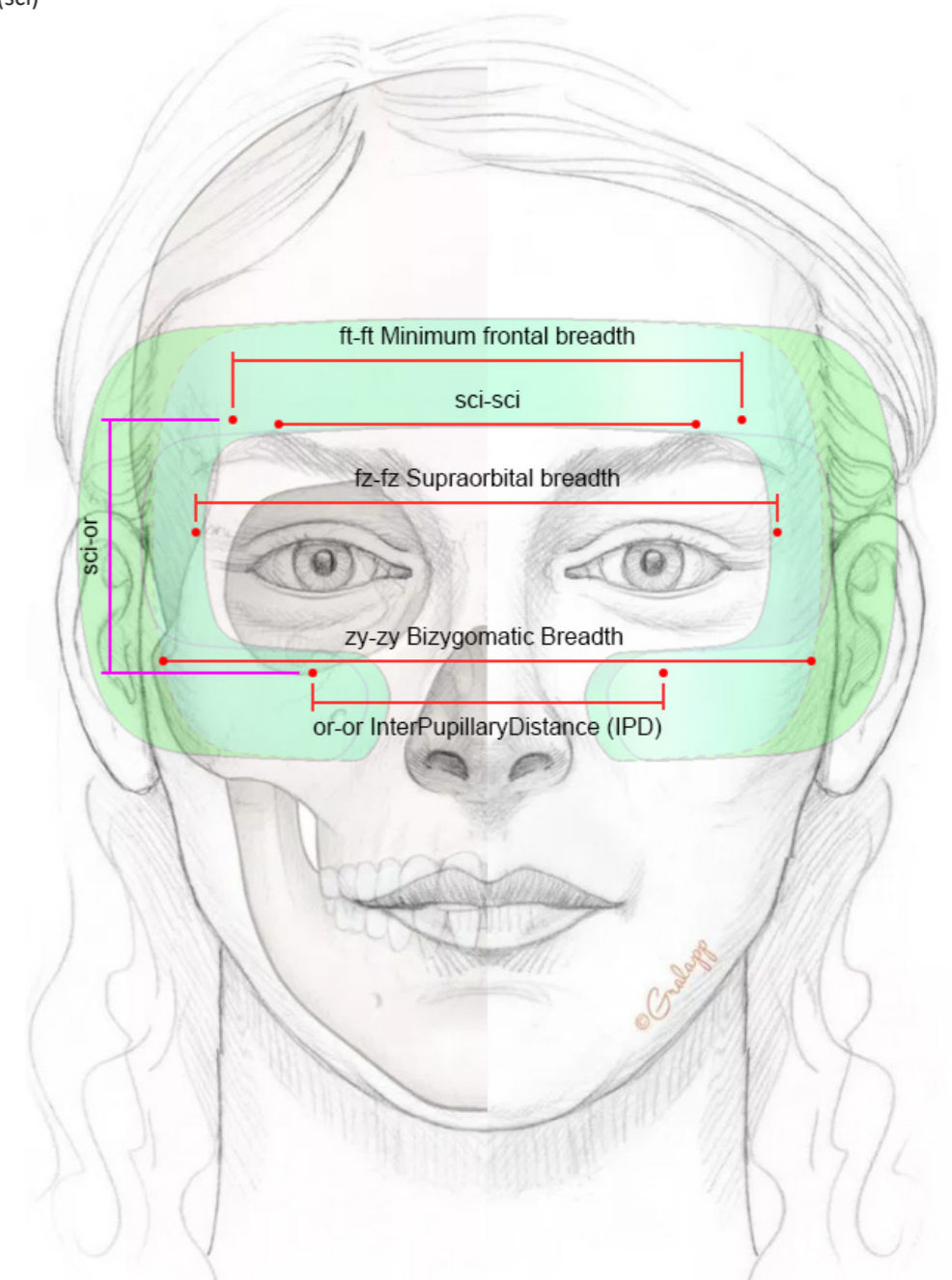
The landmarks projected were:

- Frontozygomaticus (fz)
- Frontotemporale (ft)
- Superciliare (sci)
- Zygion (zy)
- Orbitale (or)

Heights

One height was calculated by drawing a vector between the superciliare (sci) and the orbitale (or). The vector was projected onto the vector perpendicular to the Frankfort plane and then measured. Again, the left and right measurements were averaged.

Landmarks	Corresponding traditional style measurement name	Corresponding traditional style measurement picture
zy-zy (zygion-zygion)	Bizygomatic Breadth (CAESAR) Maximum facial breadth (FARKAS)	
fz-fz (frontozygomaticus-frontozygomaticus)	Supraorbital breadth (FARKAS)	
ft-ft (frontotemporale-frontotemporale)	Minimum frontal breadth (FARKAS)	
sci-sci (superciliare-superciliare)		
pupil-pupil	Inter-Pupillary Distance (IPD)	
or-or (orbitale-orbitale)		



Overview of the measurements

Widths

zy(R) - zy(L)	Zygion(R) - Zygion(L)	Bizygomatic Breadth	Traditional (CAESAR)
fz(R) - fz(L)	Frontozygomaticus(R) - Frontozygomaticus(L)	Supraorbital breadth	Digital (Python)
ft(R) - ft(L)	Frontotemporale(R) - Frontotemporale(L)	Minimum frontal breadth	Digital (Python)
sci(R) - sci(L)	Superciliare(R) - Superciliare(L)	/	Digital (Python)
or(R) - or(L)	Orbitale(R) - Orbitale(L)	InterPupillaryDistance (IPD)	Digital (CAESAR)

Depths

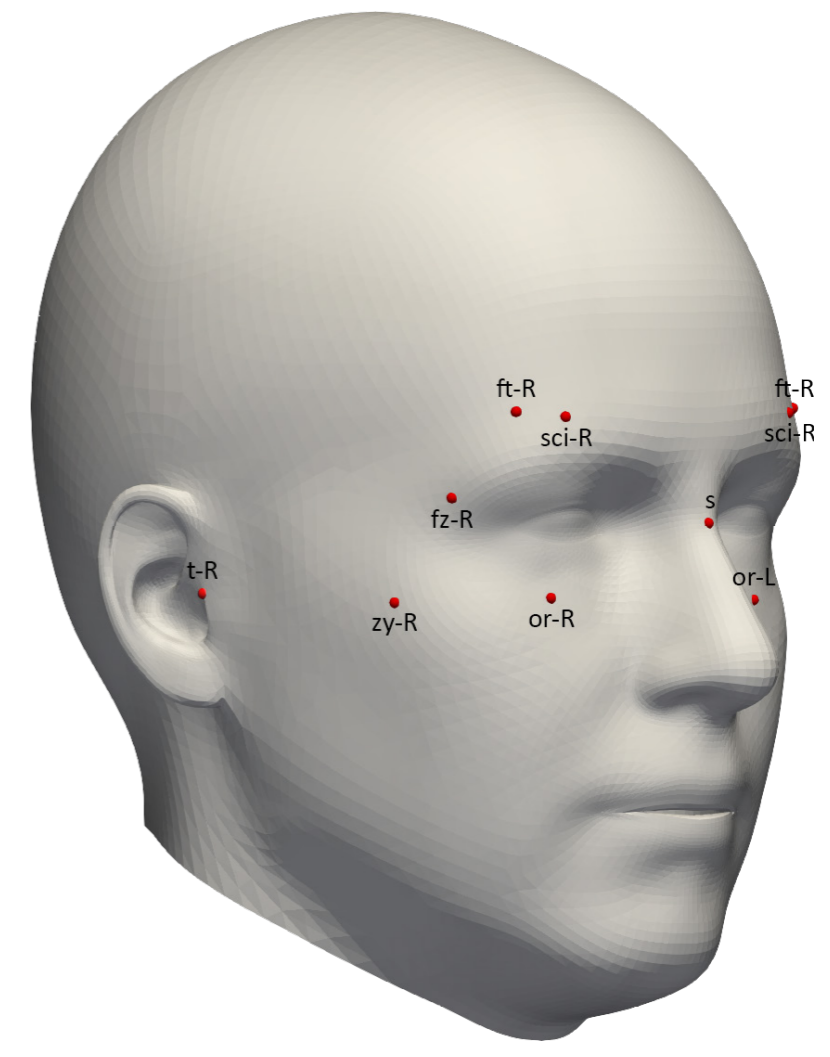
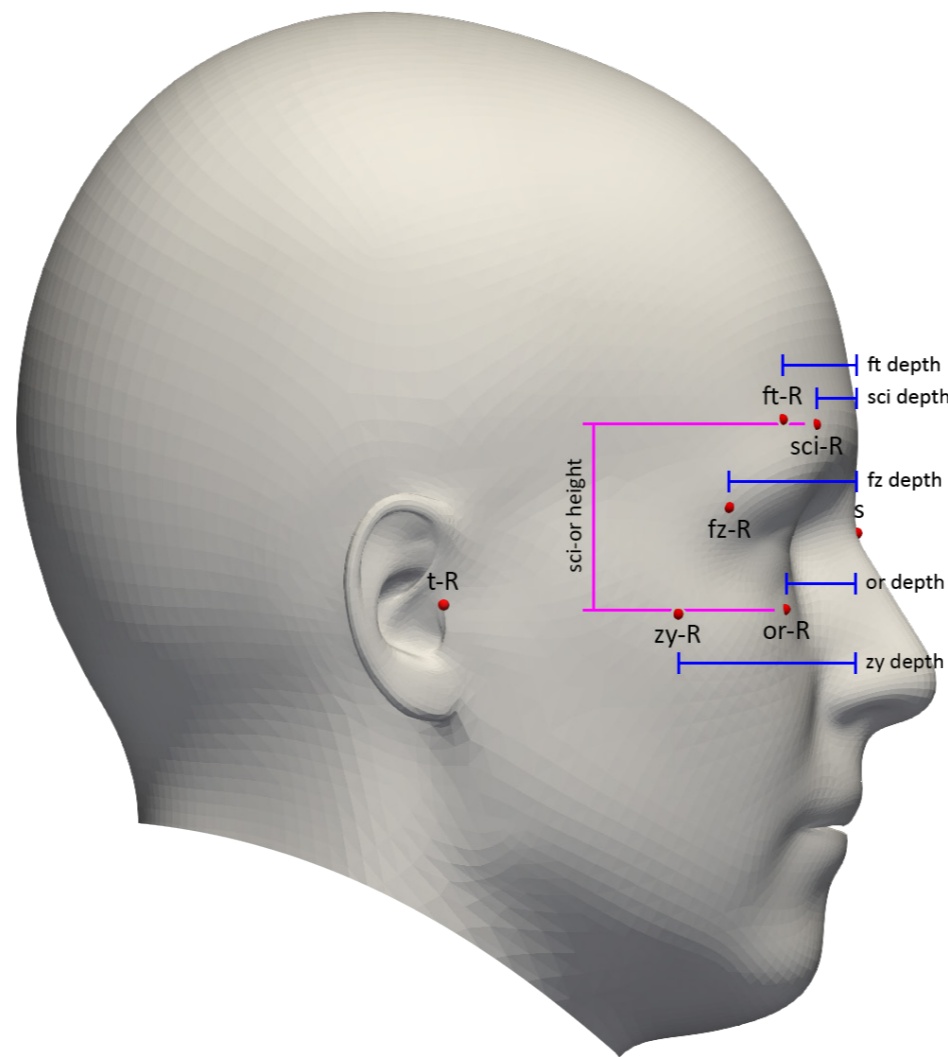
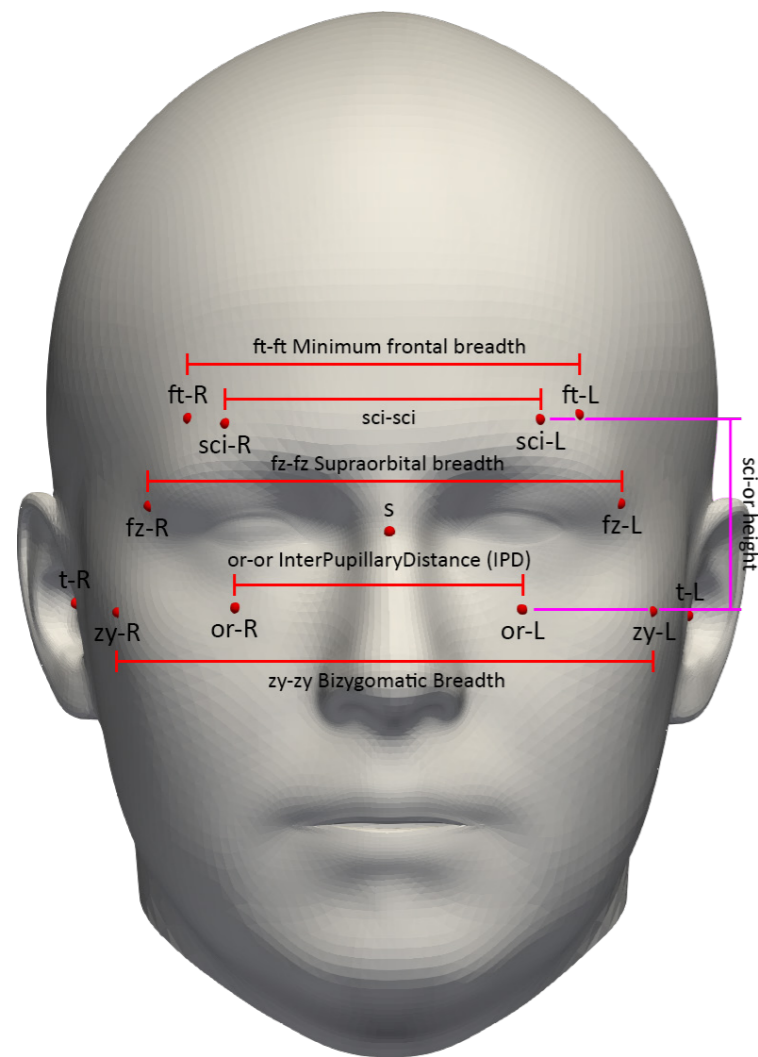
zy-FP	Zygion - Frontal plane passing through the Sellion	/	Digital (Python)
fz-FP	Frontozygomaticus - Frontal plane passing through the Sellion	/	Digital (Python)
ft-FP	Frontotemporale - Frontal plane passing through the Sellion	/	Digital (Python)
sci-FP	Superciliare - Frontal plane passing through the Sellion	/	Digital (Python)
or-FP	Orbitale - Frontal plane passing through the Sellion	/	Digital (Python)

Height

sci-or	Superciliare-Orbitale	/	Digital (Python)
---------------	-----------------------	---	------------------

	A	B	C	D	E	F	G	H	I	J	K	L	M
1	Subject Number	Gender	zy-zy-width	fz-fz-width	ft-ft-width	sci-sci-width	or-or-width	zy-depth	fz-depth	ft-depth	sci-depth	or-depth	sci-or-height
2	11001	Female	126.2	113.3	93.3	74.1	70.1	86	70.1	52	38.8	44.4	39.8
3	11009	Female	129.2	111.9	90.4	71.8	68	86	70.7	54.6	41.5	40.9	44.4
4	11017	Female	122.8	109.3	89.4	71.3	62	83	69.3	52.8	39.9	39.9	44.2
5	11021	Female	124.2	108.1	88.5	69.8	62.2	81.8	66.6	50.2	37.4	38.4	42.4
6	11024	Male	132	120.9	97.7	79.7	68.3	93.2	78.3	58.6	44.3	45.3	44.5
7	11025	Male	128.5	115.8	94.1	75.5	64.9	89	74.6	57.6	43.8	41.6	48.9
8	11026	Female	140.9	121.2	97.4	77.5	72.4	92.4	73.5	54.6	40.6	44	42.1
9	11029	Male	123.8	109.5	93.8	75.6	66.3	82.1	67.1	50.6	37.9	41	43.9
10	11031	Female	121.2	106.5	87.7	70.7	67.7	83.7	69	52.3	39.4	42.6	43.3
11	11033	Male	129.7	117.7	97.4	76.8	67.3	90.5	75.8	58.3	44	44.3	41.5
12	11035	Female	128.3	114.9	92.3	74.3	73.7	90.6	75	57.4	43.9	46.5	40.8
13	11038	Female	122	106.3	87.5	67.7	63.7	78.6	64.4	49	37.3	37.1	41.6
14	11040	Male	132.2	115.8	92.7	74.1	74.5	90.1	73.2	54.4	41.3	48.4	42.9
15	11042	Female	121.7	107.8	89	71.7	63.8	83	67.5	50.4	37.7	40.4	39.1
16	11049	Female	132.3	117.3	96.3	76.8	77.4	86.8	70.7	53.1	39.7	45.2	45.7
17	11050	Male	128.7	115.3	97	80	72.3	89.8	74.3	57.6	44.2	44.4	46.3
18	11051	Female	131.2	113.9	93.6	74.3	64.9	88.2	70.2	52	38.9	41.5	39.4
19	11052	Male	137.1	120.6	97.4	78.3	72.9	91.2	74.6	55.8	42	43.5	42.4
20	11054	Female	129.6	114.2	94.5	76.9	71.5	89.5	74.9	57.7	44	47.6	44
21	11057	Female	124.9	114	97.9	78.3	69.3	87.7	73.6	56.5	42.4	45.5	46.2
22	11074	Male	131.8	114.8	94.4	76.1	72.8	89.2	73.3	55.8	42	45.2	42

Table of measurements



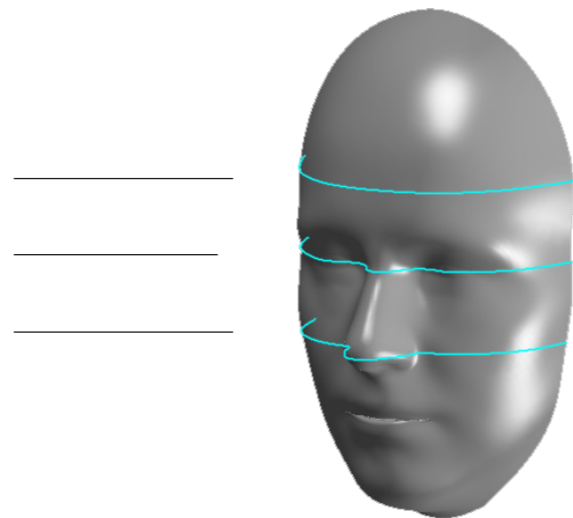
	Min (mm)	Max (mm)	Range (mm)	Average (mm)
Widths				
Zy-zy	102.5	149.1	46.6	127.48
Fz-fz	89	128.9	39.9	112.44
Ft-ft	73.9	108.2	34.3	93.13
Sci-sci	59.3	89	29.7	74.92
Or-or	49.5	85.6	36.1	68.42
Depths				
zy	65.6	105.3	39.7	87.85
fz	55.3	85.6	30.3	72.88
ft	42.4	67.1	24.7	55.83
Sci	32.9	52.2	19.3	42.32
Or	31.4	58.4	27	43.67
Height				
Sci-or	32.3	56.2	23.9	44.68

First interpretation of the results

The values of these variables describe together the position of the landmarks in space (with sellion as origin) and therefore the geometry of the subject's face portion underlying the mask.

More specifically, some variables approximately describe the curvature of different sections of the face:

- Curvature of the forehead: variables of landmarks Ft and Sci
- Curvature of the section at the height of the eyes: variables of landmark Fz
- Curvature of the Cheekbones (zygoms): variables of landmarks Zy and Or



6.3 Statistical analysis

The ultimate goal of this anthropometric study is to create digital mannequins that can be used for the design of a sizing system for VR masks in order to optimize the fit for electrodes contact.

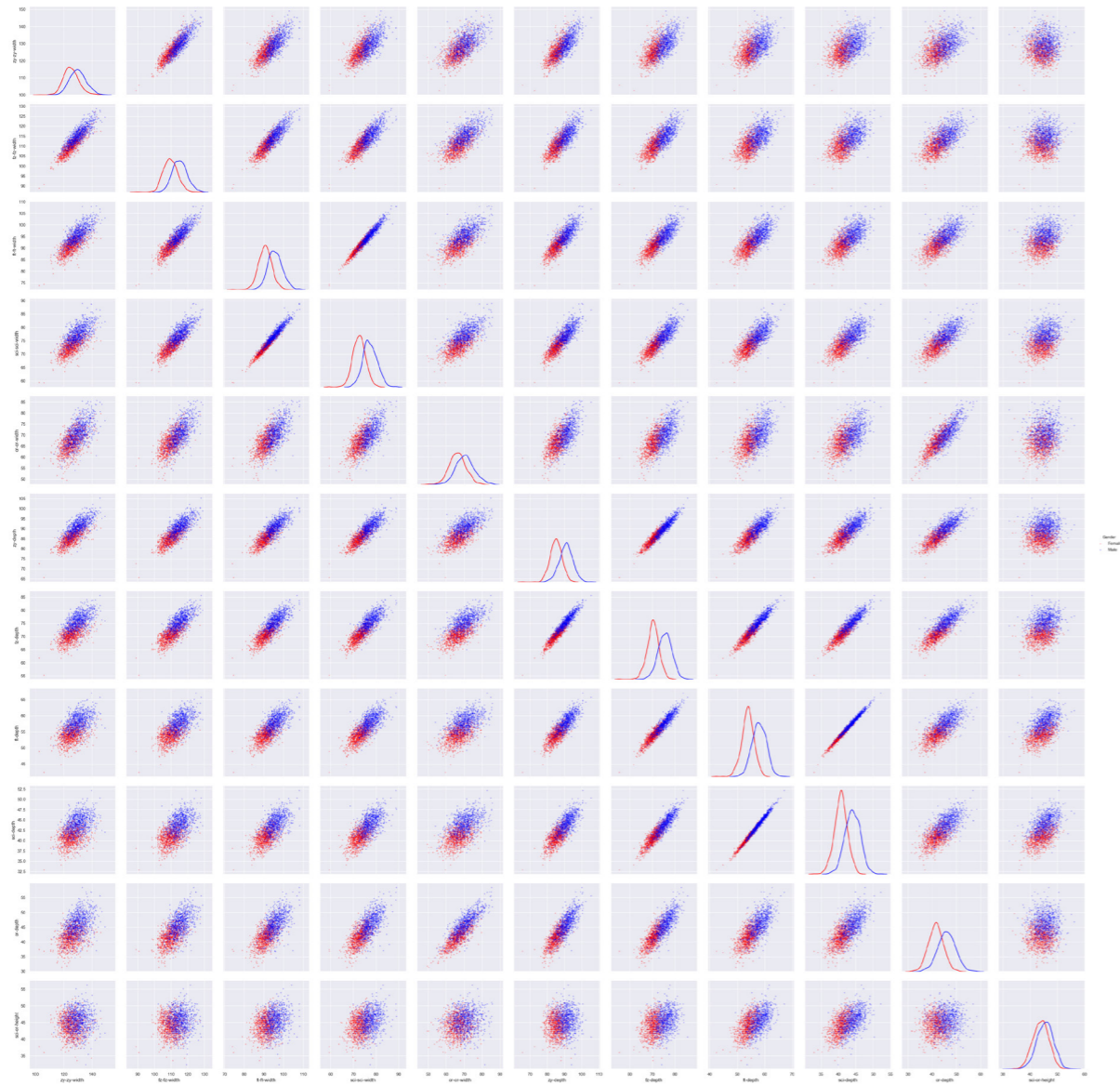
Realistic virtual mannequins, that represent body shapes that occur in the target population, are valuable tools for product developers who design near-body products. Statistical shape modelling is a promising approach to map out the variability of body shapes.

6.3.1 Visualizations

The first step of the statistical analysis was to create visualizations that are useful to investigate the relationships between the chosen anthropometric variables.

The visualization created were:

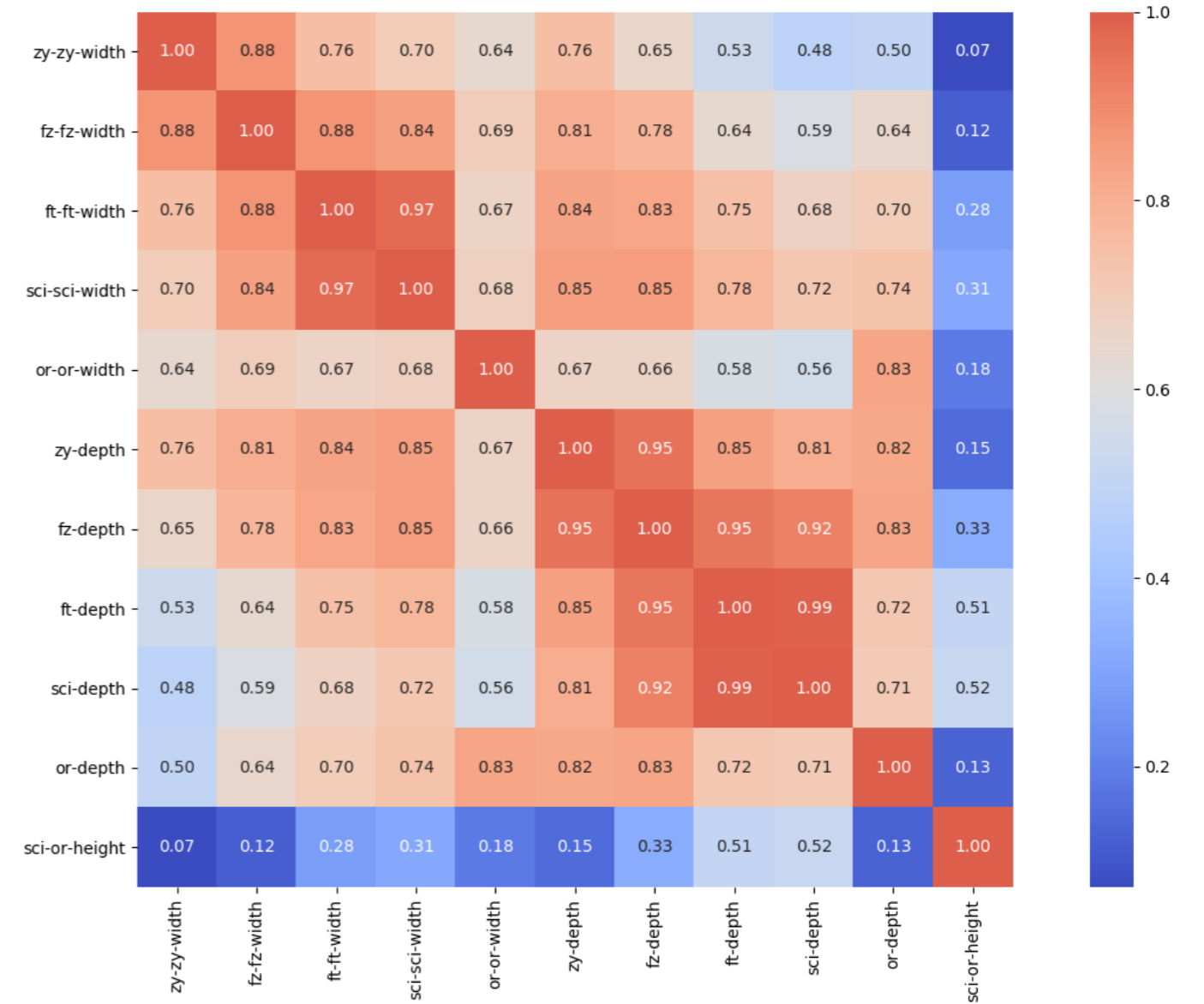
- Pair plots
- Correlation matrix
- Cluster map



Pair Plots

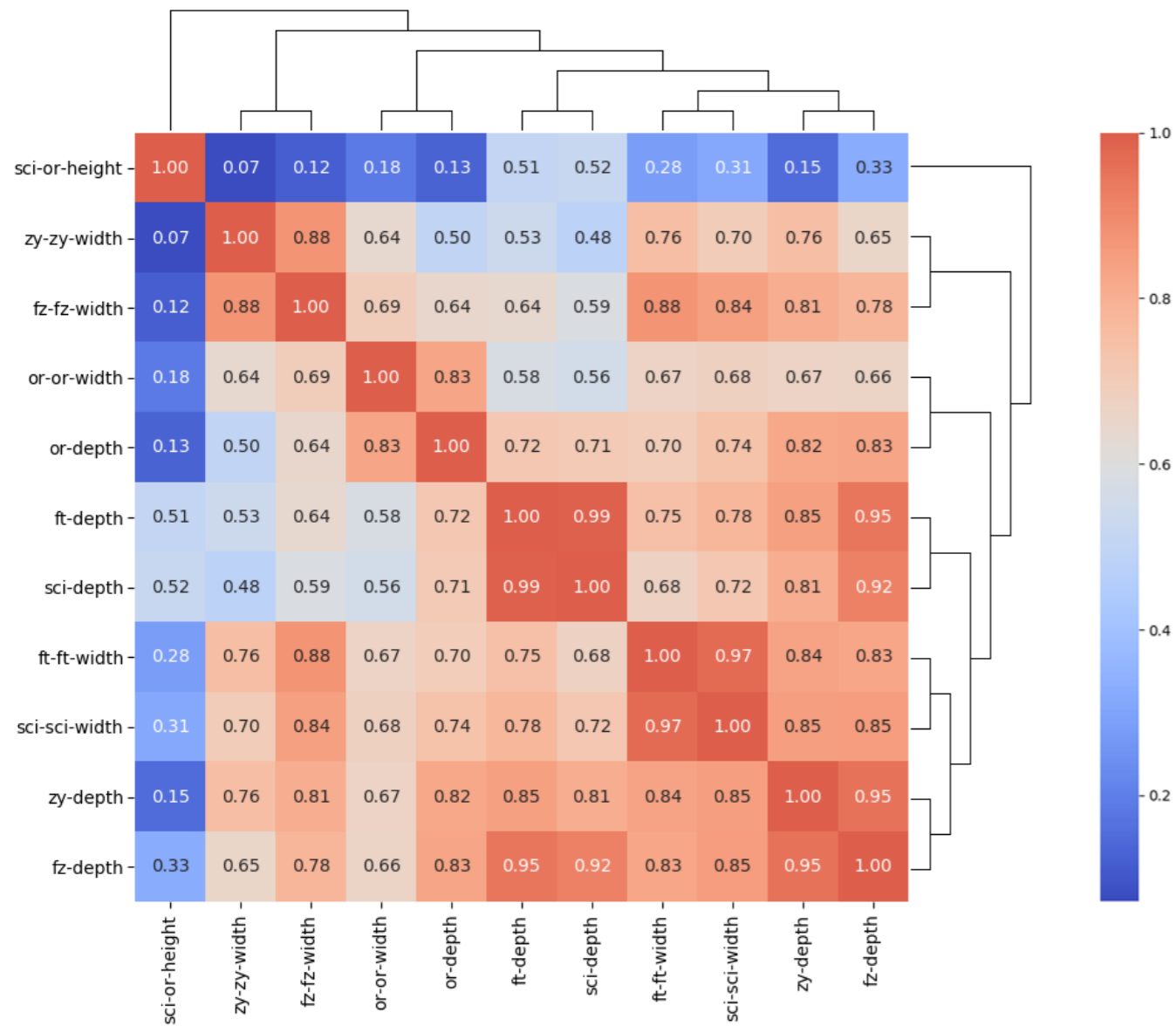
This table called pair plots displays a scatterplot for each pair of variables. It is useful to show graphically the degree of correlation between each pair of variables.

The correlation refers to the degree to which a pair of variables are linearly related. The scatterplots that are roundly distributed indicate low correlation. The scatterplots that are more linearly distributed indicate high correlation.



Correlation Matrix

This table called correlation matrix is similar to the pair plots visualization, but it shows the correlation between each pair of variables by its Pearson correlation coefficient (measure of the linear correlation between two variables). The correlation coefficient is also mapped to a colour code that goes from blue (low correlation) to red (high correlation). In this way it is possible to picture more clearly which are the variables that are highly correlated.



Cluster Map

In this table called cluster map, the pair of variables with the highest correlation are grouped together (first step). Then pairs of variables are grouped also with other pairs of variables by their correlation (second step) and so on. Finally, the variables are re-ordered following the clusters.

An empirical analysis of the visualizations

The visualizations immediately show predictable facts. This is positive because it means that no mistakes were done in the extraction of measurements and in the plotting of the data.

Firstly, all pairs of variables are positively correlated (no negative correlation coefficient). More specifically, the measurements that are of the same group are highly correlated. On the other hand, it is interesting to see how the variables of different groups can be also highly

correlated. For example, the variable or-or width is highly correlated with the depth of or itself. That indicates that a face with a large distance between the orbits is likely to generate a more curved zygomatic section.

Further than empirically analyse the visualizations, actual conclusions can be drawn by conducting a Principal Component Analysis on the data.

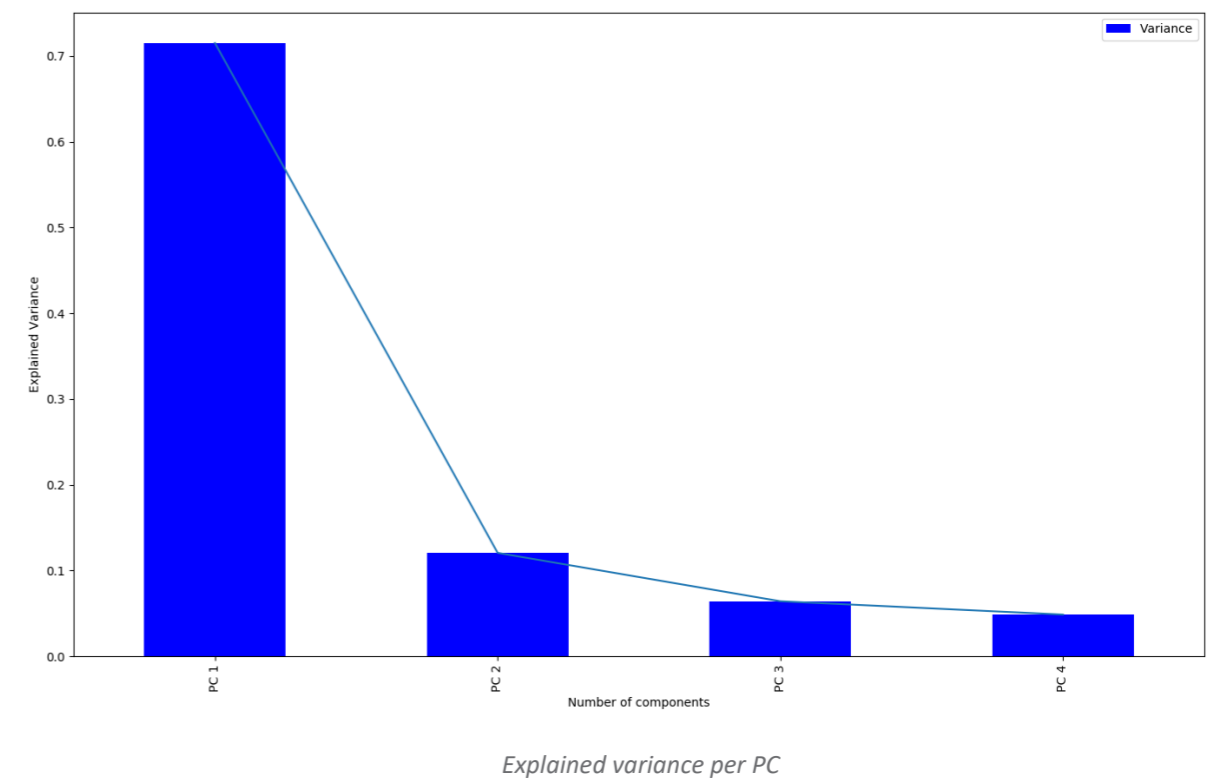
6.3.2 Principal Component Analysis (PCA)

A common approach in the analysis of anthropometric datasets is the Principal Component Analysis (PCA). It is useful to discover trends in the variation of multiple dimensions.

The PCA is a statistical procedure that transforms a set of variables into another shorter (easier to manage) set of variables called principal components. The components are then considered as a new set of variables that can characterize the variation of face shapes. The PCA transformation is defined in such a way that the first principal component explains the largest possible variance,

and each other component explain the highest variance possible under the constraint that it is orthogonal to the preceding components. The variance is a measure of how far a set of values are spread out from their average.

Beforehand proceeding with the calculation of the Principal Components, the dataset had to be normalized. After normalizing the dataset, all variables will have the same standard deviation, thus all variables will have the same weight in the PCA.



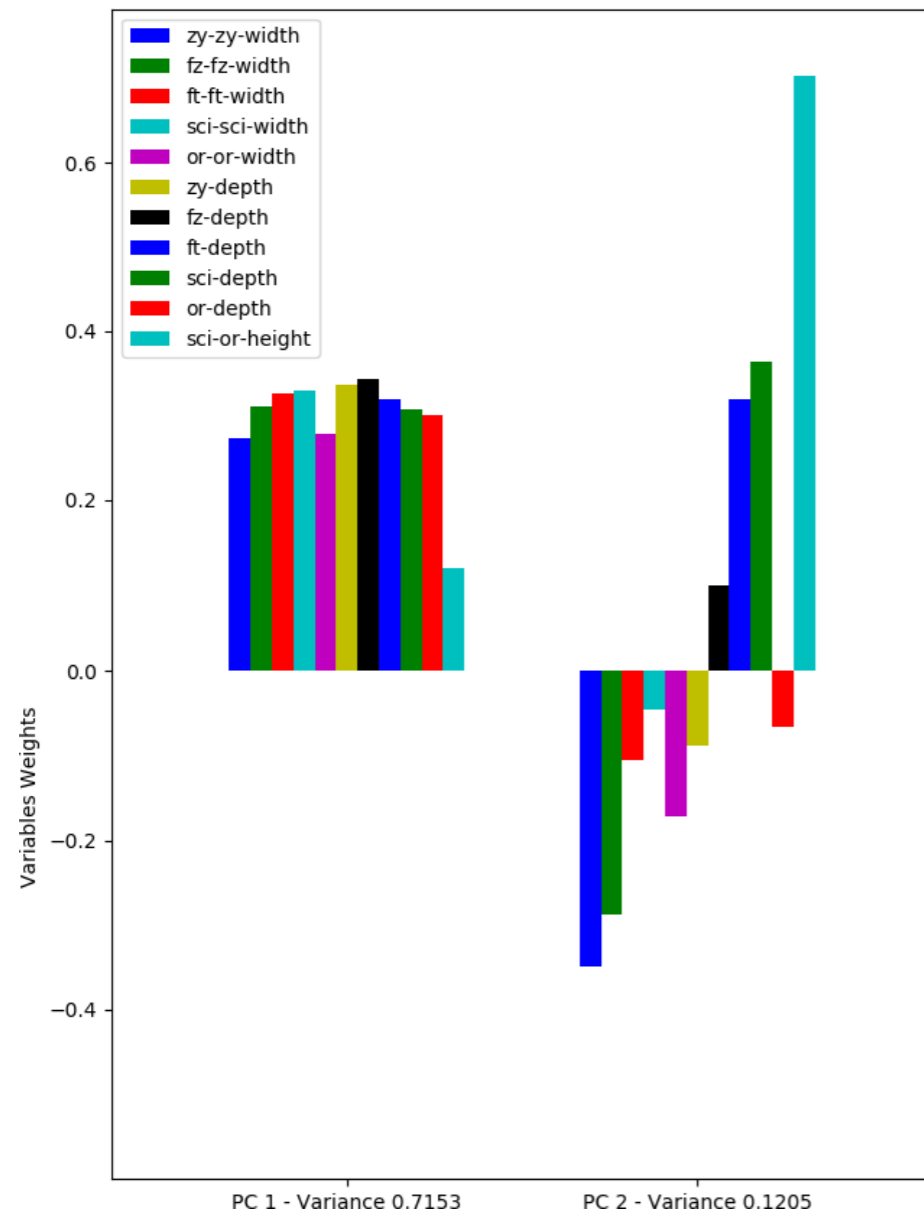
According to Lacko et al. (2017) a generally accepted method to select which components are most relevant to the shape variation is to select a number of components that explain a cumulative variance within a threshold of between 70% and 90%.

The variance of the components was calculated up to PC4, but since the two principal components explain 83.5% cumulative variance, only the PC1 and PC2 will be considered.

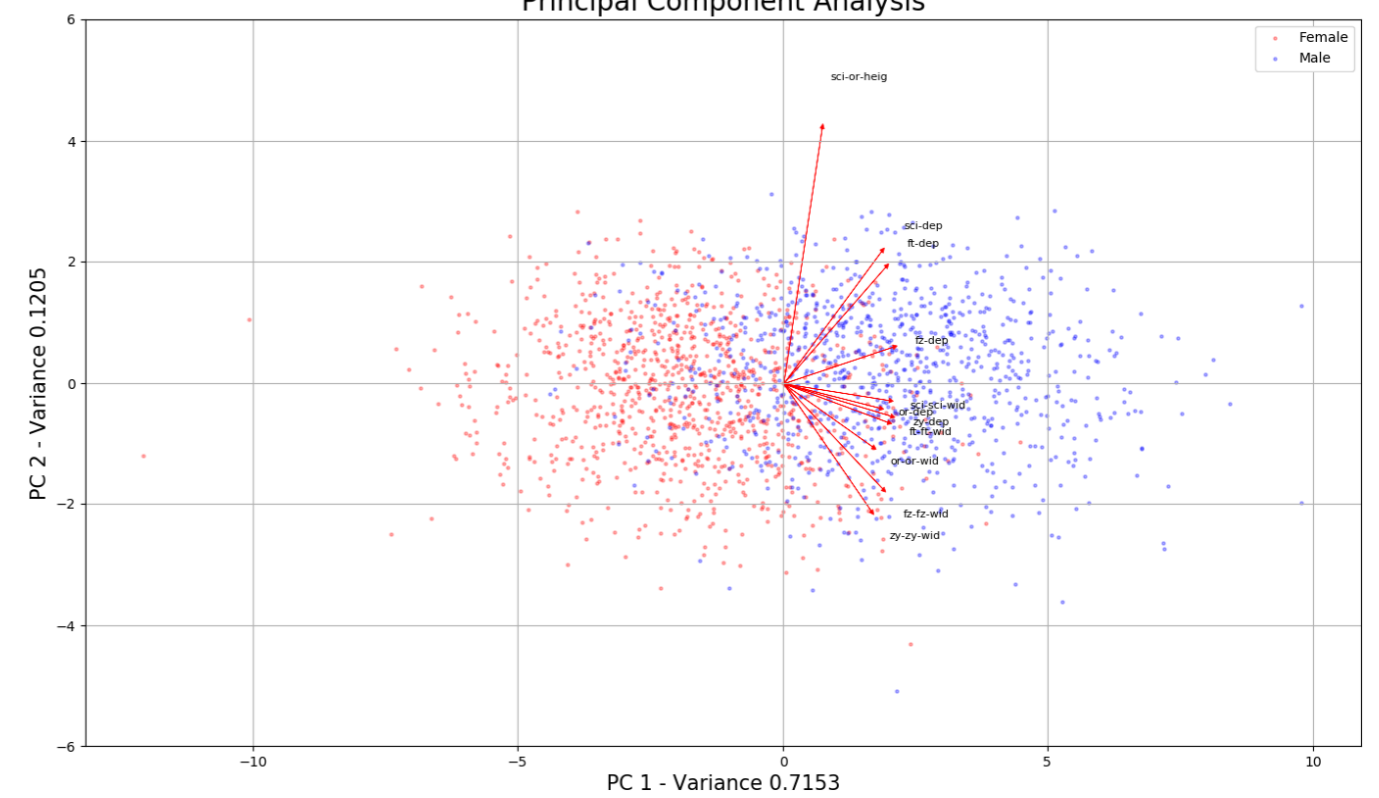
For the purpose of this project, PC1 and PC2 are sufficient to represent the variability of the face shapes underlying the mask section, and it also makes easier to display data in two-dimensional plots. More specifically, the component 1 accounted for the largest proportion of variance in the data explaining 71.5% alone, followed by 12% by component 2.

Description of the components

	PC1	PC2
1	fz depth x 0.343	sci-or height x 0.702
2	zy depth x 0.336	sci depth x 0.363
3	sci-sci width x 0.33	ft depth x 0.32
4	ft-ft width x 0.326	fz depth x 0.1
5	ft depth x 0.32	sci-sci width x -0.045
6	fz-fz width x 0.31	or depth x -0.066
7	sci-depth x 0.307	zy depth x -0.088
8	or depth x 0.301	ft-ft width x -0.105
9	or-or width x 0.279	or-or width x -0.173
10	zy-zy width x 0.274	fz-fz width x -0.288
11	sci-or height x 0.12	zy-zy width x -0.349



Principal Component Analysis



These tables and plots show the impact that each variable has on the two components and the distribution of the subjects. Overall, PC1 (horizontal scale) and PC2 (vertical scale) both reflect a combination of variables. More specifically, PC1 (horizontal scale) describes a similar and proportional variation of all variables, except for the sci-or height. On the other hand, PC2 mostly describes the variation of the sci-or height variable, together with positively and negatively correlated variables.

In practice, PC1 almost describes a uniform (except for height) scale of the human face. Thus, subject towards the right side have bigger faces than subjects on the left side. This is also confirmed by the higher concentration of male subjects

(blue points) at the right side of the plot, which have typically bigger anthropometric dimensions compared to female subjects (red points) highly concentrated at the left side of the plot.

Regarding PC2, subjects on the top of the plot have taller faces and subjects on the bottom have a shorter face. At the same time, at the top of the plot subjects have high values of ft depth and sci-depth, and low values of zy-zy width and fz-fz width, and vice-versa.

Even with these visualizations and interpretations, the meaning of each component is more easily visualized by displaying virtual mannequins of clusters and extremes that show more clearly the shape variation along each component.

6.4 Clustering and generating mannequins

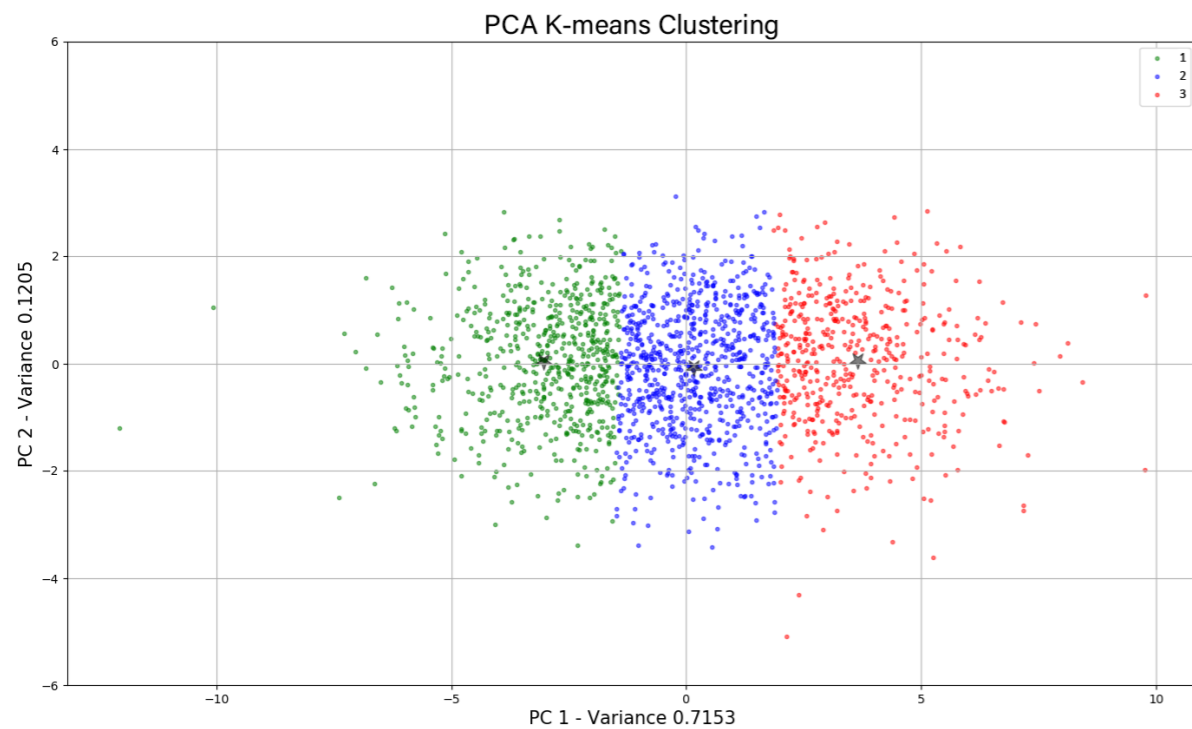
6.4.1 Clustering

Clustering is the process of grouping subjects into clusters that share similar characteristics (Lacko et al., 2017). The clustering method used in this project was the K-means algorithm.

K-means is a clustering algorithm that partitions a given set of data points into a user-specified number of clusters (Paquet, 2004). The algorithm works by iteratively clustering subjects based on

the average distance between its position in space (in this case a two-dimensional space with PC1 as X and PC2 as Y) and its closest cluster representative (centroid) which is the group mean.

The inputs given for K-means clustering were the principal components dataset and the number of desired clusters, corresponding to the number of sizes desired, set at 3 during the ideation phase.



This plot shows the result of the K-means clustering. The three clusters are displayed in different colours and their relative centroids (mean between all subjects in the cluster) are displayed by stars. The averages of the cluster 1 (green), 2 (blue) and 3 (red) will be used for the design of the S, M and L sizes respectively.

Observations

- The limits of the clusters are practically vertical. A cluster ends and the following starts at a specific value of PC1
- The clusters cover different areas, and may differ in number of subjects.

A numerical description of the clusters is provided in the following pages.

6.4.2 Averaging and extremes

From the list of subjects in each cluster, average mannequins were generated (Python - VTK Visualization toolkit, Kitware Inc.). The process of averaging 3D scans consists of:

- Extracting the points coordinates of all the 3D scans in one cluster
- Calculating the means of the coordinates of each corresponding point of the 3D scans in the cluster
- Re-building and exporting a new 3D model with the new points coordinates.

The three average mannequins will be imported in the CAD program in order to model the three sizes of the mask around them. Averages of clusters 1, 2 and 3 correspond respectively to the S, M and L sizes.

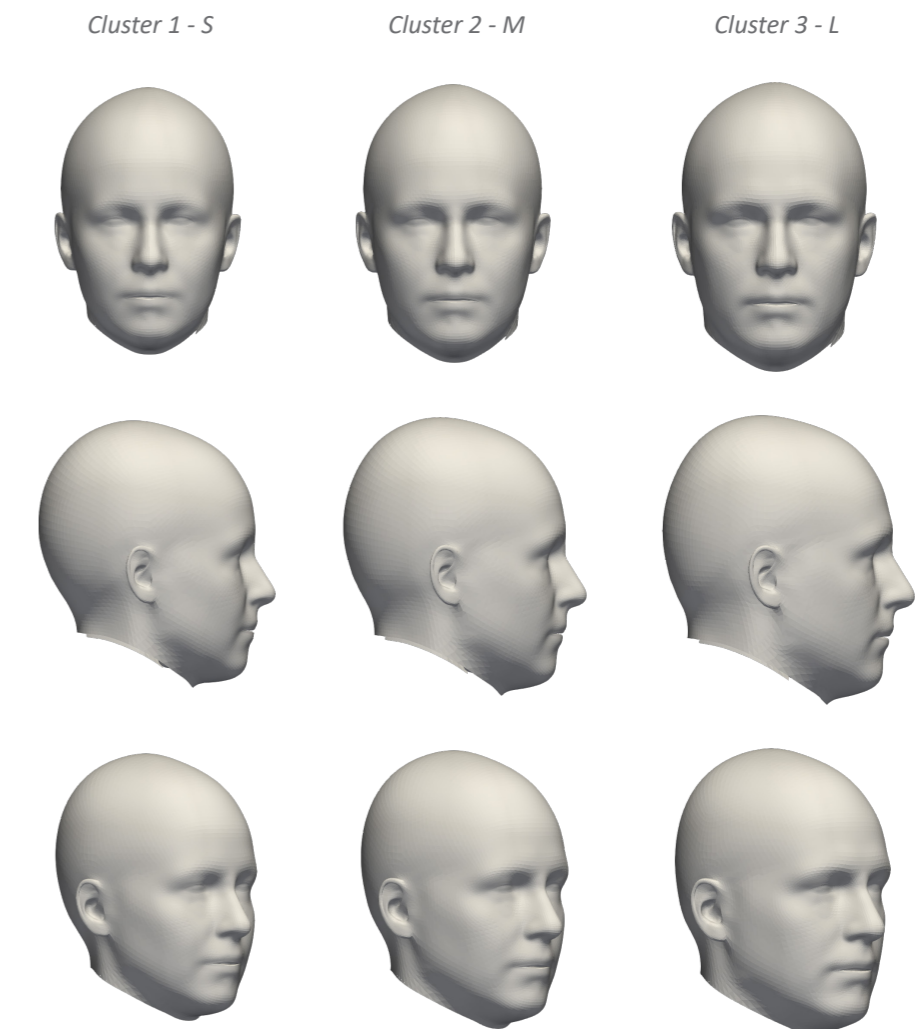
Extreme mannequins

According to Lacko et al. (2017) generating only cluster averages excludes many individuals which shapes are more extreme within the groups (Lacko et al., 2017). For this reason, other extreme mannequins were generated. For each cluster other four extreme mannequins were generated by averaging 20 extremes subjects along PC1 and PC2.

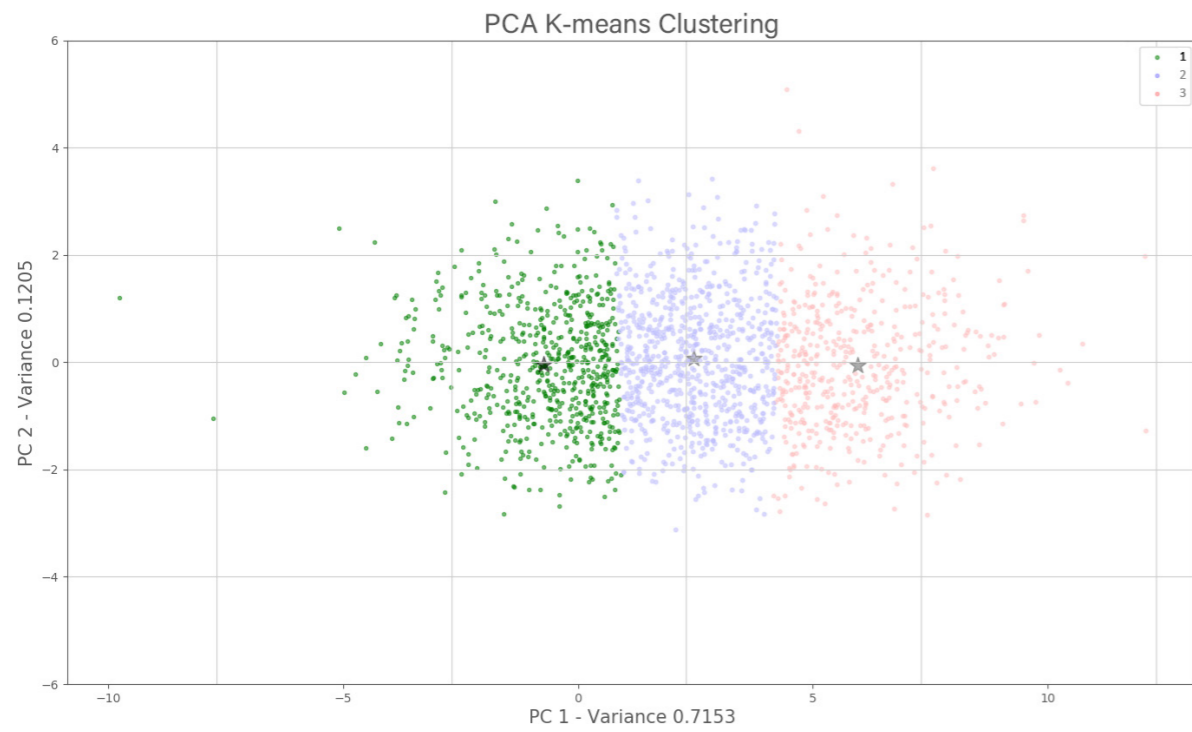
- PC1 Left
- PC1 Right
- PC2 Top
- PC2 Bottom

Four more mannequins were also generated from the combinations of these extremes.

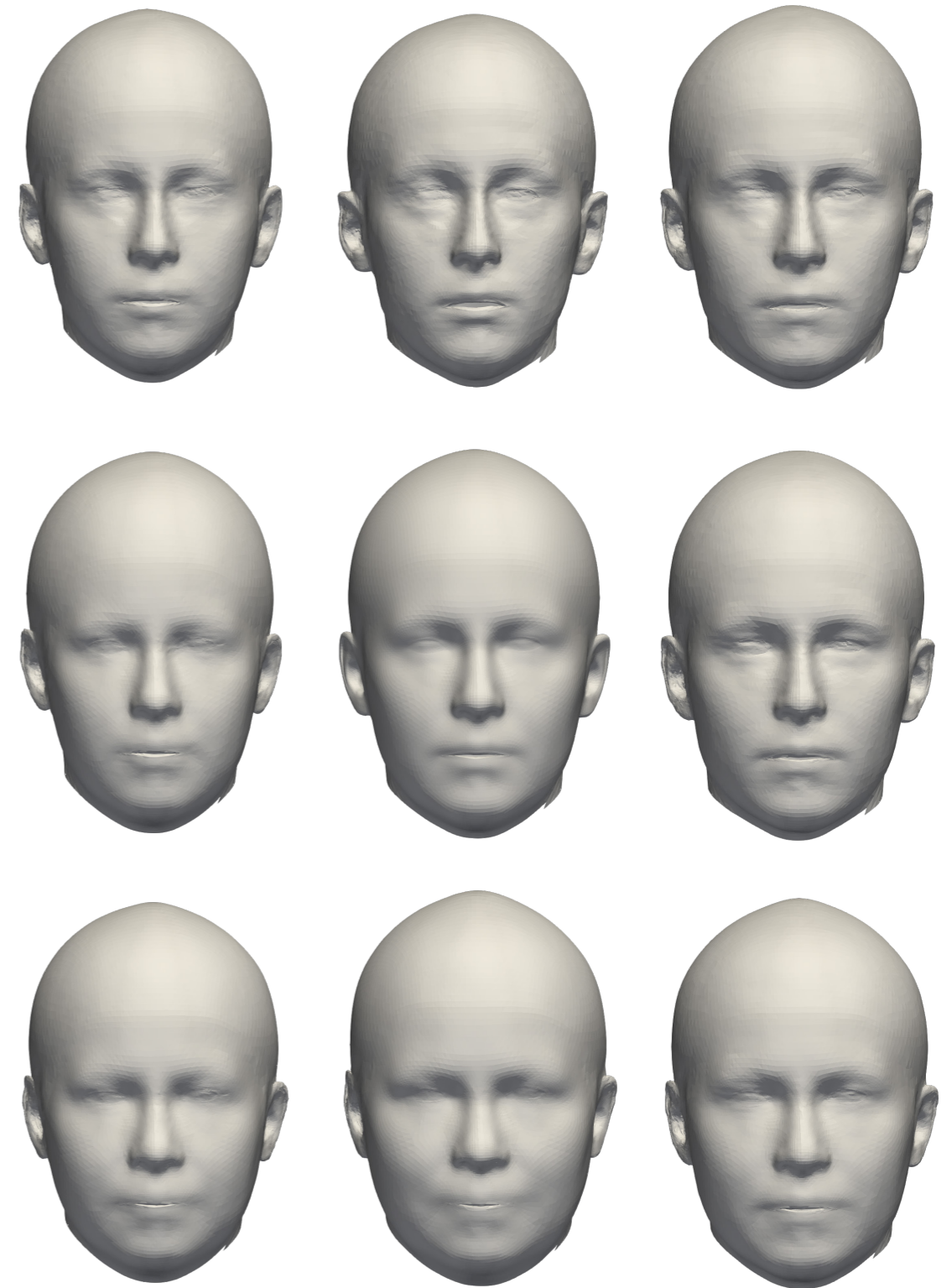
- Top/Left
- Top/Right
- Bottom/Left
- Bottom/Right



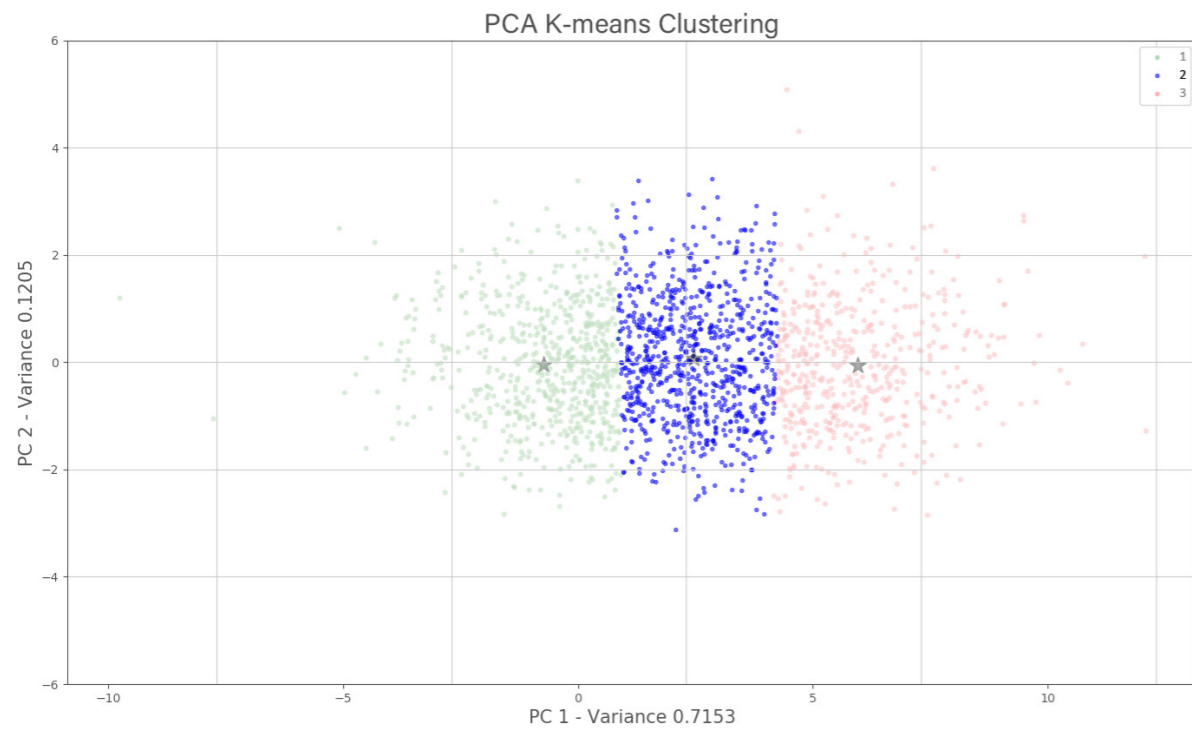
Cluster 1



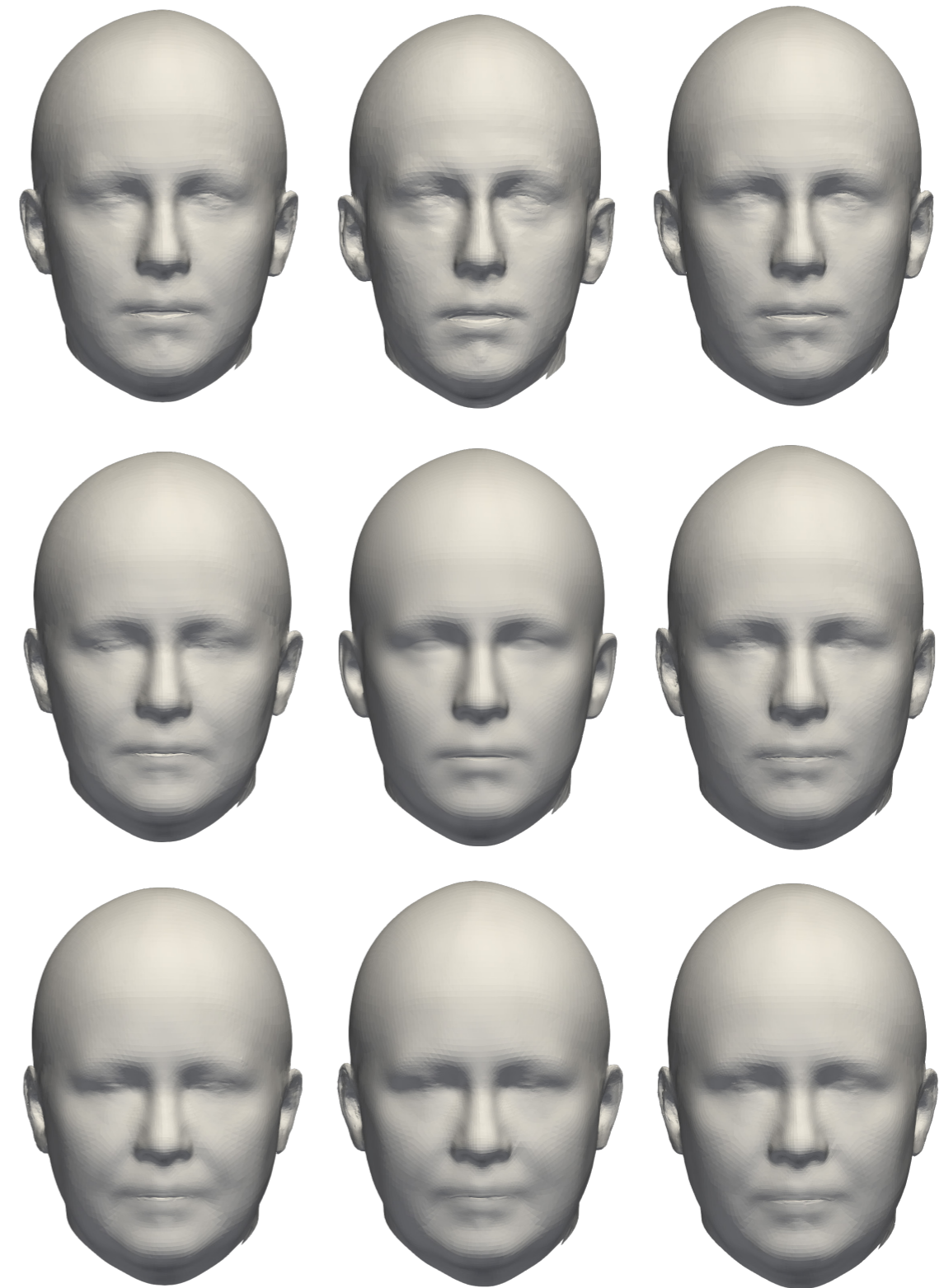
	Min	Max	Range	Average (Centroid position)
Components				
PC1 (X)	-12.06	1.39	13.45	-3.02
PC2 (Y)	-3.37	2.82	6.19	0.05
	Min (mm)	Max (mm)	Range (mm)	Average (mm)
Widths				
Zy-zy	102.5	136.5	34	122.45
Fz-fz	89	115	26	107.48
Ft-ft	73.9	94.7	20.8	88.83
Sci-sci	59.3	76.5	17.2	71.09
Or-or	49.5	74.4	24.9	64.03
Depths				
zy	65.6	89.8	24.2	83.09
fz	55.3	73.5	18.2	68.84
ft	42.4	57	14.6	52.81
Sci	32.9	43.7	10.8	39.91
Or	31.4	46.6	15.2	40.03
Height				
Sci-or	33.6	50.5	16.9	43.72



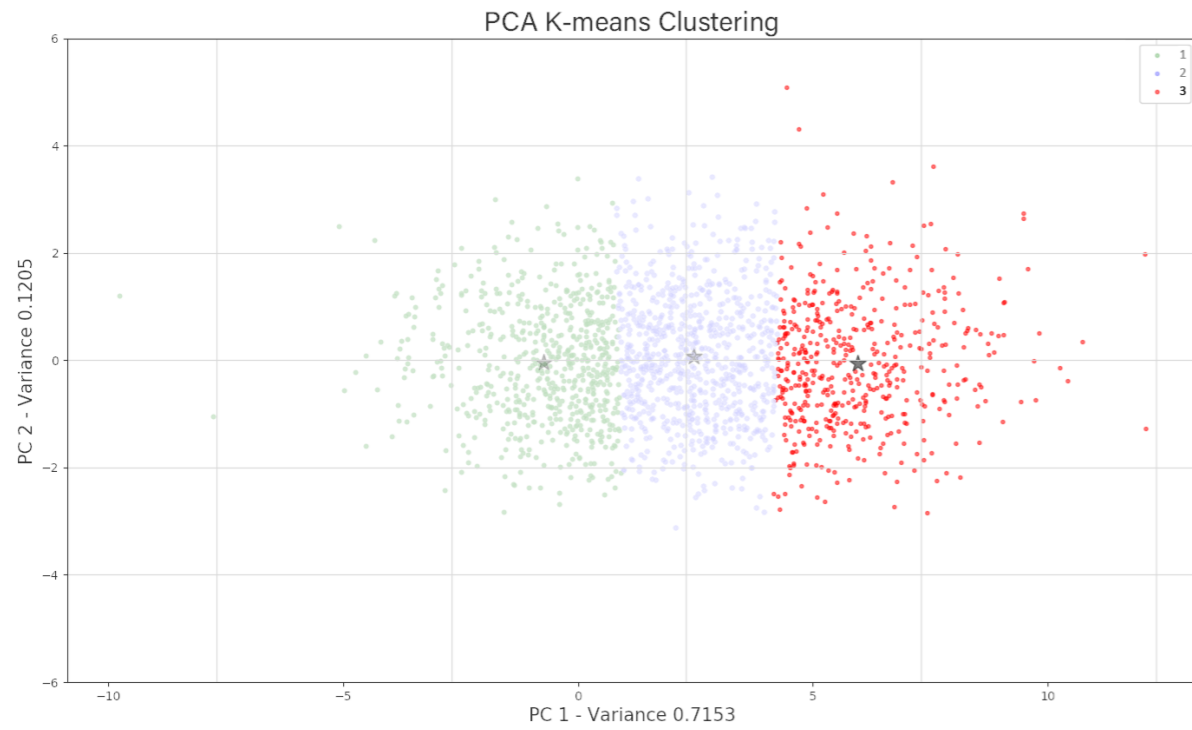
Cluster 2



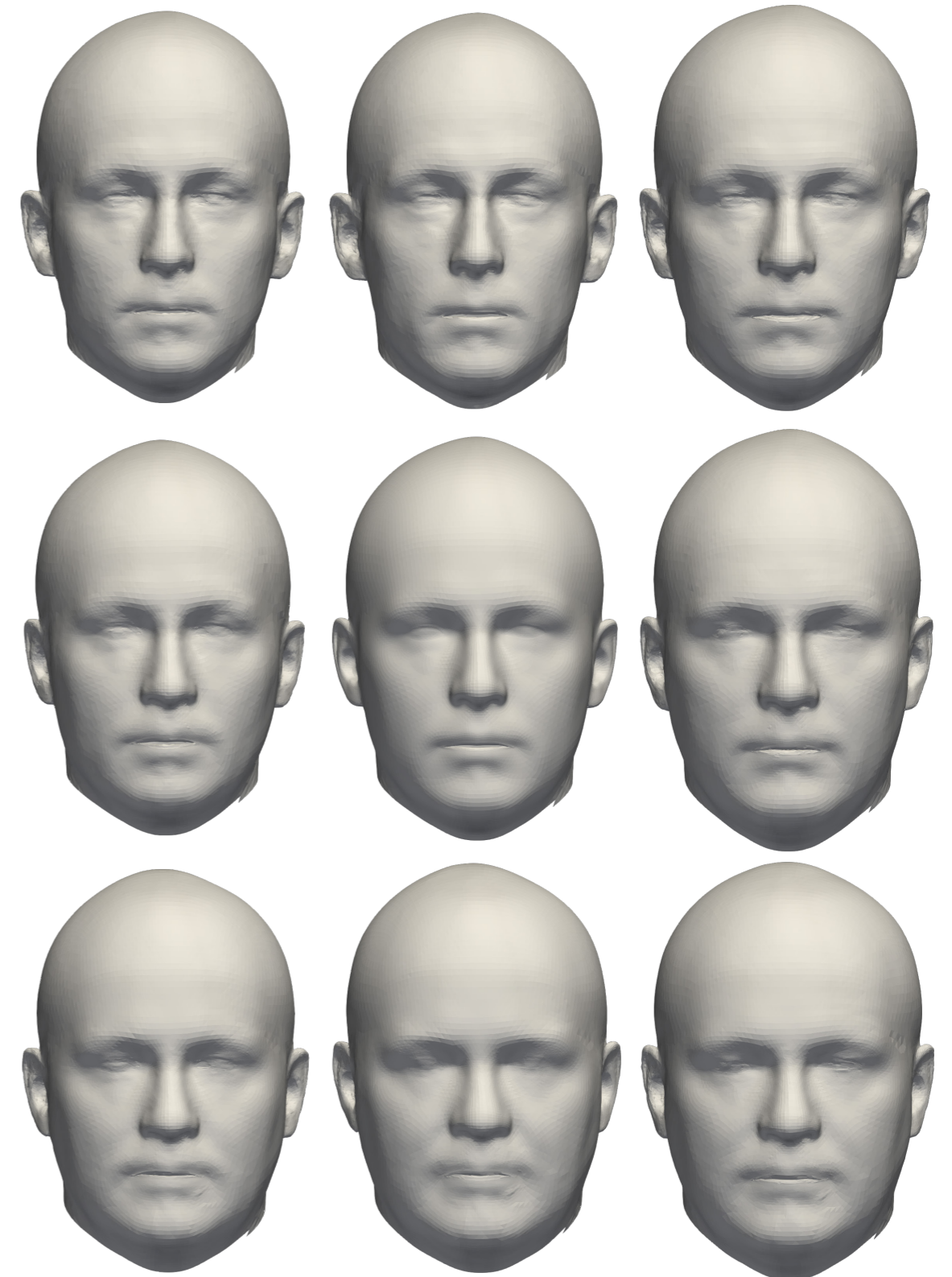
	Min	Max	Range	Average (Centroid position)
Components				
PC1 (X)	-1.49	1.91	3.4	0.16
PC2 (Y)	-3.41	3.12	6.53	-0.07
	Min (mm)	Max (mm)	Range (mm)	Average (mm)
Widths				
Zy-zy	115.9	143.2	27.3	127.88
Fz-fz	104.4	121.6	17.2	112.89
Ft-ft	86.5	99.5	13	93.41
Sci-sci	68.6	81.3	12.7	75.14
Or-or	54	79.5	25.5	68.71
Depths				
zy	80.3	95.8	15.5	88.15
fz	67.5	77.7	10.2	73.07
ft	50.9	61.3	10.4	55.92
Sci	38.1	48.4	10.3	42.38
Or	34.7	52.6	17.9	43.85
Height				
Sci-or	37.2	53.9	16.7	44.59



Cluster 3



	Min	Max	Range	Average (Centroid position)
Components				
PC1 (X)	1.85	9.78	7.93	3.66
PC2 (Y)	-5.08	2.85	8.65	0.05
	Min (mm)	Max (mm)	Range (mm)	Average (mm)
Widths				
Zy-zy	123.2	149.1	25.9	133.35
Fz-fz	109.5	128.9	19.4	118.12
Ft-ft	92.1	108.2	16.1	98.27
Sci-sci	74.1	89	14.9	79.54
Or-or	60.4	85.6	25.2	73.64
Depths				
zy	85.9	105.3	19.4	93.55
fz	72.8	85.6	12.8	77.79
ft	53.5	67.1	13.6	59.61
Sci	39.9	52.2	12.3	45.36
Or	37.1	58.4	21.3	48.1
Height				
Sci-or	32.3	56.2	23.9	46.06



6 Anthropometric study - Summary and conclusions

- The anthropometric study will be conducted on a 3D scans database of European population (represented by subjects from Italy and Netherlands). The North American database was excluded in order to simplify the study. This choice influences the results of the study but does not exclude that the fact that extra-European users will benefit from the design of a sizing system.
- The craniofacial landmarks underlying the mask section and the ones useful for the definition of the plane were selected. Whereas two or more landmarks were in extreme proximity, only one was selected and the other excluded.
- The scans were aligned by translating the sellion to the origin of the world coordinate system and by rotating them in such a way that the normal vectors of the defined planes (Frankfort translated to the sellion, frontal passing through the sellion and midsagittal) were aligned with the world coordinate system.
- 11 measurements (variables) were considered as descriptive of the face section underlying the mask and relatable to the mask dimensioning (1 Digital CAESAR, 1 Traditional CAESAR, 9 Digital Python / 5 widths, 5 depths and 1 height)
- Variables correlation results: all pair of variables are positively correlated; the variables in the same group (widths, depths) are highly correlated; some variables from different groups were also highly correlated.
- Principal Component Analysis results: PC1 explains 71.5% of the variance and seems to describe a uniform (except the height) scale of the human face; PC2 explains 12% of the variance and mostly describes the height of the face.
- The dataset was clustered in three groups, one for each size.
- For each cluster an average mannequin was created as well as 4 extreme mannequins along PC1 and PC2 and 4 more mannequins that are combinations of the extremes.
- The average mannequins will be used in the design of physical sizes for the VR headset mask. The extremes and the combination of extremes mannequins are useful to check the fit of each size against extreme subjects in the cluster.

7

Chapter 7 **PROTOTYPING AND TESTING**

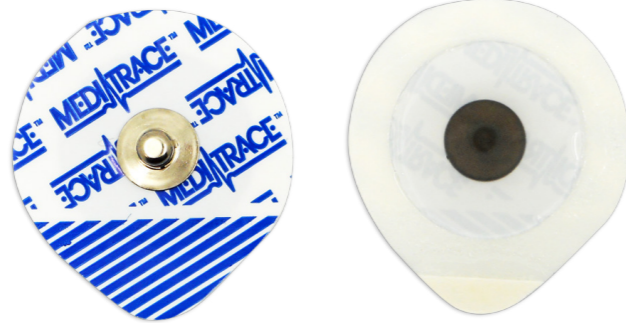
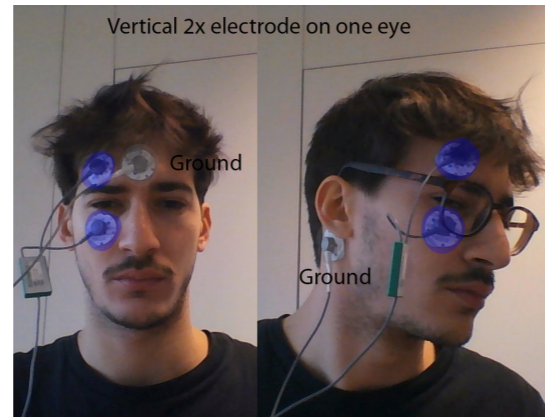
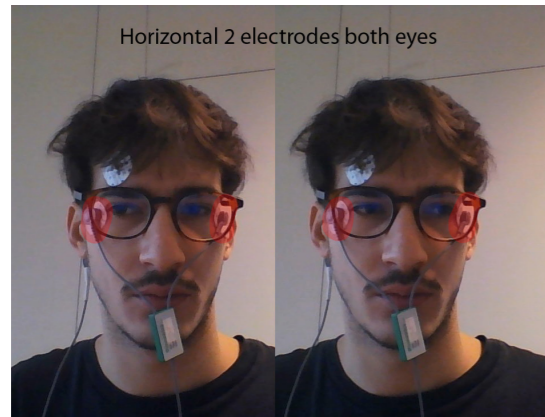
The prototyping stage followed an iterative method where several quick and dirty mock up were created at different stages to test specific aspects of the project. Then, a final prototype was designed in CAD and built for testing and demonstrational purposes. In the following sections a summary of the first iterations is presented and then the final prototype is discussed in details. Detailed information on the experiments can be found in the Appendix 6.1.

7.1 Prototyping iterations

7.1.1 Experiment with EOG signals

As first experiment, EMG instrumentation (www.biometricsltd.com) and single-use adhesive electrodes available at the faculty were used to capture and analyse EOG signals for the first time. Also, the aim was to test the different positions (configurations) of the electrodes found in literature.

The recorded signals were clearly a response of eye movements but it was impossible to discrete the proportionality of the signal to the angle of rotation. This was mostly attributable to wrong instrumentation and signal processing settings.



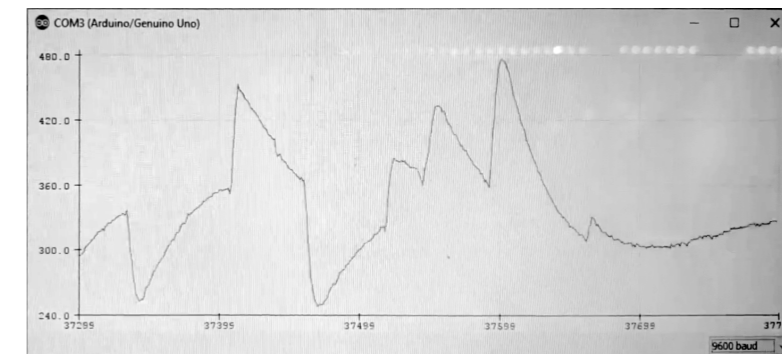
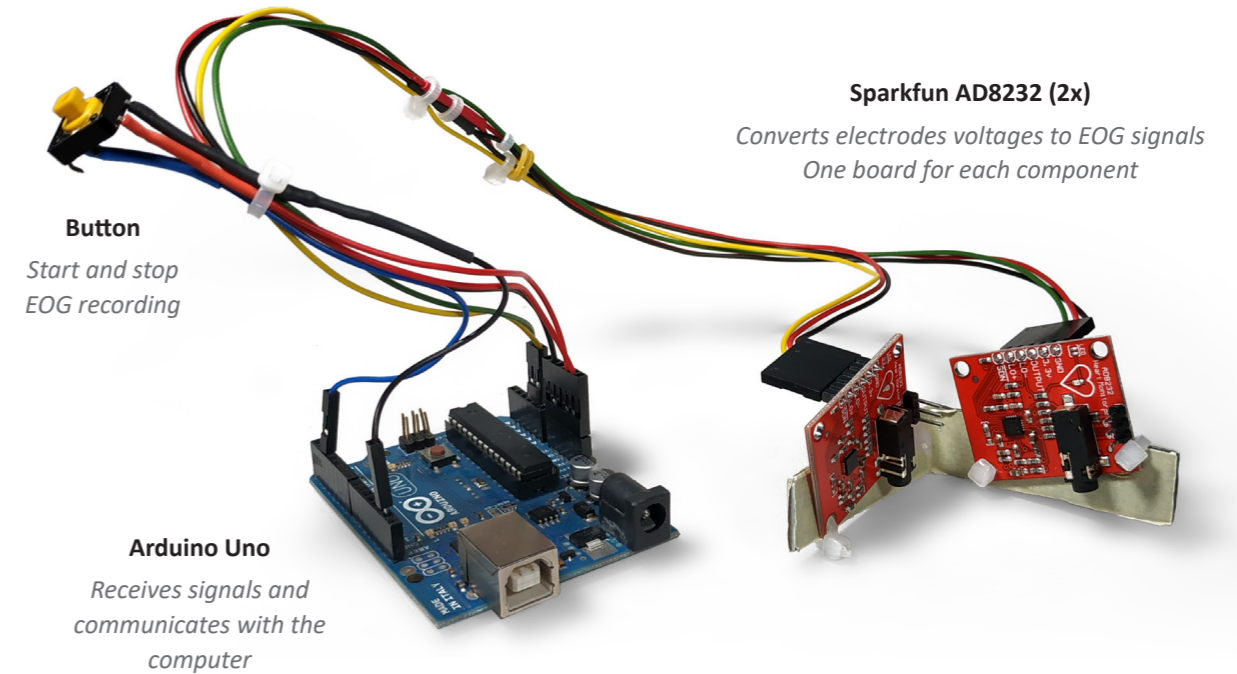
Single-use adhesive electrodes, front and back sides

7.1.2 Testing of Sparkfun board

The second iteration focused on testing the Sparkfun AD8232 ECG board to evaluate the possibility of using it for EOG measurements. The leads were connected to single-use adhesive electrodes attached in the positions chosen during the ideation phase.

Finally, the recorded signals were not only an indication of the direction of the gaze, but there was a clear proportionality between the angle of rotation of the eye and the amplitude of the signal. On the other hand, while sustaining the gaze at

any point (other than the eyes rest position), the signal would return to zero in a really short time. This behaviour would ultimately make impossible to estimate the gaze point on a surface as the VR screens. The reason is attributable to the low pass filter on the board. After several tests an optimal configuration was found by substituting two capacitors from an original value of 0.33 μF to 1 μF , triplicating the recovery to zero delay and thus allowing to discrete saccades, smooth pursuits and fixations.

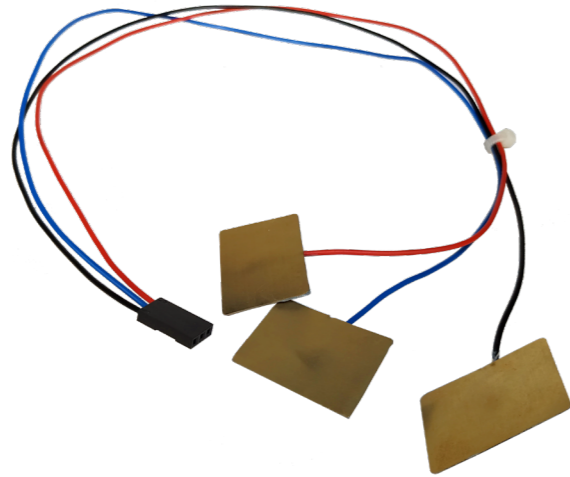


EOG signals recorded with the above setup and adhesive electrodes placed as the horizontal configuration displayed on the left page

7.1.3 Testing of custom-made dry electrodes

The third iteration regarded building and testing custom made dry electrodes. Thanks to previous experience it was immediately possible to build dry electrodes with copper plate and wiring. Since

copper plates electrodes immediately resulted in good quality signals, and also due to lack of time and budget, the performance of other materials found in literature was not further investigated.



7.2 Final prototype

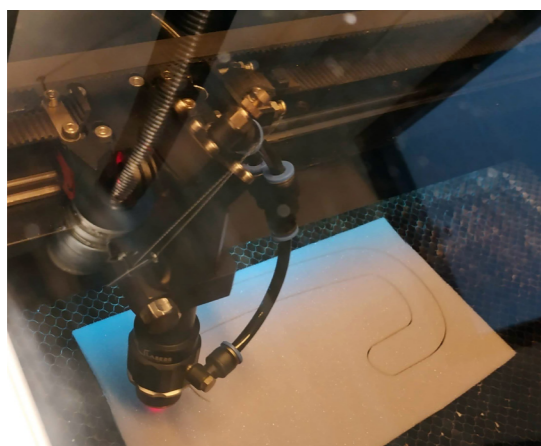
The final prototype was created with the properties discussed during ideation phase. Its purpose is to demonstrate the functioning of EOG on a VR headset and to test the comfort of the newly designed sizing system. It will be used for user testing.

7.2.1 Foam part

The foam part was prototyped by lasercutting foam. The initial intention was to lasercut an individual sheet of foam of the desired thickness. However this was not possible because the foam would burn under the intensity of the laser. For this reason, the laser was set at really low intensity in order to cut three thinner sheets of foam, that

glued on top of each other would reach 17 mm in thickness (as HTC Vive). No other thickness of foam parts were experimented for lack of time.

The foam sheets were different in properties. By emulating ski masks, the three layers were ordered by harder to softer (measured in kiloPascal) towards the contacting part with the skin.



- Yellow layer (face)
5 mm - 4 kPa (softest)
- White layer
7 mm - 8 kPa
- Grey layer
5 mm - 16 kPa

7.2.2 Translation of mannequins into physical sizes

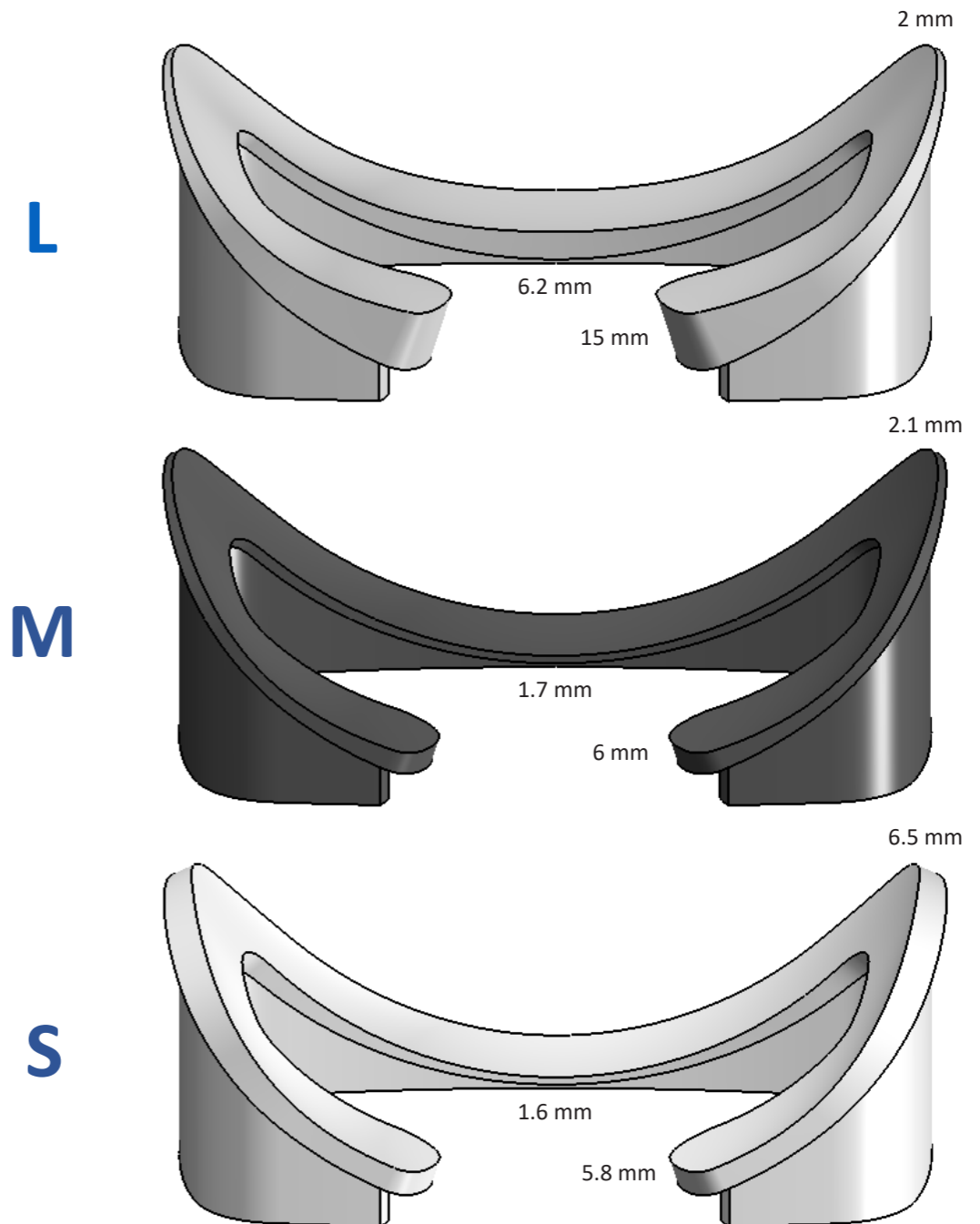
In order to translate the digital mannequins into physical sizes, three snap-ins modules were created and prototyped (3D-printing). The HTC Vive original mounting surface (lower surface) was kept identical to the original headset, while the top surface derives from a boolean subtraction of the volume of each mannequin model.

size piece it deforms taking the shape of the top surface deriving from the relative mannequin.

In the picture some thickness measurements are given at three points to give an indication of the differences in shapes between the sizes.

The extruded volume at the bottom is used to snap the sizes prototype into a body which replicates the HTC Vive headset.

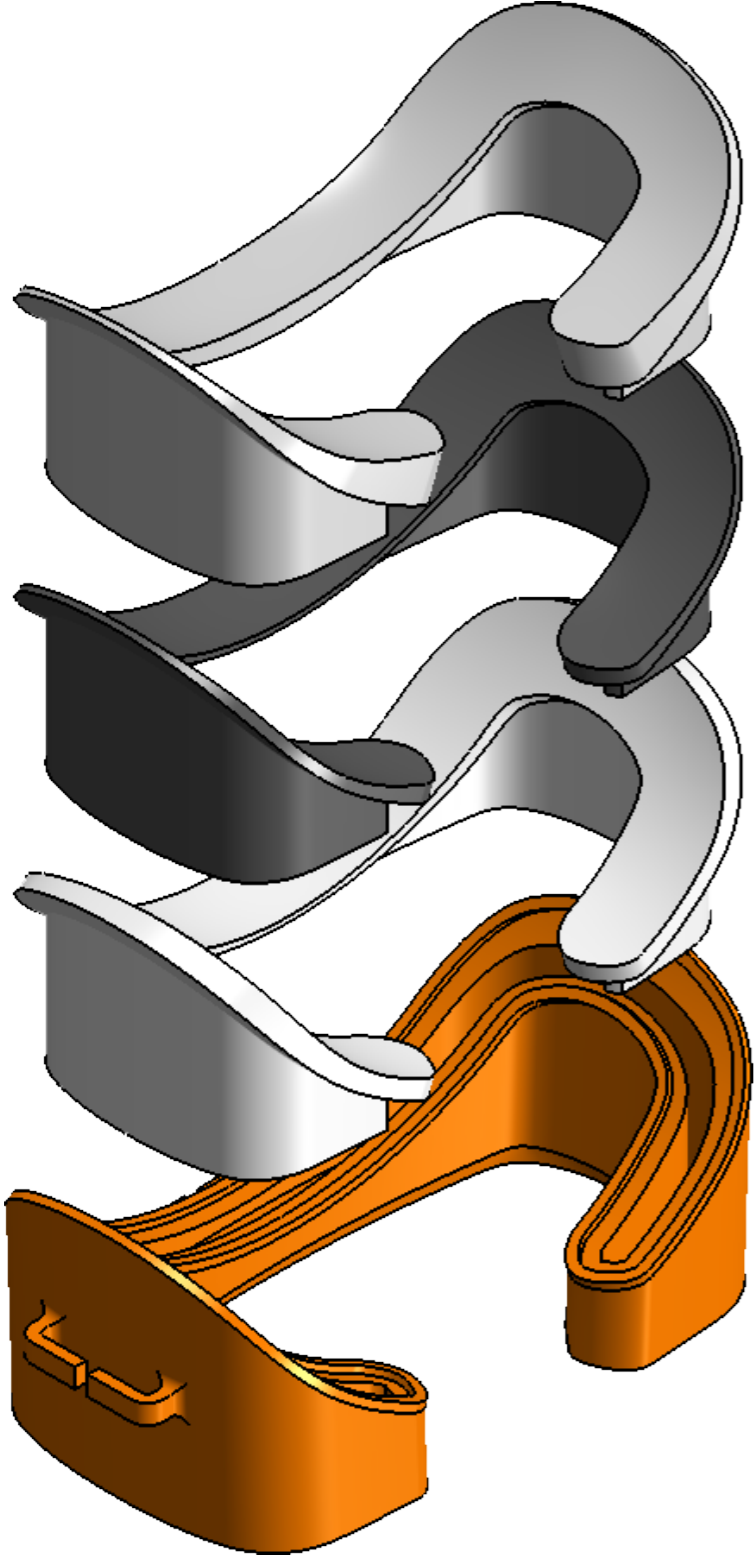
When the foam part is placed on top of the



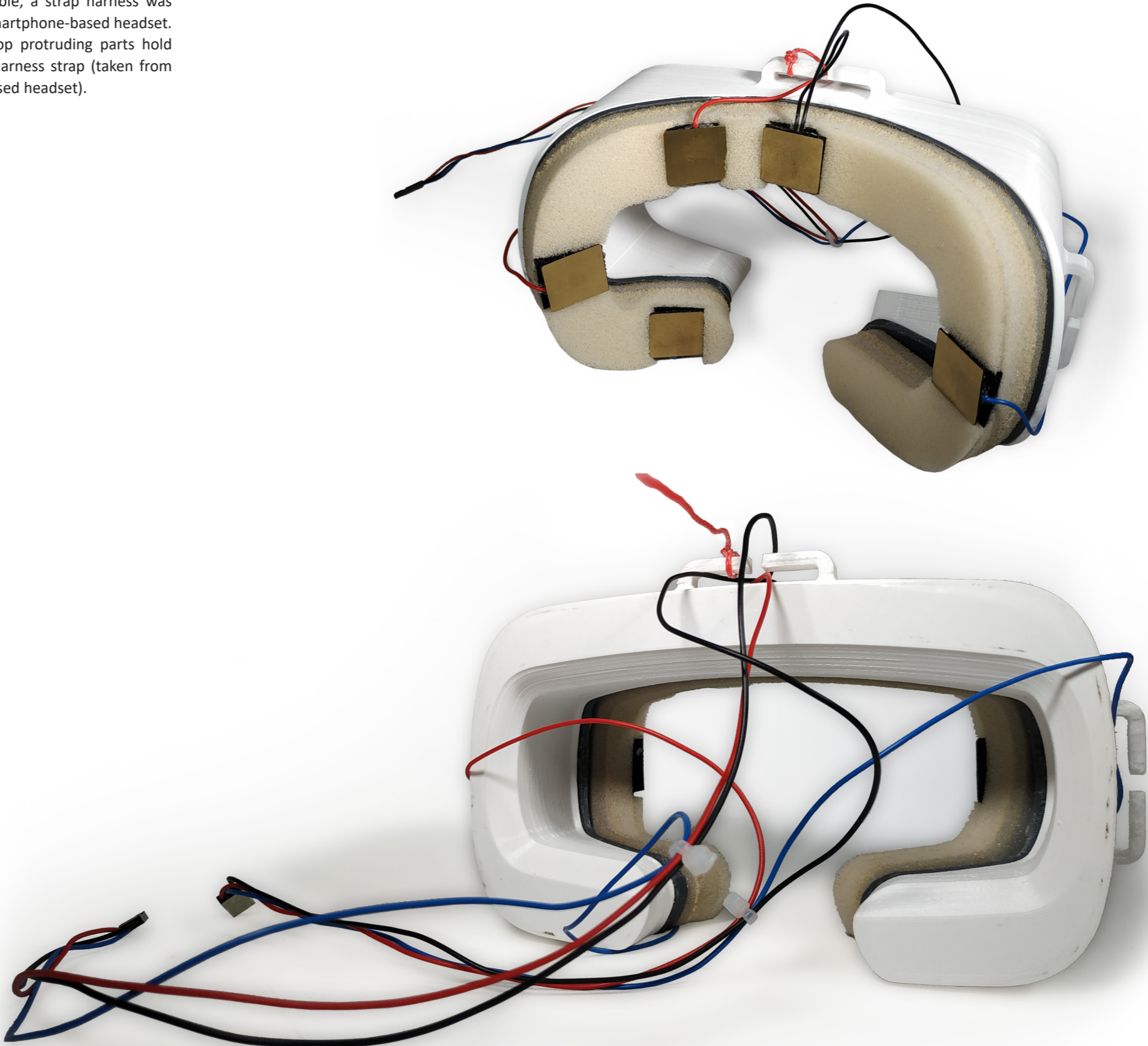
7.2.3 Main body

The prototype main body (orange) is a simplified replication of the HTC Vive. It emulates the shape of the original headset but does not contain any other hardware. The mounting surface has a three-dimensional hole where the sizes pieces can slide in and hold in place.

Since using the actual harness system of the HTC Vive was not feasible, a strap harness was taken from a cheaper smartphone-based headset. On the sides and on top protruding parts hold the three ends of the harness strap (taken from another smartphone-based headset).

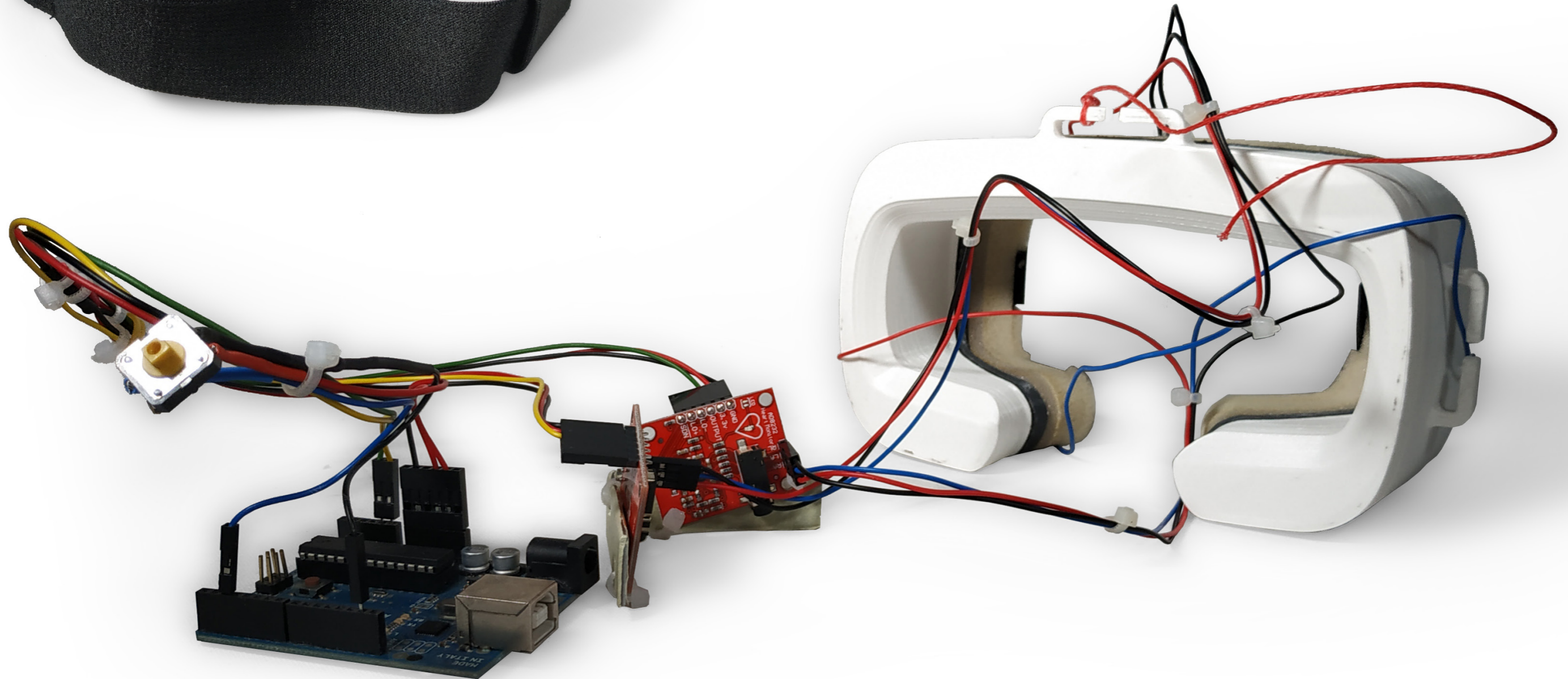


7.2.4 Physical prototype



7 Prototyping and testing - Summary and conclusions

- EMG instrumentation can receive signals that are an indication of eye-rotations but it is impossible to discrete the proportionality of the signal to the angle of eye rotation.
- With Sparkfun AD8232 it is possible to receive signals that are clearly proportional to the angle of eye rotation but the low pass filter makes the signal go to zero quickly even while sustaining the gaze at some angle. Increasing the value of two capacitors can slow down this behaviour enough to discrete saccades, smooth pursuits and fixations.
- Dry electrodes produced with copper sheet and wiring give good results in EOG signal acquisition. No other materials could be tested for lack of time.
- The foam was produced by lasercutting three layers of foam in the mask shape. The foam goes from harder to softer towards the layer that contacts the face.
- The three physical sizes are 3D-printed parts that can be mounted on a body that emulates the dimensions of the HTC Vive. They were created using the cluster mannequins.
- The foam is placed on top of the physical size parts and adapts to their shape.
- The final prototype has the purpose of demonstrating the functioning of EOG on a VR headset and testing the comfort of the newly designed sizing system. It will be used for user testing.



8

Chapter 8
USER TESTS

8.1 User test

8.1.1 Research questions

The purpose of the user test is to answer the following research questions:

Contact

- Is for each test subject, at least one (out of three) size of the mask able to ensure sufficient contact between skin and dry electrodes to provide EOG signals?
- Is each subject able to wear the mask correctly without assistance in such a way that stable EOG signals are recorded?

Signal properties

- Are the EOG signals recorded proportional to the angles of eye rotations in the horizontal and vertical direction?
- Are the different kinds of conjugate eye movements recognisable by analysing the recorded signals?

Ergonomics

- Collect subjective data on the level of comfort and discomfort that each size of the mask provides to each test subject at relevant contacting areas
- Evaluate the relationship between the perceived comfort/discomfort and the properties of the EOG signal

Other instances to be evaluated

- Evaluate the EOG signals collected from the same subject with different sizes (when applicable)
- Evaluate the EOG signals collected among the same size in different subjects

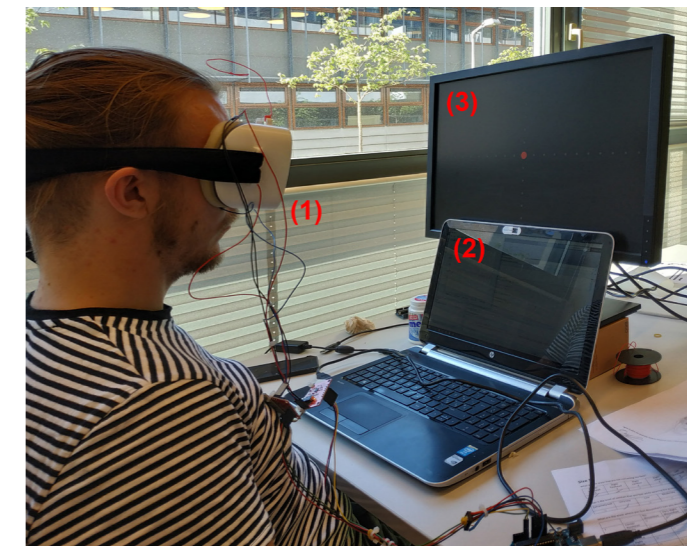
8.1.2 Equipment and test setup

The following equipment was used during the experiment:

1. Final prototype
2. Laptop computer running Matlab
3. Laptop computer connected to a 22 inches (~ 47 x 29.5 cm) screen displaying the exercise video
4. Adjustable chair

One laptop (1) was used to receive and record signals from the Arduino Uno connected to the prototype. The Arduino was communicating to the laptop with Matlab software (www.mathworks.com), used to live plot (in real time) the signals and store data in a spreadsheet file for further analysis.

The second laptop (2) was connected to a 22 inches screen with the only purpose of showing the test video (paragraph ...) displaying a series of exercises where points would appear, disappear and move around the screen.



8.1.3 Procedure

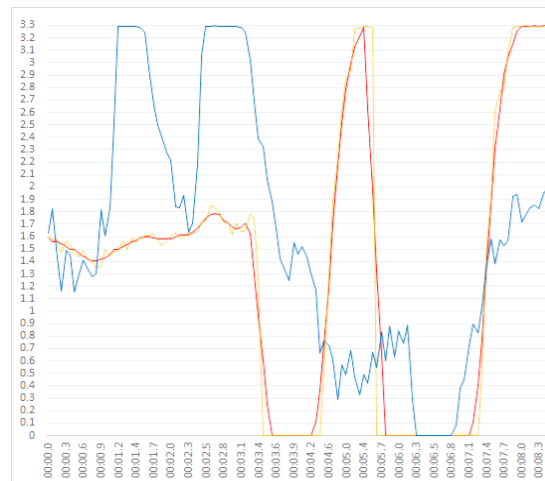
Preparation

1. The prototype is prepared with the S size of the mask
2. The test subject is asked to sit on the chair in front of the set-up.
3. The subject is asked to fill the demographic questionnaire
Meanwhile, the subject is informed about the EOG working principle and the test procedure and
4. The chair gets regulated in such a way that the subject's head (in a straight-forward position) is aligned vertically with the red dot at the center of the screen, and the prototype is at a distance of 40 cm to the screen.
The red string on the prototype is used to assure the correct distance to the screen
5. The subject is asked to wear the prototype without assistance

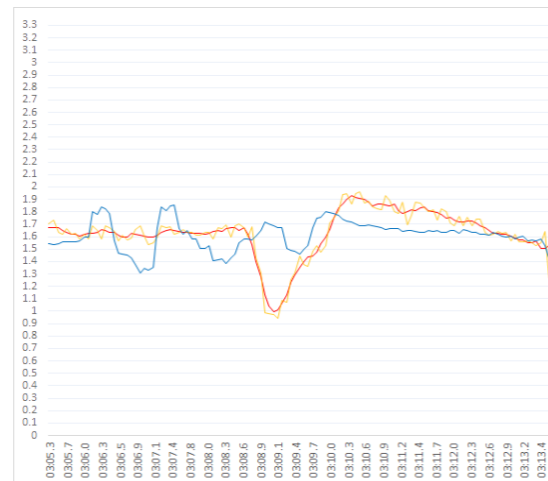
Recording

6. The Matlab program is started and the live plot is checked to see if EOG signals are being captured
If the signal randomly fluctuates reaching 0 and 3.3 V, it means that there is a lack of contact between the face and all electrodes
7. The subject has to wear the prototype for 5 minutes
8. The subject fills the comfort/discomfort questionnaire
7. The Matlab and the screen video capture software are set to record
8. The user is asked to not move the head and follow the instructions showing on the video, (duration of approximately 5 minutes).
9. The screen video capture and the signals are exported and stored on the computer for further analysis
10. The subject is asked to fill the comfort/discomfort questionnaire

The whole procedure is repeated for size M and L



Signals received whereas not all electrodes are contacting the subject's skin



Signals received with complete contact, during reading of the video instructions

8.1.3 Questionnaire description

In order to collect demographic data, and answer the research questions regarding the comfort/discomfort of the mask, subjects were asked to fill a questionnaire. The complete questionnaire is available at the Appendix ...

Demographic data

The demographic questions collected the following data:

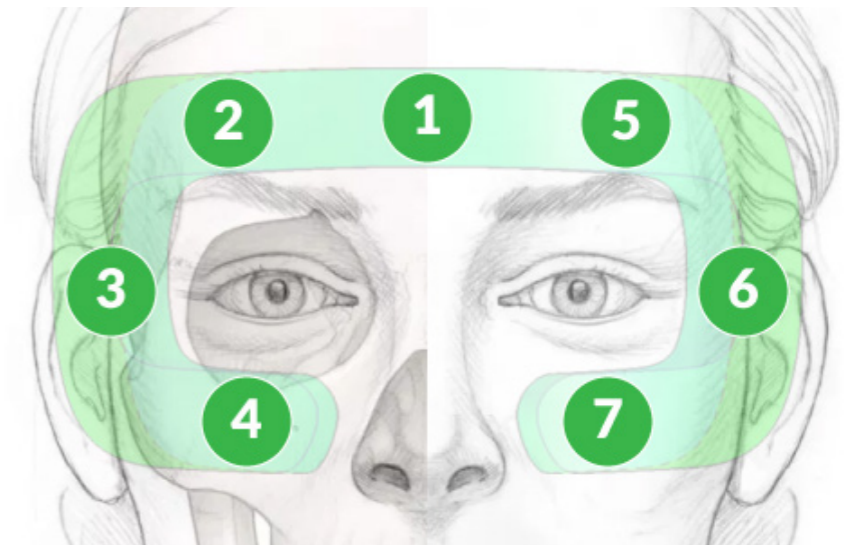
- Gender: Male / Female
- Age
- Nationality
- Nationality father / Nationality mother

Collecting detailed information on the nationality of the subjects and their parents relates to the fact that the anthropometric analysis was performed on a database of European subjects. For this reason, it is expected that the sizing system would perform best (at least one size provides contact for all electrodes) with European subjects. Nevertheless, it is also interesting to test with non-European subjects.

Contact

In case the EOG signals are not stable, it means that some electrodes are not contacting the subject's face. It is useful to note the position of the non-contacting electrodes.

1. Center forehead
2. Right forehead
3. Right canthus
4. Right cheek
5. Left forehead
6. Left canthus
7. Left cheek



Comfort/discomfort

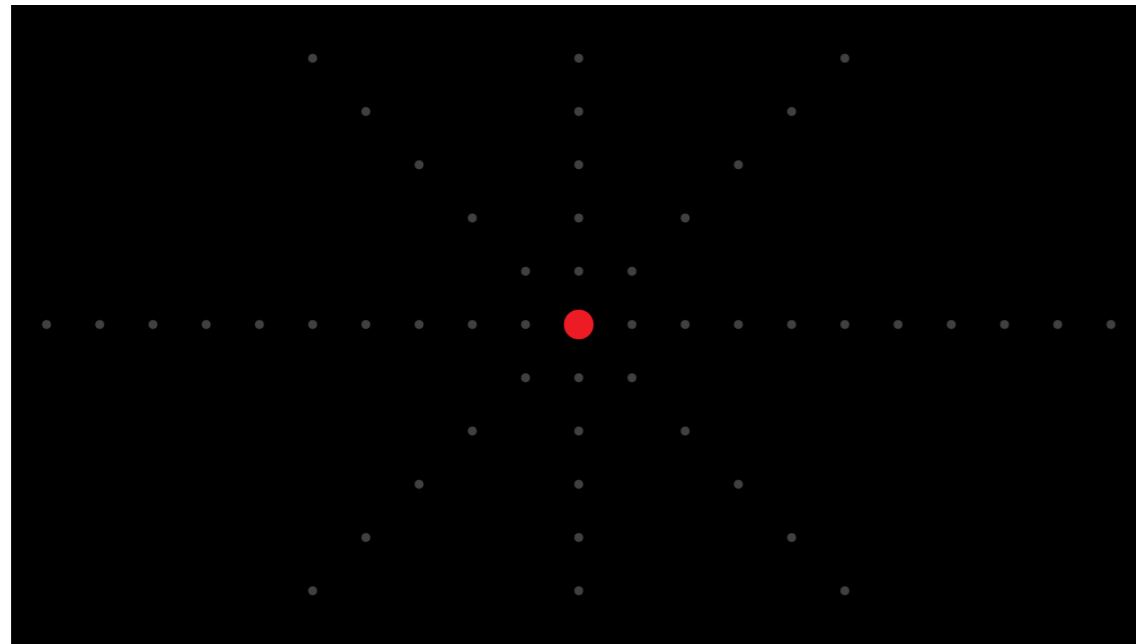
After 5 minutes of wearing the prototype, the subjects had to answer questions about the overall level of comfort of the prototype. Then the subject had to describe for each of the 7 areas, the perceived level of discomfort. A well-known tool for such ratings is Porter's seven-point comfort rating scale (Porter et al., 2003). These questions were repeated for each size of the mask.

8.1.4 Video stimuli description

The video shown to the test participant has been designed with the following purposes in mind:

- Provoke the different of eye movements that are possible in VR: saccades and smooth movements
- Evaluate whether opposite direction of a rotation (left or right, top or bottom) translates into opposite (positive or negative) signals (considering $3.3V / 2 = 1.65V$ as the zero)
- Evaluate the signal amplitudes both for small and extreme eye rotations in the vertical, horizontal and oblique directions
- Evaluate EOG signals during movements which are a combination of horizontal and vertical rotations (oblique)
- Evaluate the effect of artefacts (mainly blinking)

In order to research the aforementioned behaviours, the video consisted in 23 exercises where dots appeared, disappeared and moved on a grid in the horizontal, vertical and diagonal axes. A complete description of the exercises is available in the Appendix



Minimum angle of rotation

The distance between the dots is around 2.25 cm in the horizontal and vertical axes, and 3.25 in the diagonal axis. With the eyes at a distance of 40 cm to a screen of 22 inches (~ 47 x 29.5 cm), rotating the eyes from one point to the next in the horizontal and vertical axes would require a rotation of around 3.2 deg. Moving from one point to the next in the oblique direction would require the eyes to rotate with the same angle, in the horizontal and vertical direction at the same time.

8.1.5 Subjects

The test subjects were a total of 7, 5 males and 2 females. They all were students of the faculty of Industrial Design at TUDelft between 22 and 26 years old. All the subjects had no previous knowledge regarding the prototype and its working principle.

- Subject 1 - B*****a, Female, 24 years old, Italian (same as both parents)
- Subject 2 - D*****I, Male, 23 years old, Indian (same as both parents)
- Subject 3 - B*****n, Male, 25 years old, Turkish (same as both parents)
- Subject 4 - F*****c, Male, 25 years old, German (same as both parents)
- Subject 5 - S**a, Female, 22 years old, Turkish (same as both parents)
- Subject 6 - D*****I, Male, 25 years old, Dutch (both parents Ukrainian)
- Subject 7 - O***r, Male, 26 years old, Italian (same as both parents)

A relevant factor in results of the test is the nationality of the participants. The anthropometric analysis and the design of the sizing system was based on Italian and Dutch populations, considered as representative of the European population in general. The first research question (whether there would be for each subject at least one size of the mask that ensures sufficient contact to provide EOG signals) was expected to be verified at least for subjects with European origin. Nonetheless it was interesting to test this assumption with several subjects with extra-European origins (subjects 2 and 6), whereas Turkish population was considered as European.

8.1.6 Limits of the user test

- Small sample size due to time limitations
- The subjects were looking at a video which is not representative of VR environments
Repeating the test in VR would be beneficial to evaluate the differences between a computer screen and the VR headsets screens
- No head and body movement were allowed
Another test may evaluate the effect of head and body movements on the EOG signals.
- Lack of a specific methodology in the analysis of the EOG signal
- There is no reference to evaluate the accuracy of the EOG signal
It would be beneficial to also record eye movements with a commercial eye-tracker to compare with the EOG signals
- Literature shows that the level of the EOG signal slightly varies with the level of adaptation of the eyes to the lighting condition of the room. During the test and in the results this factor was not taken into consideration
- No different harness systems were tested
- The test did not include the evaluation of different materials which would have an influence on the comfort/discomfort and the signal properties
This includes different foams densities and different electrodes metals/plastics and metal coatings
- The comfort/discomfort data is collected after only 5 minutes
Following test may investigate longer term comfort/discomfort
- The comfort/discomfort questionnaire provides subjective qualitative data. It would be beneficial to evaluate the comfort also with quantitative sensor data
Pressure sensors might be included at relevant spots of the mask in order to produce a pressure map output

8.2 Evaluation of the signals

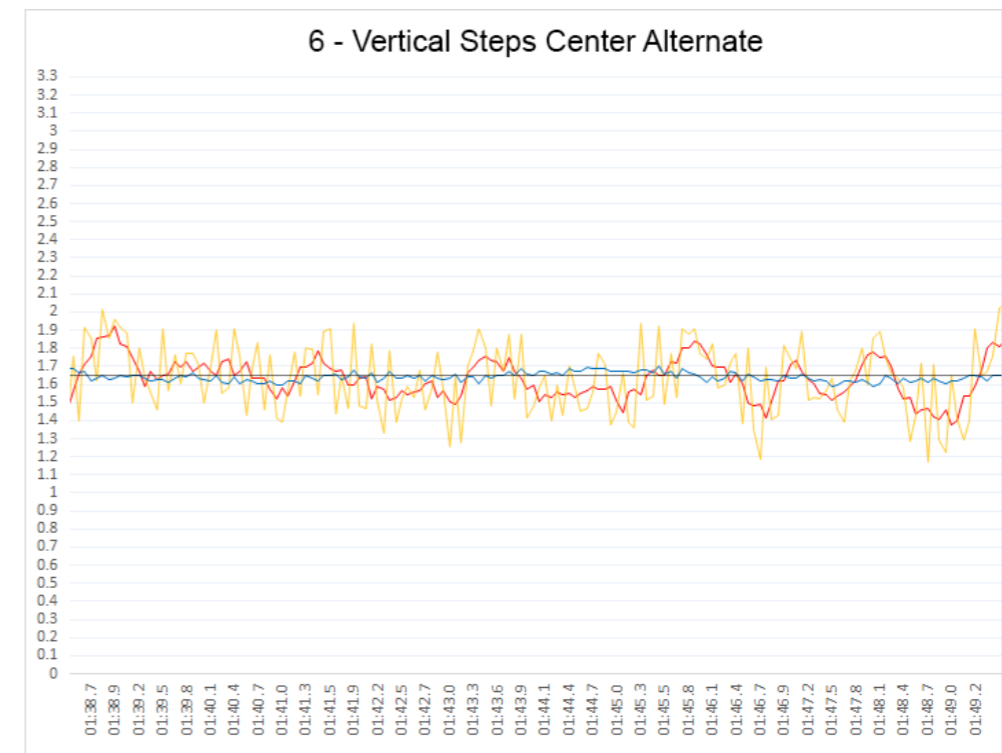
8.2.1 Filtering

The EOG signal resulting from the tests showed high disturbance in the vertical component (orange line). In order to clean the noise a filter was applied to the raw signal.

A common filter used in signal processing is the moving average filter. It is a simple low-pass filter

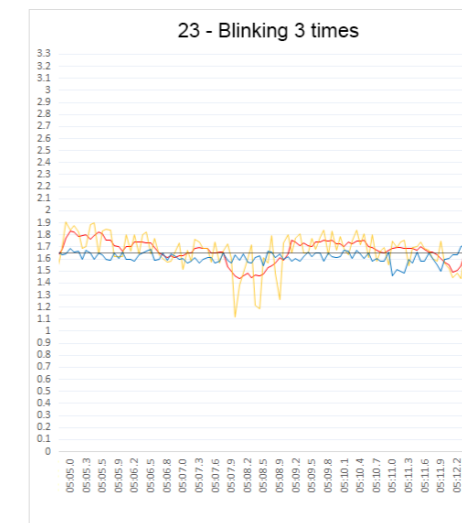
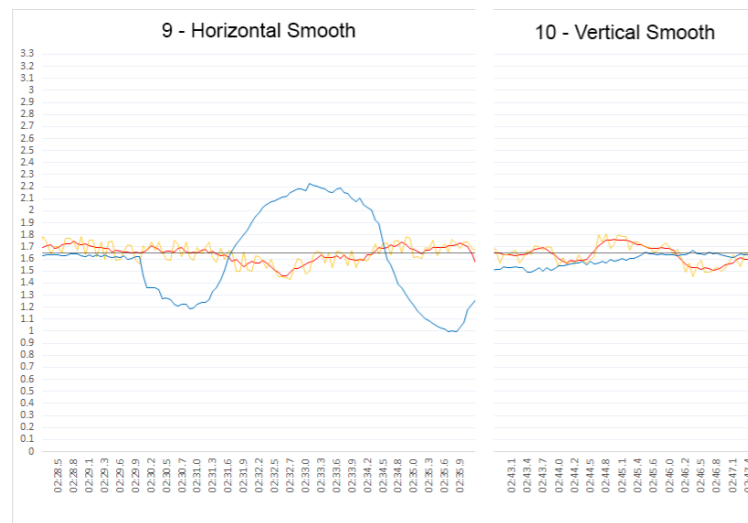
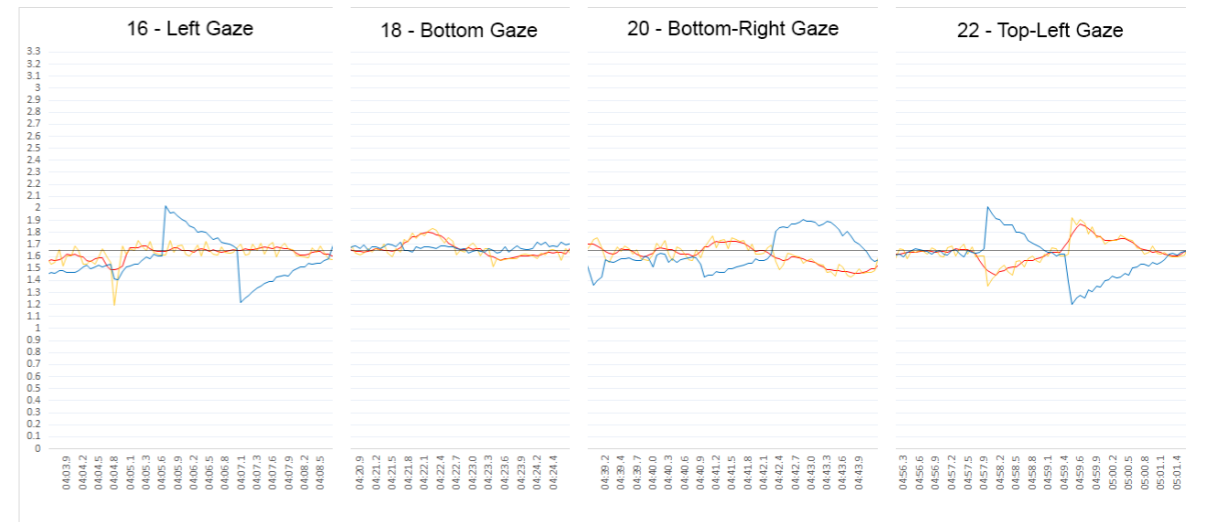
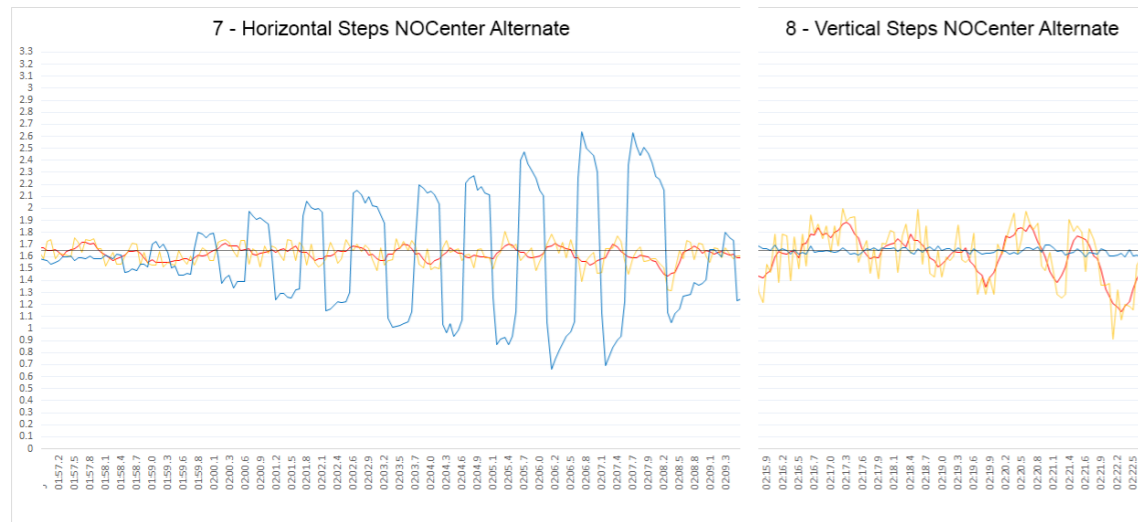
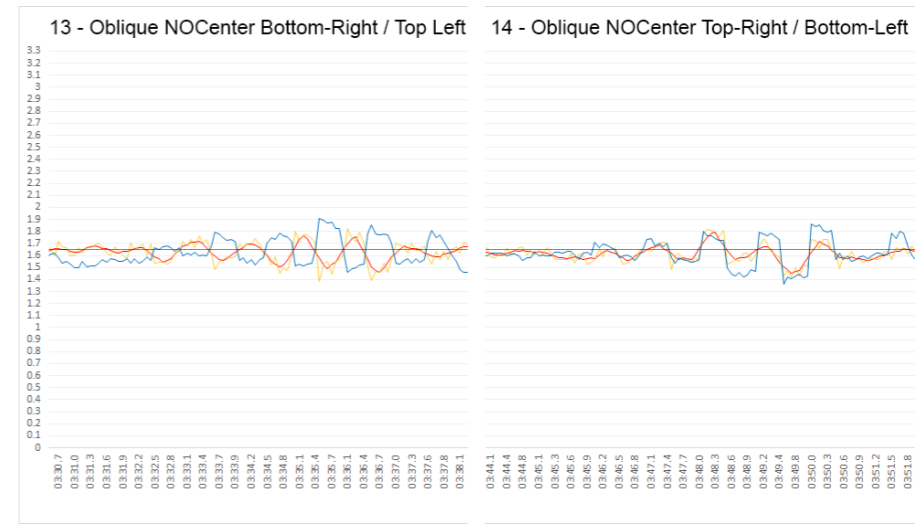
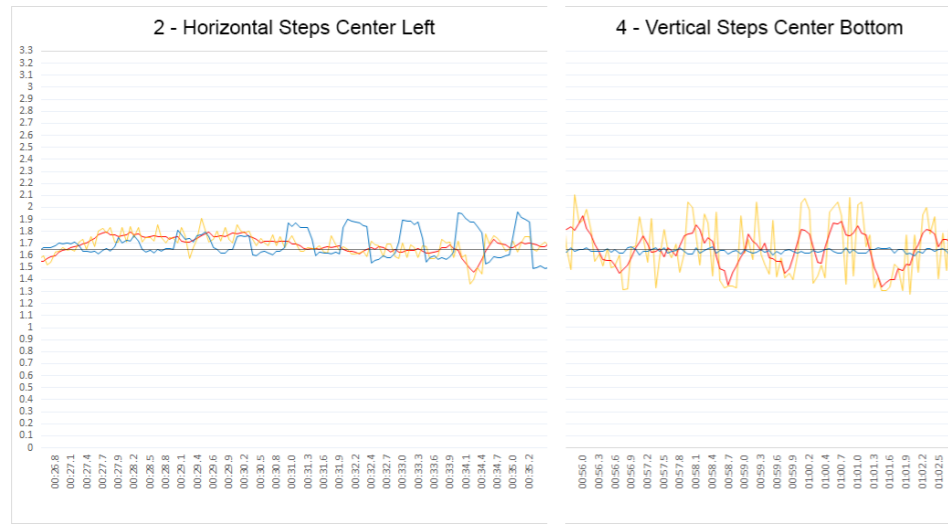
which averages a defined number of samples. The effect is a shorter but smoother output, where sharp modulations in the data are rounded.

Limited research and knowledge on filtering, as well as lack of time restricted the evaluation of more filters.



8.2.2 Plots

It is not possible to display all the data recorded during the user test sessions in this report. The following pictures are a selection of the highest quality plots among different exercises subjects and sizes.



8.3 Summary of results

Here are summarized the main results and findings from the analysis of the signal plots and the questionnaires. A complete analysis of the results for each subject can be found in the Appendix 8.3.

8.3.1 Signals

- In each case at least one size ensured contact for EOG signals
 - 4 cases - 1 size*
 - 2 cases - 2 sizes*
 - 1 case - 3 sizes*
- The vertical signals were more disturbed than the horizontal one, except in one case (the key factor is the distance of the electrodes from the eyes)
- When subjects received EOG signals from multiple sizes, in only one case there were relevant differences between the recordings
- The signal amplitude range (minimum and maximum for extreme gaze positions) varies per subject but not per size
- The zero signal (eyes rest position) may differ from 1.65V. The range is not always symmetrical (due to non-symmetrical positioning of the mask). This can be adjusted with zero position calibration

8.3.2 Comfort/discomfort

- Sizes that provided EOG signals were rated higher in comfort compared to the other sizes (relationship between contact and comfort) except in one case
- The local discomfort was mainly attributable to high pressure/compression
- The local discomfort is mostly symmetric (except one case)
- Subjects are comfortable in fitting larger size than the preferred one

9

Chapter 9
**RECCOMENDATIONS,
REFLECTIONS AND REFERENCES**

Reccomendations

- Meet, interview and gain insights from doctors that perform EOG measurements on patients
- Investigate the requirements in terms of accuracy and frequency for each application
- Repeat the anthropometric study including the North-American database
- Create a sizing system with 2 and 4 sizes and evaluate their performances by comparing them against the three sizes.
- Investigate a one-size-fits-all with regulation system approach for the final product.
- Implement the EOG in a actual virtual reality headset
- Include calibration procedure
- Repeat the test in virtual reality EOG signals are recorded also during head and body movements.
- Evaluate in detail the proportionality (line or curve diagram) between the EOG signals and the angles of eye rotations
- Investigate the effects of filters on the EOG signals

Reflection

I believe that I am somebody who pursue high quality of work. During this graduation I tried to do possibly my best to deliver good results and to meet my personal expectations and the ones of the supervisory team, while keeping the motivation high.

In the specific, the time spent in the research and forming knowledge was extremely useful to ensure the quality of the further work. Although, I believe that the lack of time to explore deeply some topics, as well as having the suport of a company and a budget may have affected the quality of technical manners such as the hardware and the realization of a prototype.

I managed this lack in two ways. Firstly, by gaining as much possible support and knowledge from the supervisory team. Secondly, by making a first step on a relatively unexplored topic, thus focusing the project on demonstrating the possibility of integrating efficiently EOG in a VR headset, rather than the design of an actual final

product. Therefore, I tried to put provide relevant insights on ergonomics and electronics and put the basis for a further research or graduation topic. I indeed believe that this EOG has serious advantages over camera-based eye-trackers and may see a future on the market.

The graduation represented a challenge in the fact that is a personal project, meaning that I felt that, in order to success, I needed to improve some less powerful competences as project/time management, as well as the communication and involvement of the stakeholders. I believe that a better project/time management still needs to be achieved, especially the ability to prioritize the activities.

Other ambitions were to gain deep knowledge regarding Virtual Reality, bio-signals acquisition technologies, and advanced ergonomics methodologies. I am really satisfied with what I have learned, and I am confident that I can apply this knowledge in my working future.

References

- Abo-Zahhad M., Sabah A.M., S.N. Abbas - A New EEG Acquisition Protocol for Biometric Identification Using Eye Blinking Signals (2015)
- Ansari M.W. & Nadeem A. - Atlas of Ocular Anatomy (2016)
- Augustyniak P. - Przetwarzanie sygnałów elektrodiagnostycznych (2001)
- Ball R.M. - SizeChina: A 3D Anthropometric Survey of the Chinese Head (2011)
- Ben Azouz, Z., Shu, C., Lepage, R., and Rioux, M. - Extracting Main Modes of Human Shape Variation from 3-D Anthropometric Data (2005)
- Collewyn H., van der Mark F., Jansen T.C. - Precise recording of human eye movements (1975)
- Donders FC - Beitrag zur Lehre von den Bewegungen des menschlichen Auges (1848)
- Drewes H., Schmidt A. - Interacting with the Computer Using Gaze Gestures (2007)
- Du Bois-Reymond E. - Untersuchungen Über Thierische Elektrizität (1848)
- Duchowski A.T. - Eye Tracking Methodology, Theory and Practice (2017)
- Farkas L. - Anthropometry of the head and face (1994)
- Goto L., Huysmans T., Lee W, Molenbroek J.F.M., Goossens R.H.M. - A Comparison Between Representative 3D Faces Based on Bi- and Multi-variate and Shape Based Analysis (2019)
- Heide W., Koenig E., Trillenber P., Kömpf D., Zee D.S. - Electrooculography: technical standards and applications (1999)
- Henn V. - Electronystagmography: the answers one might get (1993)
- Horwitz J. - The VR headset market is about to get way too crowded and confusing (2019) - Retrieved from: www.venturebeat.com
- Kolar J., Salter E. - Craniofacial anthropometry: practical measurement of the head and face for clinical, surgical, and research use (1997)
- Krachunov S. & Casson A.J. - 3D Printed Dry EEG Electrodes (2016)
- Krupiński R. & Mazurek P. – Real-Time Low-Latency Estimation of the Blinking and EOG Signals (2012)
- Lacko D., Huysmans T., Vleugels J., De Bruyne G., Van Hulle M.M., Sijbers J., Verwulgen S. - Product sizing with 3D anthropometry and k-medoids clustering (2017)
- Lang B. - Eye-tracking is a Game Changer for VR That Goes Far Beyond Foveated Rendering (2018) – Retrieved from: www.roadtovr.com
- Malmivuo J. & Plonsey R. - Bioelectromagnetism (1995)
- Mark Shelhamer M. & Roberts D.C. - Magnetic scleral search coil (2010)
- Morimoto C.H. & Mimica M.R.M. - Eye gaze tracking techniques for interactive applications (2005)
- Nowakowski M., Sheehan M., Neal D., Goncharov A.V. - Investigation of the isoplanatic patch and wavefront aberration along the pupillary axis compared to the line of sight in the eye (2012)
- Paquet E. - Exploring anthropometric data through cluster analysis (2004)
- Park R.S. & Park G.E. - The center of ocular rotation in the horizontal plane (1933)
- Porter J. M., Gyi D. E., Tait H. A - Interface pressure data and the prediction of driver discomfort in road trials (2003)
- Rashbass C. - The relationship between saccadic and smooth tracking eye movements (1961)
- Robinette, K.M., Blackwell, S., Daanen, H., Boehmer, M., Fleming, S., Brill, T., Hoferlin, D., Burnsides, D. - Civilian American and European Surface Anthropometry Resource (CAESAR) Final Report, Volume I (2002)
- Robinson D.A. - A method of measuring eye movements using a scleral search coil in a magnetic field (1963)
- Robinson D.A. - The mechanics of human smooth pursuit eye (1965)
- Rusydi M., Okamoto T., Ito S., Sasaki M. - Rotation Matrix to Operate a Robot Manipulator for 2D Analog Tracking Objects Using Electrooculography (2014)
- Schott, E. - Über die Registrierung des Nystagmus und anderer Augenbewegungen vermittels des Seitengalvanometers (1922)
- Shackel, B. - Eye movement recording by electro-oculography (1967)
- Shkoukani M. & Abusaim H. - Proposed Enhanced Object Recognition Approach for Accurate Bionic Eyes (2012)
- Westheimer G. - Eye movement responses to a horizontally moving visual stimulus (1954)
- Wilson-Pauwels L., Stewart P.A., Akesson E.J., Spacey S.D. - Cranial Nerves: Function and Dysfunction (2010)
- Wong A.M.F. - Listing's Law: Clinical Significance and Implications for Neural Control (2004)
- Wyman D., Steinman R.M. - Small step tracking; implications for the oculomotor "dead zone" (1973)
- Young L.R. & Sheena D. - Survey of eye movement recording methods (1975)
- Lacko D.,surgical,van der Mark F.

